

GEOCHEMISTRY AND GEOCHRONOLOGY  
OF METEORITE IMPACT MELTS

A GEOCHEMICAL AND GEOCHRONOLOGIC INVESTIGATION

OF

METEORITE IMPACT MELTS

AT

MISTASTIN LAKE, LABRADOR

AND

SUDBURY, ONTARIO

BY

MICHAEL MARCHAND, B.Sc. (Hon.), M.Sc.

A Thesis

Submitted to the School of Graduate Studies

in Partial Fulfilment of the Requirements

for the Degree

Doctor of Philosophy

McMaster University

January 1976

© 1976 by Michael Marchand

DOCTOR OF PHILOSOPHY (1976)  
(GEOLOGY)

McMASTER UNIVERSITY  
Hamilton, Ontario

TITLE: A Geochemical and Geochronologic Investigation  
of Meteorite Impact Melts at Mistastin Lake,  
Labrador and Sudbury, Ontario

AUTHOR: Michael Marchand, / B.Sc. (hon.) [McGill University]  
M.Sc. [McGill University]

SUPERVISOR: Dr. J.H. Crocket

NUMBER OF PAGES: 142, xiv

SCOPE AND CONTENTS:

Trace element and Sr isotopic geochemistry have been used to demonstrate what happens chemically to the rocks that have been hit and melted by the impact of a meteorite.

Two meteorite craters were studied by these techniques. The one in Labrador has a simple geology and this has allowed the construction of a model of the geochemical processes involved in the impact of a meteorite. The other, at Sudbury, has a much more complex geological history which does not allow the direct application of the model because of post-crater events.

## ABSTRACT

The meteorite crater at Mistastin Lake, Labrador, lies completely within an unmetamorphosed post-orogenic pluton composed of adamellite and mangerite and containing large lenses of anorthosite. The young age (40 m.y.) and unaltered nature of the impact melt, combined with the simple target rock geology, makes this crater an ideal place to investigate the process of impact melting.

The country rocks and the impact melt were analysed for a suite of ten trace elements. Using the multivariate statistical technique of correspondence analysis, it is shown that the impact melt samples form a linear array of points joining the anorthosite samples to the mangerite samples. This indicates that the various melt samples can be explained as a result of the complete fusion of different proportions of anorthosite and mangerite. A least-squares mixing model using the average trace element contents of the four rock types indicates that the average melt can be formed by mixing 60% anorthosite, 38% mangerite and 2% adamellite.

A Rb-Sr isochron on the combined mangerite and adamellite units of the Mistastin Lake pluton gives an age of  $1347 \pm 15$  (1s) [ $\lambda = 1.39$ ] with an initial ratio of  $.7082 \pm .0003$  (1s). The anorthosite samples do not plot on this isochron and have an estimated initial ratio of approximately  $.704 \pm .001$ , indicating that they are not

comagmatic with the granitic rocks of the pluton. On an isochron diagram the melt rocks plot along a line joining the locus of anorthosite samples to an average granite sample of the pluton. This is a further indication that the melt can be explained as the result of fusion of the local country rocks.

The Sudbury area is much more complicated because of post-impact thermal and tectonic events. Various rock units of the upper Irruptive and Grey Onaping Formation from a restricted geographic area of the North Range of the Irruptive were analysed for the suite of ten trace elements and Sr isotopes. Correspondence factor analysis of the trace element data shows the plagioclase micropegmatite to be very inhomogeneous, making it more akin to the impact melt rather than a differentiate of the norite. It has an isochron of  $1361 \pm 48$  m.y. with an initial ratio of  $.7151 \pm .0008$ . This is the lowest age recorded for a unit of the Sudbury Basin. The impact melts, country rock fragments, glasses, and norite have isochrons and errorchrons giving ages between 1430 and 1890 m.y. This wide range of ages from rocks that shared the same post-Irruptive tectonic history can be explained by the following model:

The Irruptive was intruded into a subaqueous meteorite crater below the layer of impact melt. A hydrothermal convection system was established in the crater resulting in the hydration of the units, alteration and

some metasomatism. These effects resulted in the ubiquitous presence of chlorite, epidote, albite, green amphibole and granophyric textures and in the devitrification of the glasses. Later episodes of thermal activity affected these systems which, because of their small size, variable mineralogy, and different average Rb/Sr ratios, reacted at different times producing the various ages.

## P R E F A C E

This geochemical study was started in the summer of 1969 when a suite of samples was collected from the Mistastin Lake crater in Labrador for trace element and Sr isotopic analysis. This crater has a large amount of well-exposed impact melt and a fairly simple country rock geology, both features favourable for testing the hypothesis that melt rocks were formed by fusion of various mixtures of the target rocks. In the beginning of this study there was little interest in the geochemistry of impact craters but shortly afterwards the Apollo missions to the Moon showed that impact processes were important in modifying the surface of the Moon, although very little interest seemed to be generated in terrestrial craters. This was likely due to the large amounts of money available for lunar studies. It is only now, in 1975, that some of the labs that contributed to the geochemical understanding of the Moon are becoming interested in terrestrial craters.

In spite of all the resources expended on lunar studies, the Moon is and will always remain a poorly sampled body while terrestrial craters offer the possibility of complete and accurate sampling and geological documentation. Detailed geochemical studies, preferably after detailed

geological mapping, of terrestrial craters probably offer a much better chance of understanding the geochemical processes of impact melting than does the Moon. Once there is a sufficient volume of precise geochemical data on terrestrial craters, perhaps a re-examination of lunar models will be useful.

This thesis consists primarily of two parts, one on the geochemistry of the Mistastin Lake crater in Labrador and the other on the Sudbury astrobleme. Both parts deal with geochemistry, but each is in fact a self-contained unit with little direct relationship to each other. This is primarily because the geological history at Sudbury is complex and post-crater effects have obscured many of the geochemical characteristics of the impact-produced rocks. On the other hand, the Mistastin Lake crater is young and fresh, with the geochemical relationships well preserved. These portions of the thesis have therefore been written in the form of two discrete scientific papers. To provide cohesion, an introduction containing a short review of the important aspects of shock metamorphism and crater formation along with a summary of previous geochemical work on meteorite impact craters has been provided. The data and the descriptions of the analytical techniques have been placed in appendices at the end of the thesis.



## Acknowledgments

I would like to thank James H. Crocket who acted as supervisor of this thesis and provided technical and financial support through his N.R.C. operating grant. Robert H. McNutt and P.S. Nicholson rounded out the supervisory committee to which I am most grateful for allowing me to carry out this investigation with the greatest of freedom. A special thanks must be given to the Gravity Division of the Earth Physics Branch of the Department of Energy, Mines & Resources, Ottawa, particularly to Michael Dence for whom I worked over a period of four summers (1968-71) and who introduced me to and taught me most of what I know about meteorite impact craters. His critical review of this thesis is most appreciated. Dick Grieve and Blyth Robertson, also of the Gravity Division, provided additional help and encouragement. Fred Taylor of the Geological Survey of Canada provided invaluable assistance in the form of complete logistical support at Mistastin Lake, samples from his reconnaissance mapping in Labrador and sundry geological facts. I am especially indebted to Walter Peredery of INCO who accompanied me in the field in Labrador, guided me around the Sudbury Irruptive, provided samples from his thesis work on the Onaping Formation and presented stimulating discussions on the origin of the Sudbury Irruptive. His excellent thesis

provided the geological framework for my geochemical work on the Sudbury area. I must also extend my appreciation to the other INCO geologists who provided information and assistance, Don Phipps, Ed Pattison and J.V. Guy-Bray.

I would also like to express my appreciation for courtesies and geological information to Ken Card and H. Meyn of the Ontario Department of Mines. Appreciation is extended to Jack Whorwood for photographic services and to fellow graduate students, especially to Walter Gibbins who provided discussion and arguments, sometimes irrational, on aspects of Sudbury geology and other diverse topics. A special thanks to Susan Thorp for encouragement and some technical assistance.

## TABLE OF CONTENTS

|           |   | Page |
|-----------|---|------|
| Chapter 1 | Review of Shock Metamorphism, Crater Formation, and Crater Geochemistry |      |
| 1.1       | Introduction  | 1    |
| 1.2       | Crater Formation  | 2    |
| 1.3       | Shock Metamorphism  | 8    |
| 1.4       | Previous Geochemical Work on Meteorite Impact Craters                   | 10   |
| <br>      |   |      |
| Chapter 2 | The Mistastin Lake Meteorite Crater                                     |      |
| 2.1       | Introduction  | 18   |
| 2.2       | The Rock Units  | 20   |
| 2.3       | Geochemical Appraisal of the Impact Melt                                | 25   |
| 2.4       | Least Squares Mixing Model  | 34   |
| 2.5       | Geochronology and Sr Isotopic Geochemistry                              | 38   |
| 2.6       | Conclusions   | 49   |
| <br>      |   |      |
| Chapter 3 | The Sudbury Irruptive   |      |
| 3.1       | Geological Setting  | 53   |
| 3.2       | Shock Metamorphism  | 55   |
| 3.3       | The Upper Irruptive   | 56   |
| 3.4       | Chemistry of the Upper Irruptive  | 60   |
| 3.5       | The Basal Breccia   | 68   |
| 3.6       | The Onaping Formation   | 70   |
| 3.7       | Chemistry of the Glasses and Country Rocks                              | 72   |

|   | Page |
|---|------|
| 3.8 The Melt Rocks  | 73   |
| 3.9 Geochemistry of the Melt Rocks  | 74   |
| 3.10 Geochronology  | 76   |
| 3.11 $Sr^{87}/Sr^{86}$ Ratios   | 89   |
| 3.12 Discussion   | 93   |
| 3.13 Model of Crater and Irruptive<br>Formation                               | 99   |
| Appendix A Geochronological Procedures  | 103  |
| B Trace Element Analysis  | 109  |
| C Major Element Analysis  | 111  |
| D Correspondence Analysis   | 115  |
| E Mistastin Lake Samples: Location,<br>Trace Element Data, Major Element Data | 117  |
| F Sudbury Area: Location, Descriptions,<br>and Trace Element Data             | 122  |
| List of References  | 130  |

## LIST OF FIGURES

| Figure No. |  | Page |
|------------|--|------|
| 1-1        | Model of the excavation stage of a typical terrestrial impact crater . . .                               | 5    |
| 1-2        | Two alternate post-excitation histories of an impact crater. . . . .                                     | 5    |
| 1-3        | Main rock units of a standard large complex impact crater. . . . .                                       | 7    |
| 1-4        | Progressive stages of shock metamorphism. . . . .  | 12   |
| 2-1        | Location of the Mistastin Lake crater..  | 19   |
| 2-2        | Geology of the Mistastin Lake crater...  | 21   |
| 2-3        | Variation diagrams of the melt and country rocks. . . . .  | 28   |
| 2-4        | Correspondence analysis factor plot....  | 31   |
| 2-5        | Country rock isochrons . . . . .   | 45   |
| 2-6        | Mixing lines of melt and country rocks on isochron diagram. . . . .                                      | 48   |
| 3-1        | Geological map of the Sudbury Basin. .   | 54   |
| 3-2        | Diagrammatic representation of the contact relationships of the rock units of the Sudbury Basin. . . . . | 57   |
| 3-3        | Geological map of the Upper Irruptive in the Dowling Area. . . . .                                       | 58   |
| 3-4        | Correspondence analysis factor plot. .   | 64   |
| 3-5        | Variation of Factor 3, Rb, and Sr across the South Range Blezard traverse. . . . .                       | 66   |
| 3-6        | Melt rocks and glasses on Streckeisen's double-triangle diagram. . . . .                                 | 75   |

---

| Figure No. |  | Page |
|------------|--|------|
| 3-7        | Upper Irruptive isochrons. . . . .     | .84  |
| 3-8        | Irruptive isochrons. . . . .           | .87  |
| 3-9        | Strontium development diagram. . . . . | .92  |

## LIST OF TABLES

| Table |   | Page  |
|-------|---|-------|
| 1-1   | Progressive stages of shock metamorphism . . .  | 13    |
| 1-2   | Characteristics of geochemically studied<br>craters . . . . .                         | 15-16 |
| 2-1   | Generalized stratigraphy of the crater<br>rock units . . . . .                        | 24    |
| 2-2   | Correspondence analysis results . . . . .   | 32    |
| 2-3   | Average trace element composition of the<br>rock units . . . . .                      | 35    |
| 2-4   | Mistastin Lake mixing model . . . . .   | 36    |
| 2-5   | Rb-Sr analytical data . . . . .   | 40    |
| 2-6   | Rb-Sr regression results. . . . .   | 43    |
| 3-1   | Correspondence analysis results . . . . .   | 62    |
| 3-2   | Rb-Sr analytical data . . . . .   | 78    |
| 3-3   | Geochronological results. . . . .   | 81    |
| 3-4   | Sr <sup>87</sup> /Sr <sup>86</sup> results at 1844 m.y. . . . .                       | 91    |
| 3-5   | List of ages in the Sudbury area. . . . .   | 94    |
| A-1   | Replicate determinations of SRM-987 . . . . .   | 105   |
| A-2   | Comparison of analyses of SRM-987 . . . . .   | 106   |
| A-3   | Replicate determinations of Sr isotopes on<br>rock samples . . . . .                  | 108   |
| B-1   | Trace elements - analytical parameters . . . . .                                      | 110   |
| C-1   | Major elements; replicate determinations<br>and comparisons of MgO analyses . . . . . | 113   |
| C-2   | Analyses of Benchmark sample 'B-3' . . . . .  | 114   |

## C H A P T E R 1

### Review of Shock Metamorphism, Crater Formation, and Crater Geochemistry

#### 1.1 Introduction

A short review of the more important aspects of shock metamorphism and crater formation is presented here to illustrate the environment in which craters exist. Meteorites interact with the earth at velocities of 12-72 Km./sec. but since the atmosphere is a good cushion most lose velocity and break up. Friction melts the outer layers of the larger bodies and completely vapourizes the smaller fragments forming fireballs. Meteorites in excess of about 1000 tons are little affected by the atmosphere and reach the surface of the earth at their cosmic velocities (15-20 Km./sec.). At the point of impact the pressure reaches 5 Megabars (Mb.), vapourizing most of the meteorite and a small portion of the target rocks. The remaining meteorite is melted along with some of the target rock and sprayed over the countryside. The pulse of very high pressure, which decays rapidly as it travels into the ground, creates a shock wave lasting only a few hundredths of a second. Grading outward from the zone of melted rock and meteorite, temperatures are lower but the shock pressures are sufficiently high to transform minerals



to high pressure forms. Further out the rocks show microscopic deformation planes in minerals and a conical form of striated fractures called shatter cones.

## 1.2 Crater Formation

A model for the excavation stage of crater formation is presented in Figure (1-1) (Dence, 1971). It may require minor modification since it is now thought that the peak pressure is not reached immediately, but only after a few seconds when the meteorite has penetrated the rock (Chao, 1974). This property of the impact phenomenon is supported by some field and chemical work on the Monteräqui crater in Chile (Bunch et al., 1972) where it has been shown that none of the topmost ignimbrite unit and only the deepest rock in the crater has been melted. It then follows that the hottest and most highly shocked material is the lowest in the pre-impact stratigraphy (Chao, 1974). This only alters the point of highest pressure in Dence's model, the remainder of which remains valid. The target rock shocked above 2 Mb. will be vapourized and most rock shocked between 0.5 and 2 Mb. will be fused or partially fused. The shock melted material will then be given particle velocities in the directions indicated by the arrows in Figure (1-1) and will engulf less strongly shocked and accelerated materials in the outer parts of the growing crater. During the penetration most of the meteorite is

vapourized (Chao, 1974) and a portion of the melt will be ejected from the crater with the remainder lining the cavity overlying a layer of mixed breccia and melt. Usually there is also a layer of breccia mixed with glass bombs of melt overlying the melt layer. This layer is deposited by direct fallback into the crater and is called the 'fallback breccia' or 'suevite'. Dence (1971) calls the crater at this stage the transient cavity to emphasize the fact that at this point a rapid re-adjustment takes place. The sequence of events is demonstrated in Figure (1-2). Small (<4 Km. diameter) craters are modified by slumping of the crater walls (Figure 1-2a) and the melt and breccias become interlayered lenses in the center of the craters. In large complex craters (>4 Km.) (Figure 1-2b) collapse of the uplifted rim material initiates deep slumping and causes uplift in the center of the crater floor and downdrop of the crater rim. The crater lining in this sequence of events is generally passive (Dence, 1971) and except where the central uplift causes disturbance, the lining retains the original relationships. Melt and breccia can fill fractures in the underlying basement rocks. The central uplift contains shocked rocks with melt rocks (solid black in Figure 1-2) occurring in the lower portion of the crater floor between the central uplift and rim. Dence (1971) classifies the distribution of impact melt into four different categories: (1) as glassy bombs in ejecta, (2) as glassy

Figure 1-1. Model of the excavation stage of a typical terrestrial hypervelocity impact crater based mainly on analysis of data from Brent crater. On the right, stages in the excavation are depicted with vectors of particle motion after Gault et al. (1968). On the left are shown the corresponding positions of the attenuating shock wave. [Figure 3, Dence, 1971]

Figure 1-2. Two alternate post-excavation histories of an impact crater. (A) Slumping of the crater walls to give a simple crater of the Barringer-Brent type. Melt and breccias lining the excavated cavity are disrupted and incorporated into a central bowl-shaped body of breccias. (B) Deep-seated sliding of the crater walls to give a central uplift, ring uplift, and depressed rim, as in a complex crater of the Clearwater-Manicouagan type. The crater lining remains largely intact but fills fractures in the underlying basement rocks. Limits of shock deformation of the basement rocks is shown by inverted V's.

[Figure 4, Dence, 1971]

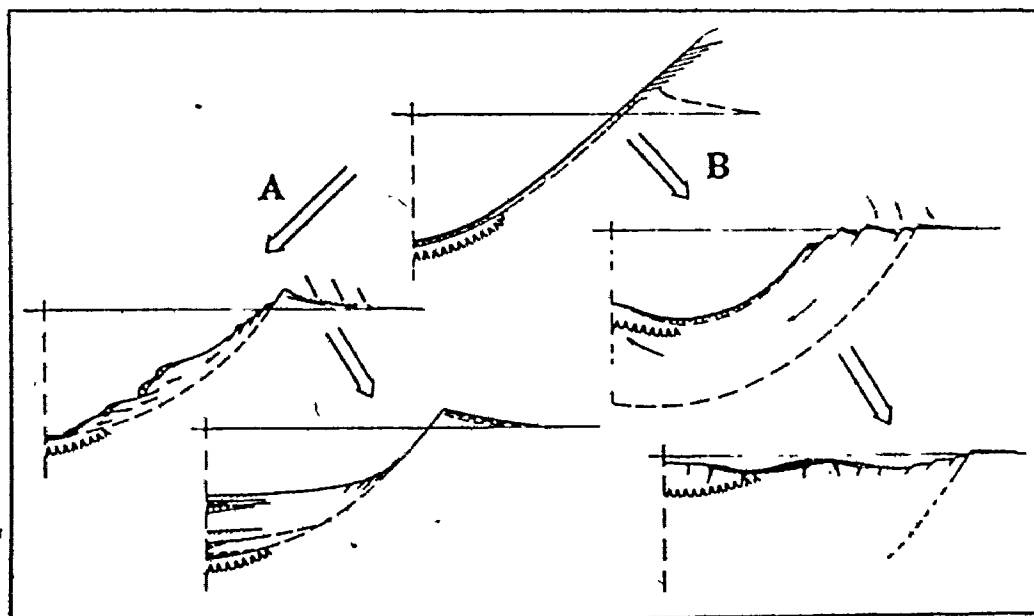
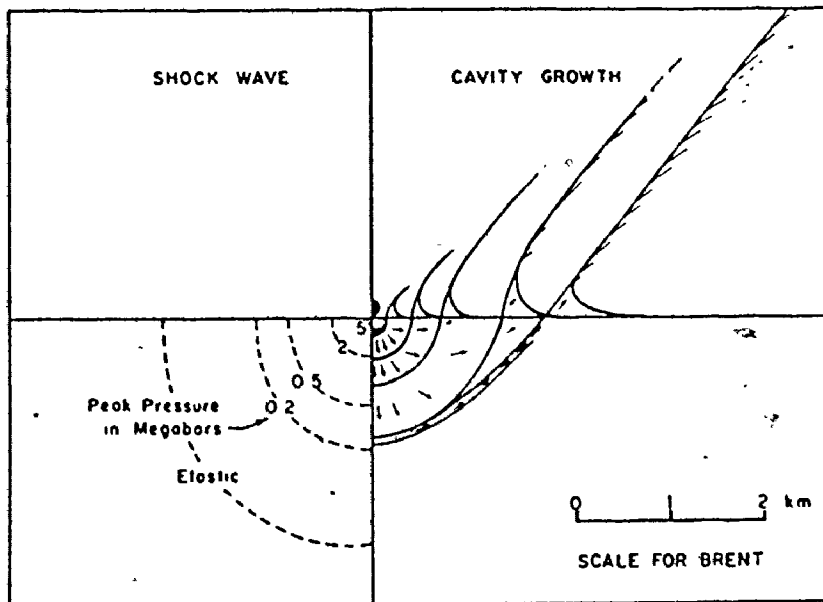


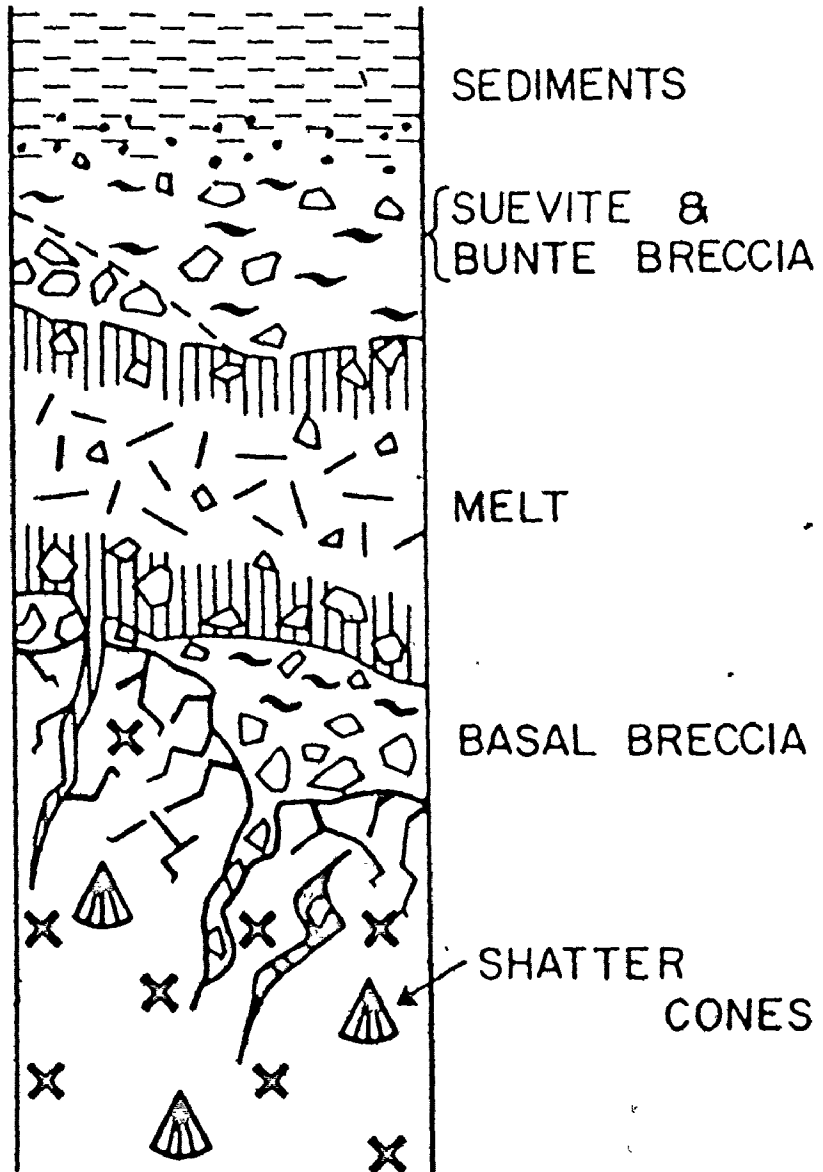


Figure 1-3. Main rock units of a standard large complex impact crater. The Main units are:

- (1) Basement crystalline rocks (crosses) mildly shocked (shatter cones), fractured, and cut by pseudotachylite breccia veins (black matrix).
- (2) Lower breccia unit: basal breccia of shocked basement rocks including shocked melted glasses.
- (3) Igneous rock unit: melt rocks with fine-grained inclusion rich margins and coarser grained center.
- (4) Upper breccia unit: Bunte breccia or equivalents of weakly shocked upper target rocks in a clastic matrix.
- (5) Fallout breccia unit: Suevite breccia of variously shocked and melted fragments.
- (6) Sedimentary fill unit: clastic or chemical sedimentary rocks.

[ Figure 5, Dence, 1972 ]

STANDARD  
IMPACT CRATER



bombs or recrystallised masses in mixed breccias (suevite), (3) as thick sheets, (4) as minor dykes in the base of the crater. A generalised stratigraphy of the resultant complex crater is presented in Figure (1-3) (after Dence, 1972).

### 1.3 Shock Metamorphism

In most cases the crater morphology has been subdued by erosion and often the only means of recognizing ancient impact craters is by the shock metamorphic features in the minerals. Much has been written about the effects of meteorite impact and the criteria for recognition of shock metamorphism (see papers in French & Short, 1968). Therefore only a very brief outline will be presented here.

The characteristics of shock metamorphism can be divided into three main groups:

(1) High pressure effects which result in the formation of high pressure polymorphs such as coesite, stishovite and diamond.

(2) High strain rate effects which involve progressive dislocation and destruction of crystal lattices. Typically this is the formation of microscopic shock lamellae, especially in quartz and feldspar, which are multiple sets of planar optical discontinuities that are oriented parallel to low index crystallographic planes (Carter, 1965; Robertson et al., 1968). These minerals have been termed diaplectic

minerals (Stoffler, 1971). Under the highest pressure the end product of this process is an amorphous phase of short range order which is called a diaplectic glass. Maskelynite is the result of in situ formation of isotropic feldspar and is one such diaplectic glass.

(3) High temperature effects are produced by relaxation from pressures so high that the resultant relaxation temperatures are hundreds of degrees above the normal melting temperature of the minerals. The melting of quartz to lechatelierite and the decomposition of zircon to baddeleyite are examples. These features indicate temperatures in excess of 1500°C., much too high for any normal igneous geologic process (French, 1968).

The occurrence of shatter cones (Dietz, 1963,1968) is the major megascopic feature of shock metamorphism and these are found outside and below the crater in the target rocks.

The orientations of shock lamellae, particularly in quartz, have been used to demonstrate shock metamorphic effects. Certain crystallographic directions predominate and the difference between shocked quartz and tectonically deformed quartz has been described (Carter, 1965,1968). Tectonites do not contain planar features with the orientations found at impact sites.



Stoffler (1971) has produced a scheme for classification of progressive stages of shock metamorphism in quartzofeldspathic crystalline rocks (Figure 1-4; Table 1-1). It relates the deformation observed in the rocks to peak pressures and temperatures attained by the specimen and therefore provides some information on the location in the crater from which it came.


#### 1.4 Previous Geochemical Work on Meteorite Impact Craters

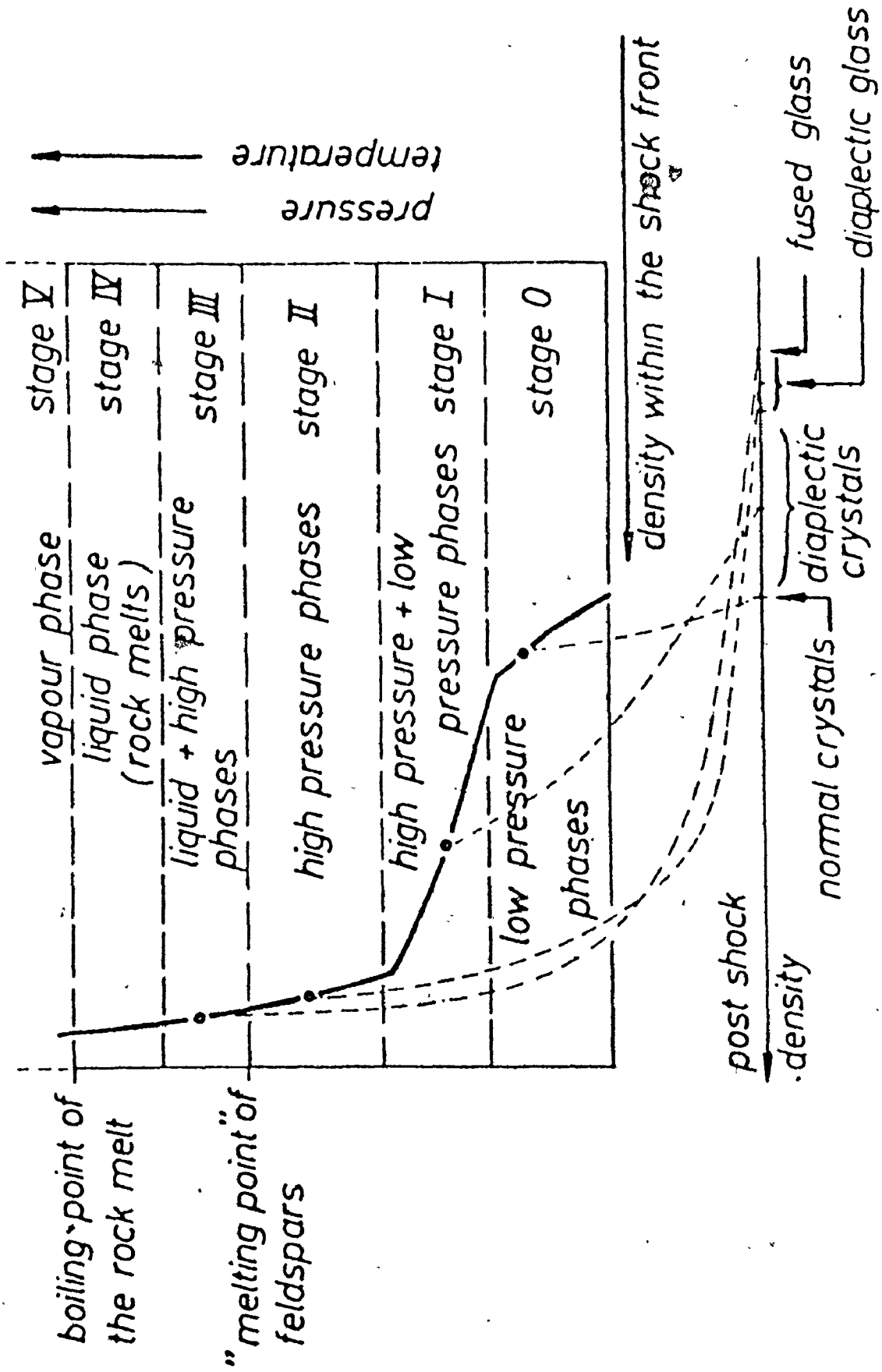
Previous work (Table 1-2) on impact craters utilizing trace element and Sr isotopic geochemistry has been minor and has suffered from inadequate sampling, especially in the restricted sampling of the country rocks. No crater with a large body of igneous textured melt has yet been studied. The impact melts analysed have been from small dyke-like occurrences and from bombs and other isolated occurrences of glass as thin coatings on the country rocks or in suevite breccias. The major problem with these impact melts from the ejecta are that they originate from a restricted locality deep in the crater (Engelhart, 1967) and are therefore not representative of the bulk of the melted rock. The specific parent of these melts has proven difficult to establish because of the inhomogeneous target rock and sparse sampling.

~~A Rb-Sr study of the impact glasses from the~~

Figure 1-4. Derivation of progressive stages of shock metamorphism from the generalized Hugoniot curve (heavy line) of the framework silicates (pressure versus density within the shock front). Lower scale (postshock density) replaces the abscissa of the Hugoniot plot to show the peak-pressure, postshock density relations on which the classification is based. The qualitative temperature scale refers to the postshock temperature on which the derivation of stages III-V is based. Dashed lines may help to relate the postshock density with the corresponding shock states in the Hugoniot plot (these lines do not represent the release adiabats measured by Ahrens and Rosenberg (1968)).

[ Figure 2, Stöffler, 1971 ]





temperature  
pressure

stage V  
stage IV  
stage III  
stage II  
stage I  
stage 0

vapour phase  
liquid phase (rock melts)  
liquid + high pressure phases  
high pressure phases  
high pressure + low pressure phases  
low pressure phases

boiling point of the rock melt  
"melting point of feldspars"

density within the shock front

post shock density

normal crystals  
diaplectic crystals  
fused glass  
diaplectic glass

TABLE 1-1  
Progressive Stages of Shock Metamorphism

| Stage | Shock Effects<br>Observed  | Peak Pressure<br>Kb. | Postshock<br>Temperature<br>°C. |
|-------|--|----------------------|---------------------------------|
| 0     | Fractured quartz<br>& feldspar;<br>shatter cones                 | 100                  | 100                             |
| I     | Diaplectic quartz<br>& feldspar                                  | 350                  | 300                             |
| II    | Diaplectic quartz<br>& feldspar glasses<br>e.g. maskelynite      | 450                  | 900                             |
| III   | Fused feldspar<br>(vesiculated glass)                            | 550-600              | 1300-1500                       |
| IV    | Inhomogeneous<br>rock glasses;<br>impact melt;<br>lechatelierite | > 800                | > 3000                          |
| V     | silicate vapour  |                      |                                 |

[ from Table 2, Stoffler, 1971 ]

small Henbury crater (Compston & Taylor, 1969) shows that the glasses fall on the country rock isochron. Further, the trace elements of the glasses are only slightly different from the analysed country rocks (Taylor, 1967). Taylor (1967) interprets the trace element properties as due to either preferential melting of the clay matrix of the greywacke target rock or to natural variation in the greywacke (ie.-a sampling problem). The Bosumtwi crater is quite large but no melt layer has yet been found. Impact melt occurs as glass in a few isolated locations outside the crater rim. The country rocks are a complex assemblage of interbedded metamorphosed phyllites, tuffs, greywackes, quartzites and shales which forms a severe sampling problem. From a restricted data base the Rb-Sr and REE geochemistry indicate that the melt is similar in composition to the country rocks (Kolbe et al., 1967). Some of the melt samples fall to the left of the country rock isochron indicating possible vapour fractionation of Rb (Kolbe et al., 1967) but there are also some points lying to the right of the isochron. This suggests that Kolbe's interpretation may be premature. The work on the Ries (Schnetzler et al., 1969) is inconclusive because of the scatter in the data and a restricted data Rb-Sr range. Sr isotopic work on the Tenoumer, Rochechouart, and Charlevoix craters consists of one or two samples of melt and is probably not statistically

TABLE 1-2  
Characteristics of Geochemically Studied Craters

| Crater                 | Diameter        | Age of Impact     | Age of Country Rocks (m.y.) | Impact Melt  | Remarks  | References  |
|------------------------|-----------------|-------------------|-----------------------------|--|--|---|
| Bosumtwi<br>Ghana      | 11 Km.          | 1.3 m.y.          | 2100-60 <sup>+</sup>        | no massive layer, scattered localities of glass  | complex country rocks REE similar to country rocks, indication of vapour fractionation | (Kolbé et al., 1967)<br>(Schnetzler et al., 1967) |
| Henbury<br>Australia   | 0.2 Km. largest | <4700 yrs.        | 730                         | scattered ejecta of impact glass, falls on same isochron as country rock                               | country rocks: sub-greywacke & quartzite; trace elements similar to the country rocks  | (Compston & Taylor, 1969)<br>(Taylor, 1967)       |
| Ries<br>Germany        | 24 Km.          | 15 m.y.           | 300                         | no massive layer, as bombs in ejecta or suevite, inconclusive Rb-Sr results                            | country rocks: poor outcrop, granite; analysed samples from fragments in suevite       | (Schnetzler et al., 1969)                         |
| Tenoumer<br>Mauritania | 1.8 Km.         | 2.5 m.y.          | 2500 approx.                | as small dyke-like bodies outside the crater; 2 samples give a high Sr <sup>86</sup> /Sr <sup>87</sup> | country rocks complex, granite, paragneiss, & Pliocene sediments                       | (French et al., 1970)                             |
| Rochechouart<br>France | 15 Km.          | <300 m.y.<br>>150 | 300                         | thin, discontinuous, altered, massive, crystalline, less than 2 meters thick, one Sr isotope analysis  | granites & schist country rocks, no analyses   | (Kraut & French, 1971)<br>(Hurley, 1969)          |

TABLE 1-2 continued

|                      |        |          |                 |   |  |
|----------------------|--------|----------|-----------------|---|--|
| Charlevoix<br>Québec | 35 Km. | 350 m.y. | 1200<br>approx. | one small outcrop<br>of massive melt,<br>one Sr isotope<br>analysis | country rocks<br>mostly charnokite,<br>no analyses<br>(Hurley, 1969) |
|----------------------|--------|----------|-----------------|---|--|

significant.

A potentially important consideration noted by Dence (1971) but not evaluated in most of the previous studies is that in some craters there has been considerable alteration and element mobility due to circulating groundwaters in the hot rocks.



## C H A P T E R 2

### The Mistastin Lake Meteorite Crater

#### 2.1 Introduction

The Mistastin Lake meteorite crater is located in the Churchill Province of the Canadian Shield in central Labrador (Fig. 2-1) and lies completely within the Mistastin Lake Batholith. The batholith consists mostly of adamellite but reconnaissance mapping (Taylor, 1969, 1970, 1972) shows several lenses of anorthosite, especially within the crater area itself. The batholith is one of numerous unmetamorphosed post-tectonic plutons of the Adamellite-Anorthosite suite that are found in central Labrador (Emslie et al., 1972). The adamellite is considered to be later than the anorthosite because of intrusive relationships but gradational contacts are also common (Emslie et al., 1972). In the region of Mistastin Lake these relationships are usually indistinct but seemingly gradational (Currie, 1971b). The mineralogical relationships of the Adamellite-Anorthosite suite suggest a pressure of crystallization of 5 Kb. (Emslie et al., 1972; Emslie, 1975) while the presence of rhyolitic volcanics (Taylor, 1972) grading into adamellite in a pluton further east shows the high-level nature of these plutons.

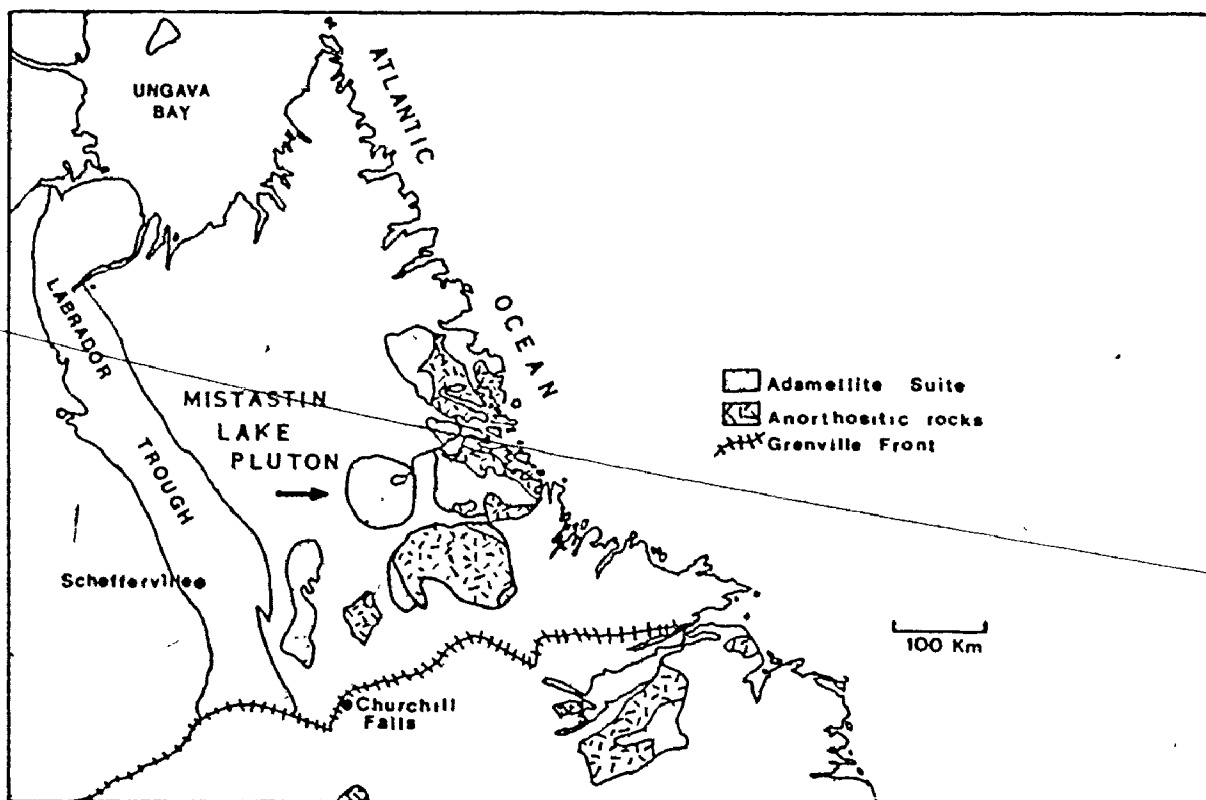


Figure 2-1. Location of the Mistastin Lake pluton with respect to the other plutons of the Anorthosite-Adamellite suite in central Labrador.

The crater at Mistastin Lake is classified as one of the complex types (Dence, 1972) and it has a diameter of approximately 20 Km. with a central uplift expressed as the island in the center of the lake. Shatter cones, planar features in quartz and feldspar, and fresh diaplectic glass, all unique indicators of meteorite impact (French & Short, 1968; Hörz, 1971), are present in the country rocks (Taylor & Dence, 1969). Abundant outcrops of fresh impact melt overlying brecciated and shocked country rocks are found around the edge of the lake (Fig. 2-2). It is the geochemical relationship of the melt rocks to the adjacent country rocks that forms the basis of this study.

## 2.2 The Rock Units

The adamellite of the batholith (Taylor, 1969, 1970, 1972) is part of the Adamellite suite (Wheeler, 1942, 1955, 1960, 1968), a series of gradational rock types consisting of adamellite, granodiorite, granite, syenodiorite and diorite. At Mistastin Lake, Currie (1971b) has distinguished two members of the suite, one which he termed 'augen granodiorite' and which is the typical adamellite described by Wheeler, and the other a green quartz mangerite. The adamellite is a coarse-grained equigranular rock consisting of potassium feldspar, plagioclase, and quartz with minor

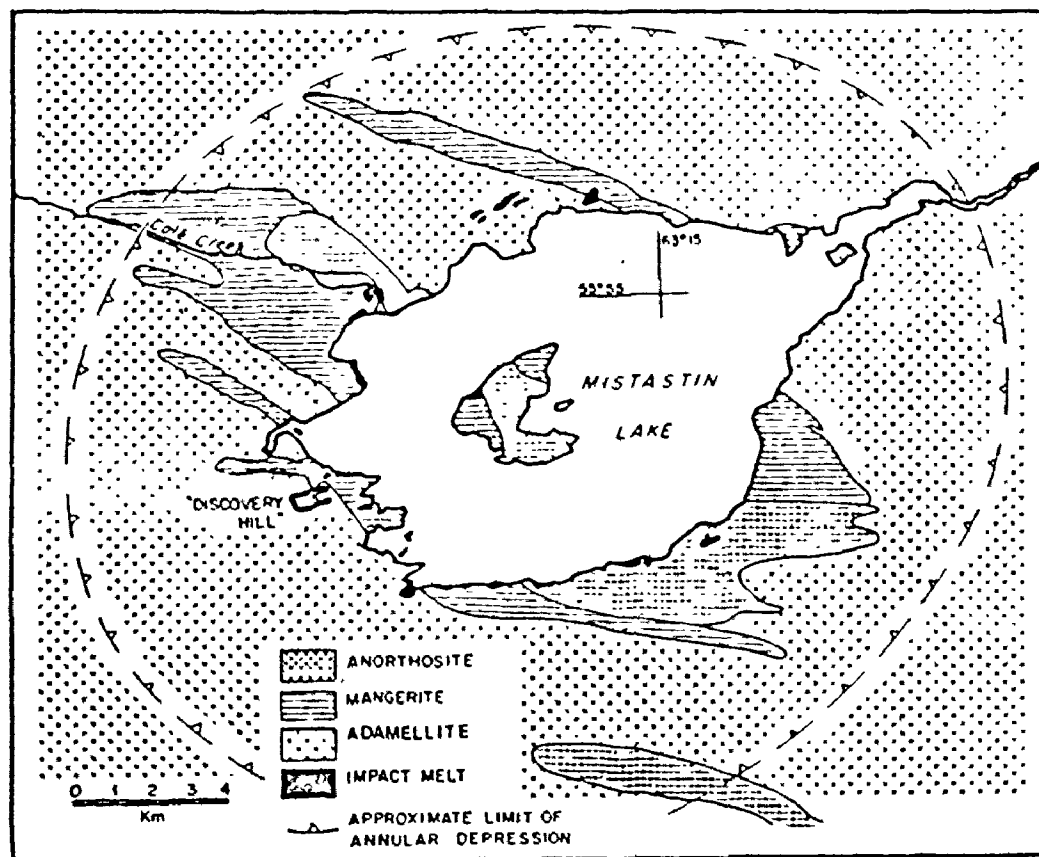


Figure 2-2. Geology of the Mistastin Lake crater (after Grieve, 1975).

amounts of hornblende, clinopyroxene, hypersthene, biotite, olivine, fluorite, apatite, zircon, and opaques. The potassium feldspar crystals are usually rounded and quite large, up to 20 cm. diameter in places, and Rapakivi texture is often well developed. The mafics are very iron rich, indicating an origin at a late stage of fractional crystallization (Emslie *et al.*, 1972). The green quartz mangerite is commonly associated with the anorthosite bands though not uniquely so (Currie, 1971b). The mineralogy of the mangerite is very similar to the adamellite though it has less quartz and more plagioclase, and the potassium feldspar is perthite. It can be distinguished chemically from the adamellite by its higher iron content and very high contents of  $TiO_2$  and MnO (Currie, 1971b). Wheeler (1968) reports a complete gradation of mangerite to adamellite in the Nain region to the east of Mistastin Lake.

The anorthosite occurs principally as two bands in the crater area (Fig. 2-1) though smaller patches have been found throughout the adamellite (Currie, 1971b). Fresh anorthosite consists of coarse-grained dark-grey calcic andesine with minor amount of mafics, including hypersthene and augite, and small widely dispersed pockets of ilmenite and quartz. The unshocked anorthosite within the crater is often altered to a pale, white coloured rock containing calcite, sericite and argillitic minerals with the mafics

altered to chlorite. Even fresh looking anorthosite sometimes displays incipient alteration along grain boundaries suggesting that some of the alteration is pre-impact in origin.

The petrography and mineral chemistry of the impact melt was described briefly by Taylor and Dence (1969) and in considerable detail by Grieve (1975). Consequently, only a brief outline of the mineralogical and textural varieties of the melt is presented here.

The melt rocks occur as isolated outcrops around the edge of the lake (Fig. 2-2), probably remnants of a once continuous layer lining the crater cavity. The stratigraphy of the crater rocks (Table 2-1) shows mainly the variation and location of different breccia types with little discrimination possible within the melt itself based on the field criteria. Several layers with columnar jointing in 'Discovery Hill' and sets of curved cooling joints parallel to the melt-country rock contact in Cote Creek indicate the rapid cooling of the melt. The largest outcrop of the melt is at 'Discovery Hill' where a vertical section of 100 m. is exposed, although the rock is relatively uniform in character, varying only slightly in grain size (Grieve, 1975).

Grieve (1975) divides the melt into three sub-units:

TABLE 2-1

## Generalized Stratigraphy of the Crater Rocks

- 
- 6 Melt - massive and vesicular in places
  - 5 Melt - scoriaceous, up to 1-2 m. thick; flow indicated by aligned elongate vesicles
  - 4 Suevite - containing bombs of melt up to 3 cm. diameter; unit often missing; several centimeters thick
  - 3 Breccia - fine-grained, 2-5 cm. diameter fragments; cut by glassy melt veinlets in places; the lower few centimeters locally coloured red; unit missing in places; 3-25 cm. thick
  - 2 Breccia - very coarse-grained, fragments 20 cm. diameter and up; mostly in situ fractures in country rock
  - 1 Country Rock - massive
- 

The complete stratigraphy is visible at only some locations and seems to be quite variable in detail. Table lists the main features and those common to all localities.

(i) glassy fine-grained melt with numerous inclusions, (ii) fine-grained micro-porphyrific melt with numerous inclusions, (iii) fine to medium-grained poikilitic melt with few recognizable inclusions. These divisions represent a continuum with no sharp boundaries. The whole melt sequence can be considered a single unit with subordinate amounts of the more glassy and fine-grained varieties at the base grading upwards to the fine to medium-grained poikilitic melt [unit(iii)] which forms the bulk of the unit. This melt consists of poikilitic pigeonite and laths and tabular crystals of plagioclase [An<sub>65-34</sub>] in a light brown interstitial glass with some opaques and apatite (Grieve, 1975). Distinctive features of the melt in outcrop are the development of vesicles close to the base of the melt, even to the extent of development of a scoriaceous texture in places and the rare occurrence of pure unaltered homogeneous glass at the basal contact of the melt.

### 2.3 Geochemical Appraisal of the Impact Melt

If the melt rock was formed by impact melting of the country rocks, its composition should reflect the mixing of different proportions of the local country rocks. To demonstrate the reality of such a process it is necessary to obtain a representative suite of the relevant country rocks and compare their composition with that of



the melt rock. To do this, a large number of samples: 7 anorthosites, 27 adamellites, 19 mangerites and 40 melt rocks, were analysed for major and trace elements (Appendix E). The samples analysed were predominantly from the islands within the lake and the area immediately surrounding the lake (sample locations - Appendix E) but some samples were also obtained from Taylor's (1970, 1972) mapping project of the whole batholith.

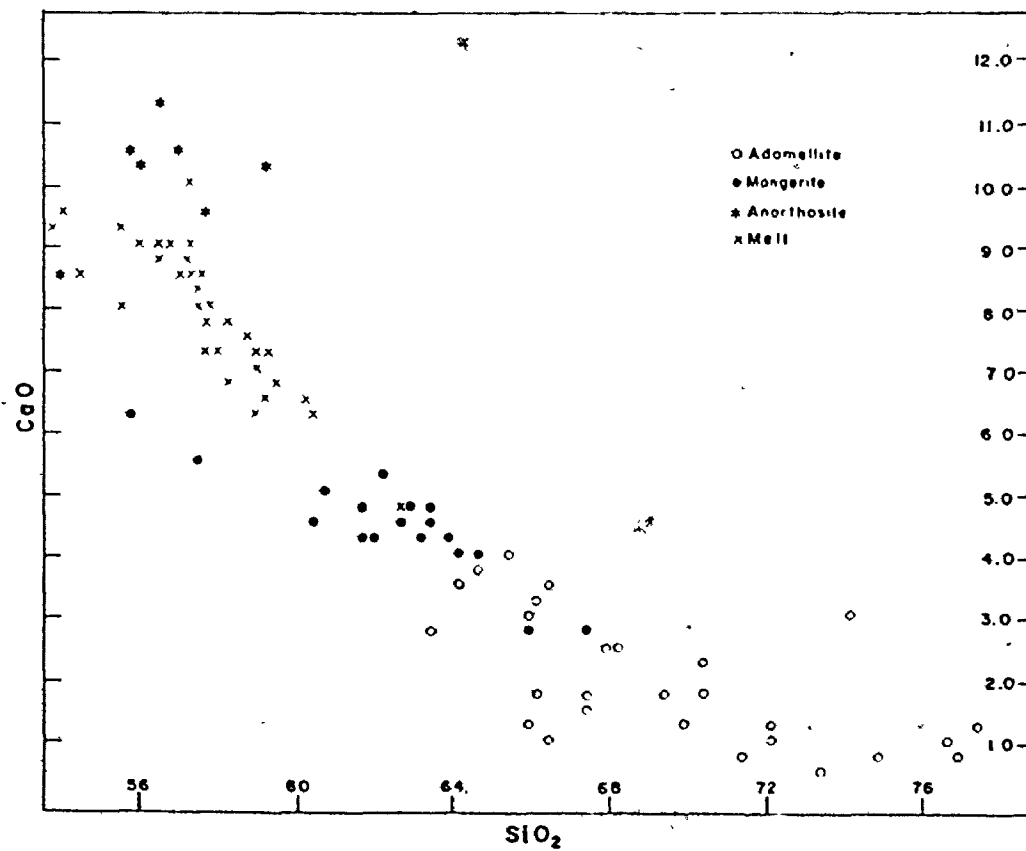
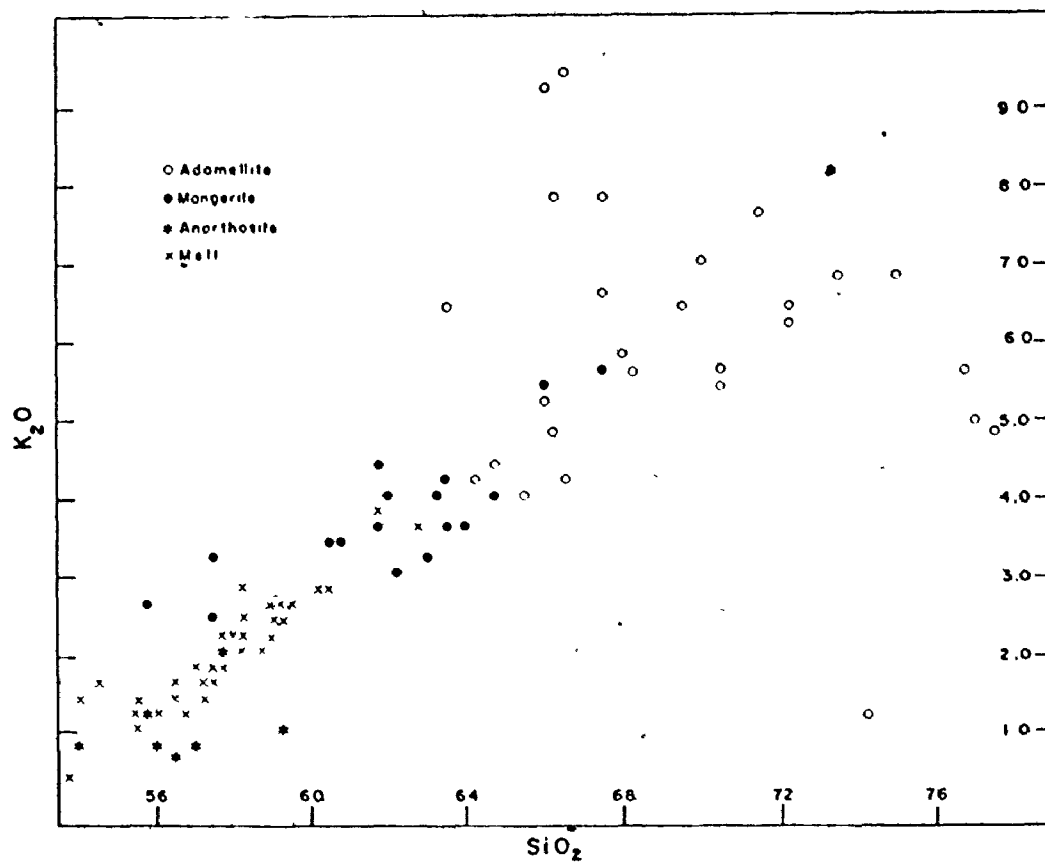
As mentioned earlier, the contact relationships between the various country rocks are indistinct and in some cases gradational; therefore, the distinction between the adamellites and the mangerites was based on Currie's (1971b) observation that the mangerites are significantly higher in  $MnO$ ,  $TiO_2$  and  $P_2O_5$  and lower in Rb than the adamellites. The gradational nature of the Adamellite-Anorthosite suite and the inhomogeneity of the adamellite is shown on the  $K_2O-SiO_2$  and  $CaO-SiO_2$  variation diagrams (Fig. 2-3a,b)

The anorthosite and melt rocks are also plotted on these diagrams (Fig. 2-3). The position of the melt along the linear trend between the anorthosite and mangerite groups indicates that it could be a mixture of anorthosite and mangerite. It is not possible to say whether adamellite is necessary to form the melt but this is a possibility. Similarly, Grieve (1975) notes that from his microprobe analyses of the melt matrix and Currie's (1971b) country rock

Figure 2-3.

A -  $K_2O$  -  $SiO_2$  variation diagram of impact melt  
and country rocks. [weight percent]

B -  $CaO$  -  $SiO_2$  variation diagram of impact melt  
and country rocks. [weight percent]



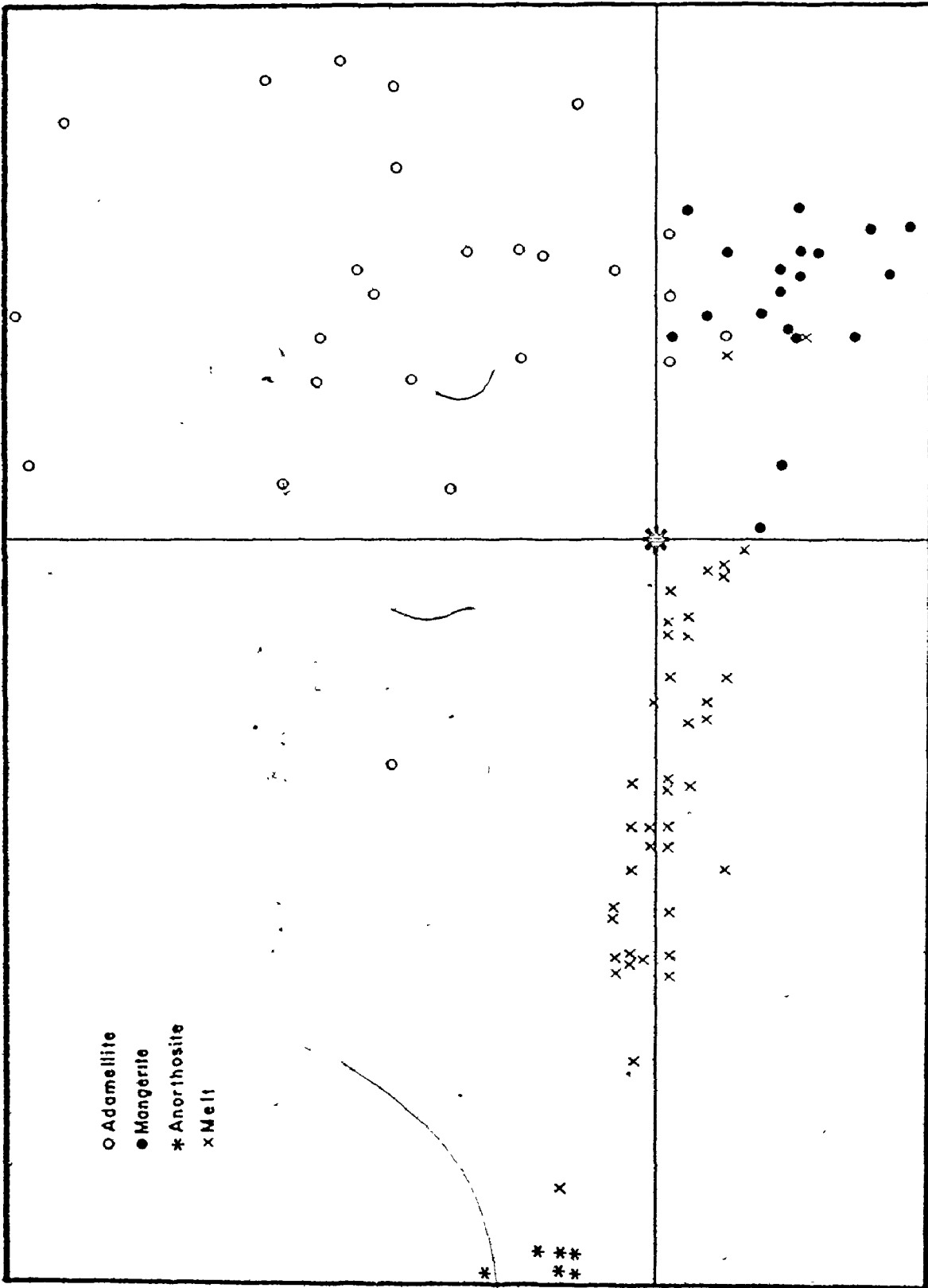
analyses, mixing of varying proportions of country rocks could give rise to the melt compositions.

Correspondence analysis, a form of factor analysis (David, 1973; Teil, 1975; Appendix D) has been used to evaluate the process of impact melting by means of a data base which incorporates the ten trace elements; Nb, Zr, Y, Sr, Rb, Th, Pb, Zn, Cu, and Ni. Q-mode analysis was used to detect patterns and relationships between the different rock units utilizing the computer program of David and Beauchemin (1974).

The results of this analysis are displayed as a factor diagram, a binary plot of factor 1 vs. factor 2 (Fig. 2-4). The factors are combinations of the trace elements (Table 2-2) with factors 1 and 2 accounting for 94% of the trace element variation in the data base. The factor diagram (Fig. 2-4) can be considered as a petrographic variation diagram showing the variation of the samples for the ten trace elements. The same data could be presented as 45 binary trace element variation diagrams but the factor plot is more efficient since it condenses the same data to a single diagram, the plane of factor 1 and 2 in ten dimensional space on which the sample points are projected.

A visual inspection of the factor diagram shows distinct groupings of the different rock units. It is

Figure 2-4. Correspondence analysis factor plot for the analysed rocks from the Mistastin Lake crater area. \* symbol indicates the zero point or center of the plot.



FACTOR 2

FACTOR 1

TABLE 2-2  
Correspondence Analysis Results

| Contribution of each factor to total variation among samples |       |       |      |     |
|--|-------|-------|------|-----|
| Factor:  | 1     | 2     | 3    | 4   |
| Percent(%)   | 74.26 | 19.60 | 2.89 | .96 |

Cumulative percent of Factors 1 + 2 : 93.86%

| Element | Factor 1<br>*CA(%) | Factor 2<br>*CA(%) |
|---------|--------------------|--------------------|
| Nb      | 2.28               | .07                |
| Zr      | 28.85              | 16.57              |
| Y       | 2.10               | .06                |
| Sr      | 55.30              | .46                |
| Rb      | 8.71               | 64.52              |
| Th      | .61                | 3.02               |
| Pb      | 1.51               | 7.10               |
| Zn      | 1.10               | 6.57               |
| Cu      | 2.48               | .05                |
| Ni      | .05                | 1.57               |

\*CA - Absolute contribution of element to dispersion  
along each factor.

the relationship between these groups that demonstrates the process of impact melting and indicates which rock types were involved. The melt rocks occupy a well-defined linear grouping on the factor diagram between the anorthosite group and the mangerite group. This grouping is interpreted as the result of the linear mixing of two end-members, anorthosite and mangerite, to produce the impact melt. Each melt sample is formed from slightly different proportions of the two rock units. This also indicates that the process of impact melting tends to homogenize the product but that the process is not complete. Even the mechanical mixing that results from the outward flow of particles and melt from the center of the crater fails to achieve complete homogenization. It appears that rapid cooling has locked in the inhomogeneity and since the diagram shows no discernible evidence of fractional crystallization, it has apparently inhibited this process. Grieve (1975) reached virtually the same conclusion on the basis of petrography and defocused beam microprobe analyses of the matrix of the melt rock.

The adamellite group is seen to be very inhomogeneous, compositionally overlapping the mangerite, a result not unexpected for two comagmatic rock types. As a consequence, the impact melt does not require material of average adamellite composition but it could easily have an adamellite component of extreme composition, one close enough in



composition to mangerite as to be indistinguishable geochemically.

#### 2.4 Least Squares Mixing Model

The results of the correspondence analysis indicate that it would be appropriate to calculate a mixing model for the origin of the impact melt. Averages of the trace elements for each of the rock types were calculated (Table 2-3) and used in a least squares mixing calculation (Bryan et al., 1969; Wright & Doherty, 1970).

The results (Table 2-4) show that the average melt can be made up of 38% mangerite and 60% anorthosite with less than 2% adamellite. The goodness of fit of the mixing model can be judged by the use of the residual factor which is the difference between the observed and the calculated composition of the melt divided by the standard deviation of the element in the melt rocks. A value of 1.0 or less indicates a perfect fit to the model (Schonfeld & Meyer, 1972). The calculated model for Mistastin Lake is a perfect fit by this criterion as no residual factor is greater than 1.0 (Table 2-4).

The extremely low amount of adamellite required by the model may seem a bit surprising at first when the amount of adamellite in the area is so great. However, the rocks that were melted came from the central portion of the lake

TABLE 2-3  
Average Trace Element Compositions of Rock Units

|                           | Adamellite |                            | Mangerite |       | Anorthosite |      | Melt  |       |  |
|---------------------------|------------|----------------------------|-----------|-------|-------------|------|-------|-------|--|
|                           | Av.        | S.D.                       | Av.       | S.D.  | Av.         | S.D. | Av.   | S.D.  |  |
| Nb                        | 26.2       | 8.4                        | 22.2      | 17.5  | 0.3         | 0.5  | 8.5   | 6.0   |  |
| Zr                        | 736.1      | 129.0                      | 474.3     | 244.2 | 21.8        | 14.5 | 294.5 | 141.5 |  |
| Y                         | 52.9       | 14.3                       | 40.4      | 27.0  | 4.3         | 2.9  | 23.1  | 8.6   |  |
| Sr                        | 315.7      | 62.2                       | 256.6     | 96.5  | 736.1       | 25.4 | 559.4 | 95.0  |  |
| Rb                        | 68.3       | 8.0                        | 161.4     | 58.0  | 10.0        | 9.7  | 32.9  | 15.1  |  |
| Th                        | 8.0        | 3.4                        | 22.1      | 41.9  | 1.0         | 0.8  | 5.4   | 2.1   |  |
| Pb                        | 24.0       | 4.1                        | 38.4      | 10.8  | 4.6         | 2.2  | 11.7  | 4.5   |  |
| Zn                        | 139.0      | 37.2                       | 64.4      | 34.9  | 24.5        | 12.7 | 71.9  | 25.1  |  |
| Cu                        | 1.5        | 4.9                        | 0.0       | --    | 19.3        | 15.9 | 9.2   | 4.4   |  |
| Ni                        | 20.6       | 7.4                        | 26.3      | 13.1  | 23.6        | 16.7 | 23.4  | 8.5   |  |
| Number                    | 27         |                            | 19        |       | 7           |      | 40    |       |  |
| S.D. - standard deviation |            | Number - number of samples |           |       |             |      |       |       |  |

TABLE 2-4  
Mistastin Lake Mixing Model

| Proportions of components used to form average melt |       |          |  |
|---|-------|----------|--|
| Adamellite  | 0.14  | + 1.77 % |  |
| Mangerite   | 38.26 | + 1.19 % |  |
| Anorthosite   | 59.55 | + 0.24 % |  |

|    | Calculated<br>Composition | Residual | Residual<br>Factor |
|----|---------------------------|----------|--------------------|
| Nb | 10.2                      | 1.7      | .28                |
| Zr | 295.3                     | .8       | .01                |
| Y  | 22.9                      | - .2     | .03                |
| Sr | 559.5                     | .1       | .00                |
| Rb | 32.3                      | - .6     | .04                |
| Th | 3.7                       | -1.7     | .82                |
| Pb | 12.0                      | .3       | .06                |
| Zn | 67.9                      | -4.0     | .16                |
| Cu | 12.1                      | 2.9      | .65                |
| Ni | 22.0                      | -1.4     | .17                |

Residual Factor: [Residual/S.D. of melt]; this factor should be less than 1.0 for a perfect match.

and the geology of the central uplift along with that of the shoreline indicates that the rocks from the zone of melting would have been anorthosite and mangerite with only a small proportion of adamellite. It is also important to realize that in the mixing model the adamellite is an average of an inhomogeneous group of rocks. It is quite conceivable that a large proportion of the adamellite which was melted was of a composition closer to that of the mangerites. The most significant conclusion obtained from the mixing model is that a large amount of anorthosite is required to form the average impact melt.

Other mixing models have been calculated using major element compositions (Currie, 1971b) and microprobe analyses of the various melt types (Grieve, 1975). However, these calculations have used the data of Currie (1971b) for the country rock compositions and this consists of only nine chemical analyses. The discrepancies between the various results may in part be due to this small data base. Grieve (1975) calculates mixtures of 67-71% anorthosite, 32-47% mangerite and 0-14% adamellite to form the various melt types. While these results are not exactly like those in Table 2-5, they are really quite similar since they do point out the predominance of anorthosite and the small amount of adamellite required to form the impact melt.

## 2.5 Geochronology and Sr Isotopic Geochemistry

Since impact melting is the total fusion of the target rocks without the significant addition of new (Rb-Sr) components, Sr isotopes are ideal tracers to document the process. As long as the Rb-Sr system remains closed during the melting, though it may tend to become homogenized, the melt rock data points should fall on the target rock isochron. Since there is usually a considerable time difference between the age of formation of the target rocks and that of the impact melt, the fact that the melt maintains the older Rb-Sr age of the target rocks is anomalous with respect to the true age of the melt. This demonstrates that a closed Rb-Sr system was maintained during impact melting. At Mistastin Lake there are two isotopically different rock units, the granitic rocks (adamellite and mangerite) and the anorthosites. If the impact melting affected only the granitic rocks then the melt data points should fall on the existing granite isochron. However, if both the anorthosite and granitic rocks were involved in the melting, then the melt points would fall along a mixing line joining the anorthosites and an average granite point on the granite isochron.

Rb/Sr ratios were determined by X-ray fluorescence spectrometry to a precision of better than 2% (1s). Standard techniques (Appendix A) were used in the chemical

extractions and mass spectrometric determinations of  $\text{Sr}^{87}/\text{Sr}^{86}$  for which a precision of .046% is indicated. Fifteen replicate analyses of the NBS standard carbonate (SRM-987) gave a value of  $.7100 \pm .0003$  (1s). Isochrons were calculated according to the method of York (1966) using the  $\lambda = 1.39 \times 10^{-11} \text{yr.}^{-1}$  decay constant. All errors in the ages and initial ratios have been expressed as single standard deviations unless otherwise indicated. The data for each isochron were analysed by the statistical treatment recommended by Brooks et al. (1972) where the regression treatment of McIntyre et al. (1966) is used to evaluate whether the scatter of the data about the fitted regression exceeds the scatter predicted from the uncertainties in the analytical technique. This occurs when the Mean Square of Weighted Deviates [MSWD] is greater than the F-ratio. In only one case is the MSWD greater than the F-ratio (Table 2-6) but here the difference is so small that, for practical purposes, it is considered the data fits an isochron.

The age of impact is  $40.8 \pm 2.5$  m.y. as determined on a suite of melt samples by the  $\text{Ar}^{39}/\text{Ar}^{40}$  step heating dating method (Mak, 1973). This is the youngest event in that area of the Shield where no rocks are younger than Precambrian. The granitic rocks, adamellites and mangerites (Table 2-5) give a combined isochron age of  $1347 \pm 15$  m.y.

TABLE 2-5  
Rb-Sr Analytical Data

| Sample      | Rb <sup>87</sup> /Sr <sup>86</sup> | Sr <sup>87</sup> /Sr <sup>86</sup> <sub>n</sub> |
|-------------|------------------------------------|---|
| ADAMELLITE  |                                    |   |
| TA-633      | .555                               | .7201; .7201                                    |
| BT-143      | 1.978                              | .7447; .7454                                    |
| TA-606      | 3.158                              | .7665; .7666; .7663                             |
| TA-678      | 4.935                              | .8012; .8005; .8013                             |
| TA-729      | 5.849                              | .8196   |
| TA-601      | 6.483                              | .8315; .8316                                    |
| MANGERITE   |                                    |   |
| TA-609      | .295                               | .7136; .7128                                    |
| LM-32       | .317                               | .7133; .7141                                    |
| LM-56D      | 1.054                              | .7283; .7282                                    |
| ANORTHOSITE |                                    |   |
| 11318       | .014                               | .7039   |
| LM-33A      | .014                               | .7038   |
| TA-707      | .025                               | .7050   |
| LM-29G      | .030                               | .7043   |
| LM-51B      | .036                               | .7047; .7048                                    |
| LM-29A      | .109                               | .7071   |

n = normalized to Sr<sup>86</sup>/Sr<sup>88</sup> = .1194

TABLE 2-5 cont'd

| Sample   | Rb <sup>87</sup> /Sr <sup>86</sup> | Sr <sup>87</sup> /Sr <sup>86</sup> <sub>n</sub> |
|--|------------------------------------|---|
| MELT   |                                    |   |
| LM442C   | .009                               | .7047   |
| LM-34C   | .043                               | .7055   |
| LM-51Z   | .065                               | .7054   |
| LM-45A   | .079                               | .7065   |
| LM-41M   | .099                               | .7048; .7055                                    |
| LM-44A   | .132                               | .7068   |
| LM-57  | .137                               | .7074; .7077                                    |
| LM-38A   | .163                               | .7084   |
| LM-55A   | .178                               | .7076   |
| LM-7-A   | .212                               | .7095   |
| LM-38C   | .237                               | .7095   |
| LM-7-B   | .244                               | .7096   |
| LM-6   | .261                               | .7101   |
| TA-T30   | .286                               | .7106   |
| LM-F-1   | .498                               | .7160   |
| n = normalized to Sr <sup>86</sup> /Sr <sup>88</sup> = .1194 |                                    |   |



(1s) (Table 2-6; Fig. 2-5d). The adamellite and the mangerite were also regressed separately (Table 2-6; Fig. 2-5a,b), but considering: (1) the lack of Rb/Sr variation in the mangerites, (2) that the isochrons overlap within two standard deviations of the ages, (3) that geologically the rocks are both units of the same intrusive body, it seems reasonable to interpret the 1347 m.y. age as that of intrusion of the pluton. The high initial ratio [.7082] of the granitic rocks indicates that the granitic magma was derived from remobilized lower crust or at least had a significant component of crustal contamination. Some zircons from another adamellite pluton associated with the Nain anorthosite, 115 Km. to the east of Mistastin Lake, have turbid cores which are remnants of earlier formed zircons. This suggests that there was a component of contamination in that magma (Krogh & Davis, 1973).

The anorthosite samples have such a small range of  $Rb^{86}/Sr^{87}$  ratios (Fig. 2-6a) that an isochron cannot be calculated. The  $Sr^{87}/Sr^{86}$  values of the anorthosite samples are considerably lower than the initial ratios of the granitic rocks (Fig 2-6b) indicating that the two rock units were not part of the same Rb-Sr system. This is in agreement with the field relations which often show the adamellite cutting anorthosite, perhaps an indication of

TABLE 2-6

## Rb-Sr Regression Results

| ISOCHRON              | N* | AGE  | +/- | IR    | +/-   | MSWD | F-ratio |
|-----------------------|----|------|-----|-------|-------|------|---------|
| Mangerite             | 3  | 1409 | 57  | .7074 | .0004 | .03  | 4.26    |
| Adamellite            | 6  | 1318 | 17  | .7095 | .0005 | 1.32 | 2.78    |
| Pluton                | 9  | 1347 | 15  | .7082 | .0003 | 2.48 | 2.42    |
| Melt                  | 15 | 1605 | 58  | .7043 | .0002 | 1.27 | 2.16    |
| Melt +<br>Anorthosite | 21 | 1684 | 61  | .7041 | .0001 | 1.61 | 2.06    |

\* N = number of data points regressed

+/- = one standard deviation (1s)

F-ratio for 24 replicates at the 95% confidence level (Brooks et al., 1972)

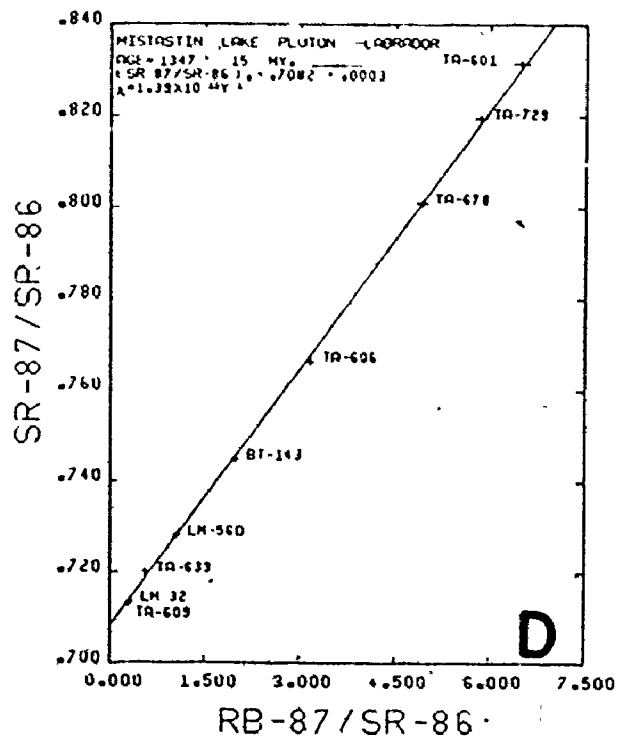
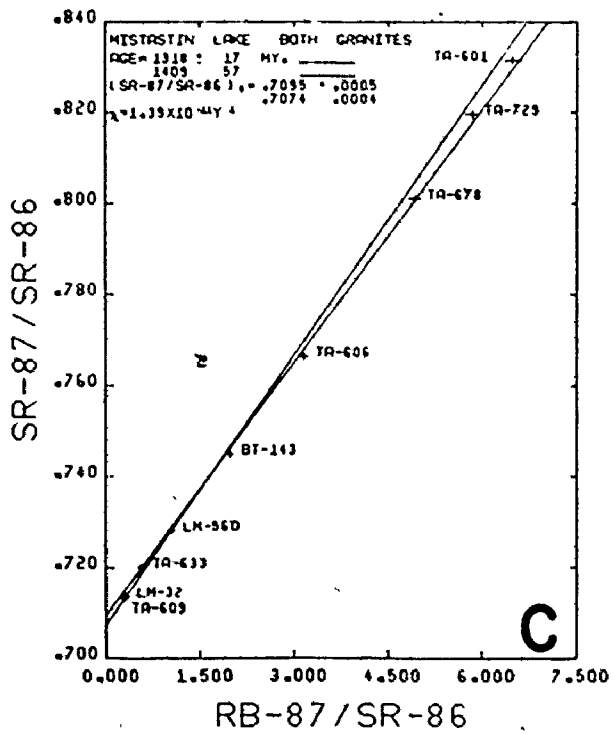
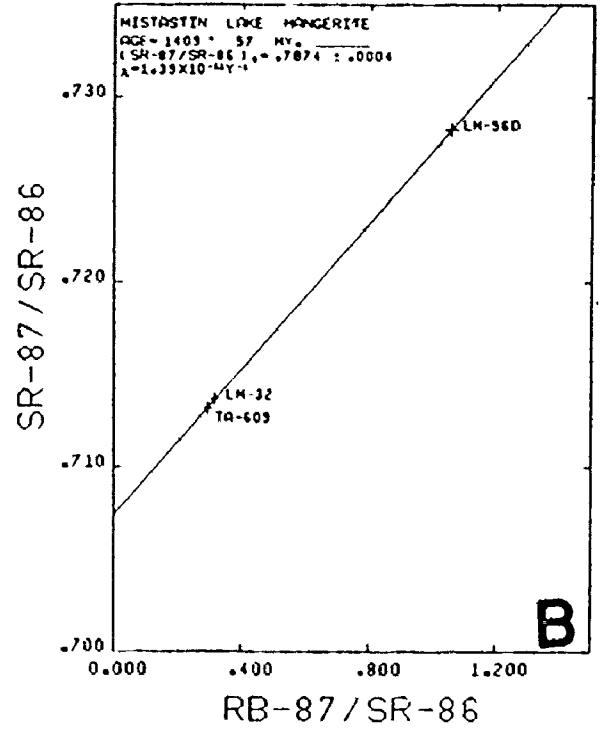
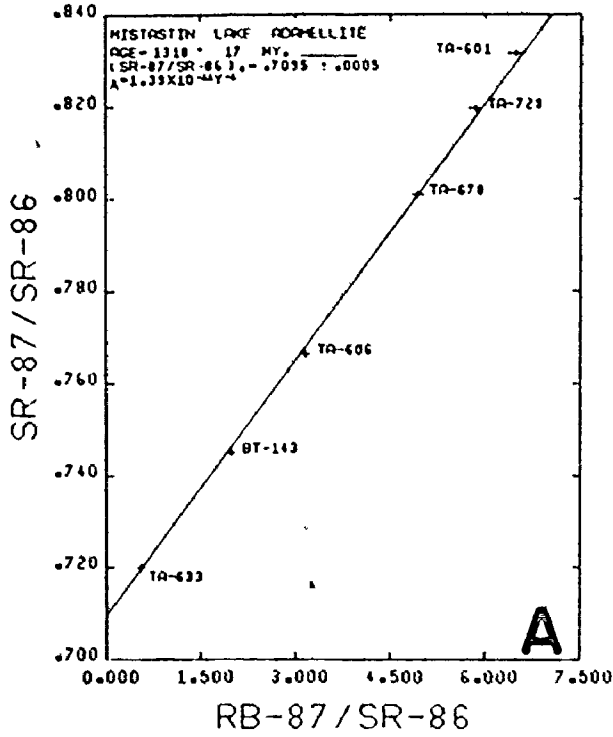
Errors used in isochron calculation:  $Rb^{87}/Sr^{86} = 2.0\%$  ;  $Sr^{87}/Sr^{86} = .046\%$

AGE in m.y.

IR = Initial Ratio ( $Sr^{87}/Sr^{86}$ )<sub>0</sub>

Figure 2-5. Country rock isochrons from Mistastin Lake, Labrador. All errors given at the one sigma (1s) level.

- A - The adamellite isochron.
- B - The mangerite isochron.
- C - Adamellite and mangerite isochrons plotted together.
- D - The isochron generated by the combined adamellite and mangerite samples.



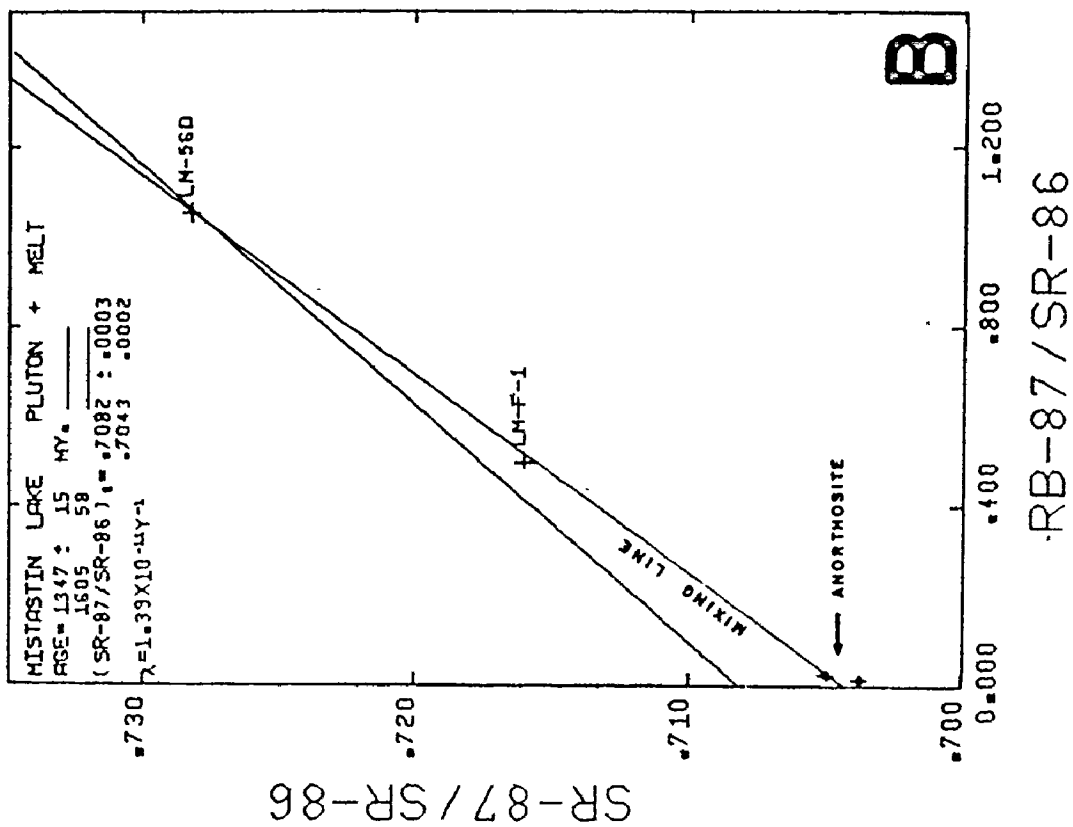
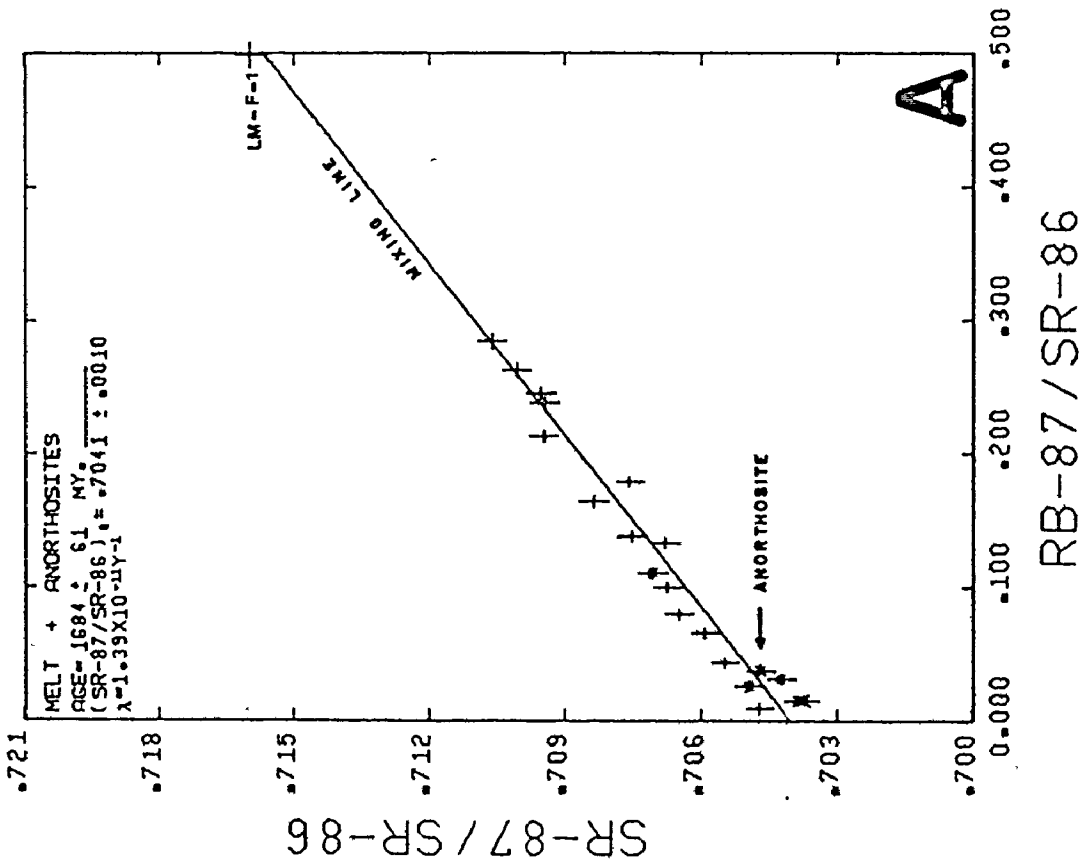
two separate magmas.

The fifteen samples of impact melt form a statistically perfect line of 1605 m.y. according to the MSWD < F-ratio criterion of Brooks et al. (1972) (Table 2-6). If the anorthosite samples are also included in the isochron calculation, the perfect line is still retained. The 1605 m.y. age for the melt rock isochron is an impossible age since the melt's K-Ar age is known to be 41 m.y. (Mak, 1973) and the melt is geologically younger than the pluton which is 1347 m.y. old. However, the linear relationship does fit a mixing model that makes the melt isochron a mixing line joining the locus of anorthosite data points and the average granite. This is a demonstration that the impact melt is a mixture of these two different Rb-Sr systems and that the spurious age of 1605 m.y. can be used to fingerprint the phenomenon.

The variation of  $\text{Rb}^{87}/\text{Sr}^{86}$  in the melt rocks can be attributed to different proportions of anorthosite component involved in the melting episode for each specific sample. The anorthosite exerts a large influence on the isotopic character of the melt due to its high Sr content. The melt rocks fall within the lower 30% of the mixing line but since the anorthosite has about twice as much Sr as the granitic rocks, the melt represents a mixture of about 60% anorthosite and 40% granite. This is comparable to the

Figure 2-6. Mixing lines showing the relationships of the anorthosite and melt samples. All errors given at the one sigma (1s) level.

- A - Regression [mixing] line calculated for the anorthosite and melt samples.
- B - Regression [mixing] line calculated for the melt only. Diagram shows the location of the anorthosites; only two are plotted for clarity. Isochron for the pluton is also plotted. Sample LM-F-1 has the highest  $Rb^{87}/Sr^{86}$  of the melt rocks. LM-56D is a mangerite sample on the pluton isochron plotted to show the position of line intersection.



proportions calculated (Table 2-4) for the mixing model from the trace element data.

## 2.6 Conclusions

The Mistastin Lake crater has proved to be an extremely favourable example of impact melting in that the unaltered nature of the melt combined with a simple country rock geology has allowed precise geochemical documentation of the impact process. This has not been possible at any other large complex terrestrial crater to date. The presence of anorthosite at the impact site is favourable because its geochemistry contrasts markedly with the granitic rocks. It has been shown that there are significant compositional differences between the mangerites and the adamellites but the gradational nature, the inhomogeneous geochemistry of the adamellites and the fact that the geological mapping has not been done in the greatest detail, makes it preferable to consider the impact melting as essentially a mixing of two components, anorthosites and granites. The correspondence analysis demonstrates the mixing model in 10-dimensional trace element space and the least squares mixing model places the average melt rock composition at 60% anorthosite and 40% granite. However, it must be pointed out that the melt rocks are variable enough to form a compositional trend, caused by the mixing



of different proportions of anorthosite and granite. Since the melt rocks can be explained exclusively in terms of complete melting of the local country rocks, neither fractional crystallization within the melt body nor partial melting of basement are significant or required processes.

The age of intrusion of the Mistastin Lake pluton is 1347 m.y. and that of the anorthosite is indeterminate, but based on the difference of initial Sr ratios the anorthosite and the granites are not part of the same Rb-Sr system. The melt rocks, which formed 41 m.y. ago, give a 1605 m.y. pseudo-isochron by the Rb-Sr technique showing the impossibility of an endogenic source for the melt. The 1605 m.y. line is actually a ~~mixing line~~ with anorthosite and average granite as end members and the melt rocks falling along it. The fact that the melt is not completely homogenized can be attributed to its rapid cooling and to ~~the~~ different proportions of country rocks involved in the original melting at different points in the target area.

The endogenic explosive volcanic origin for all meteorite impact craters has very few proponents. However, Currie (1971a) has advocated such an origin for the Mistastin Lake rocks. Currie considers that the areal geology, with the overwhelming predominance of adamellite, could not have been the source for the melt rocks. However, as argued in this study, the area melted by impact was contained

within the area of the lake and the geology of the shoreline and islands shows the importance of anorthosite and mangerite rather than adamellite in the formation of the melt rocks. Currie's (1971a) calculation for the best mix of country rocks to form the melt, from data on only 10 country rocks and 6 melt rocks, is 51% anorthosite, 40% mangerite and 9% adamellite, a result comparable to that obtained in this study on a more extensive data base. Currie (1971a,b) proposes that shock metamorphic features are formed by endogenic volcanism but also states "...[Currie's theory]... appeals to geological processes as yet unobserved". It is difficult to accept such an undocumented form of volcanism that seems to mimic the evolution of a meteorite crater and produce the shock features that are currently regarded as unequivocal evidence for meteorite impact (French, 1970). In fact, Currie (1971b) states that ".....presence of abundant shock metamorphic features leaves a nagging doubt of the adequacy of endogenic mechanisms". It would seem that without new evidence for volcanic origins, there really does not exist an alternative to the meteorite impact hypothesis with its ability to explain all the features found at craters.

The successful documentation of the simple geochemical process of mixing at this large complex crater allows its use as a model for other terrestrial and lunar craters. Any anomalous geochemical behaviour must be ascribed to either

complex and undocumented target geology or to post-impact  
geochemical mobility.

## CHAPTER 3

### The Sudbury Irruptive

#### 3.1 Geological Setting

The Sudbury Basin (Fig. 3-1), situated north of the town of Sudbury, Ontario, is defined by the outer ring of the Nickel Irruptive, which consists of a lower unit of norite and an upper unit of granophyre (called 'Micropegmatite') separated by a transition zone of oxide-rich gabbro (Naldrett & Kullerud, 1967; Naldrett et al., 1970, 1972). At the base of the norite is a discontinuous layer of ore-bearing sulphide-rich igneous rock containing exotic xenoliths of mafic and ultramafic cumulates called the 'sub-layer' (Souch & Podolsky, 1969), which also intrudes the country rocks as radial and concentric dykes called offsets (Fig. 3-1). Near the margin of the Irruptive, all the country rocks have been locally shattered and brecciated, forming a complex unit called the 'Sudbury Breccia' (Fairbairn & Robson, 1944; Speers, 1957). The offsets occur in areas of high concentration of Sudbury Breccia. In the Levack area, the sub-layer is in contact with a zone of highly brecciated country rock which has been named the 'grey breccia' (Greenman, 1970).

The Irruptive intrudes Archean granites, gneisses and migmatites on the North and East sides. On the South

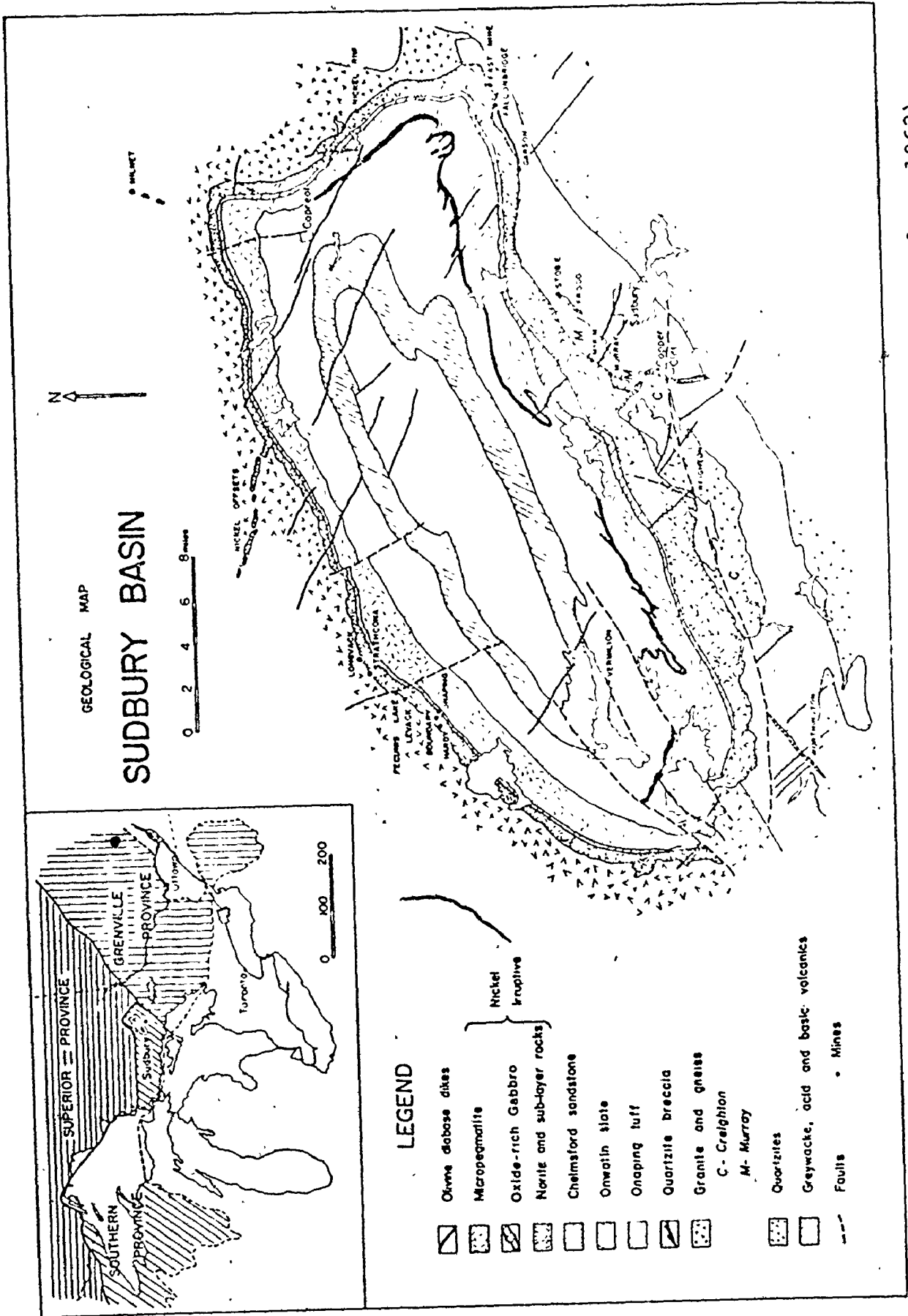


Figure 3-1. Geological Map of the Sudbury Basin (modified after Hawley, 1962).

it cuts the Huronian sequence of meta-sediments and meta-volcanics, and the Murray and Creighton granites. Overlying the micropegmatite of the Irruptive is the Whitewater group of sediments which has not been correlated with any rocks outside the Irruptive. The Whitewater group, from stratigraphic bottom to top (Fig. 3-1), consists of the Onaping Formation, a vitrophyric breccia with little or no stratification; the Onwatin Formation, a thinly bedded carbonaceous slaty shale; and the Chelmsford Formation, a carbonaceous and arenaceous proximal turbidite (Rousell, 1972; Cantin & Walker, 1972). Contacts between the units are conformable and gradational (Fig. 3-2). Late WNW trending olivine diabase dykes cut all other rocks in the area. The regional, metamorphic, and tectonic synthesis of the area has been described in Card et al. (1972) while a more restricted synthesis of the tectonics of the Irruptive region is available in Brocum & Dalziel (1974).

### 3.2 Shock Metamorphism

In 1964 Dietz and Butler discovered shatter cones in the rocks outside the Irruptive and proposed (Dietz, 1964) the meteorite impact theory for the origin of the Sudbury Irruptive. Guy-Bray et al. (1966) showed that the shatter cones are found in a zone up to 13 mi. wide around the

Irruptive. French (1967,1968,1970) described the petrographic shock features found in inclusions of basement rock in the Onaping Formation and Dence (1972) outlined the distribution of shock features in the basement rocks north of the Irruptive. These are found up to 8 Km. north of the Irruptive contact. The Onaping Formation has been interpreted as the 'fallback breccia' unit, comparable to analogous units found in other meteorite craters (Peredery, 1972a). Peredery (1972a,b) subdivided the lower Onaping Formation into several distinct units formed by impact (Fig. 3-2), including a melt rock unit which he interpreted as the remains of the impact melt. Dence (1972) suggested that there originally would have been 1200 mi<sup>2</sup> of shocked and melted rock.

### 3.3 The Upper Irruptive

A plagioclase-rich variety of micropegmatite occurring as a discontinuous band overlying the granophyric micropegmatite has been identified (Fig. 3-3) by Peredery (1972a,b) and Peredery & Naldrett (1975). The upper contact of the unit known as the plagioclase-rich micropegmatite (hereafter known as 'plagioclase micropegmatite') with the basal breccia of the Onaping Formation is sharp but sinuous. The basal breccia is intruded by numerous apophyses of the plagioclase micropegmatite, some extending for several hundred feet

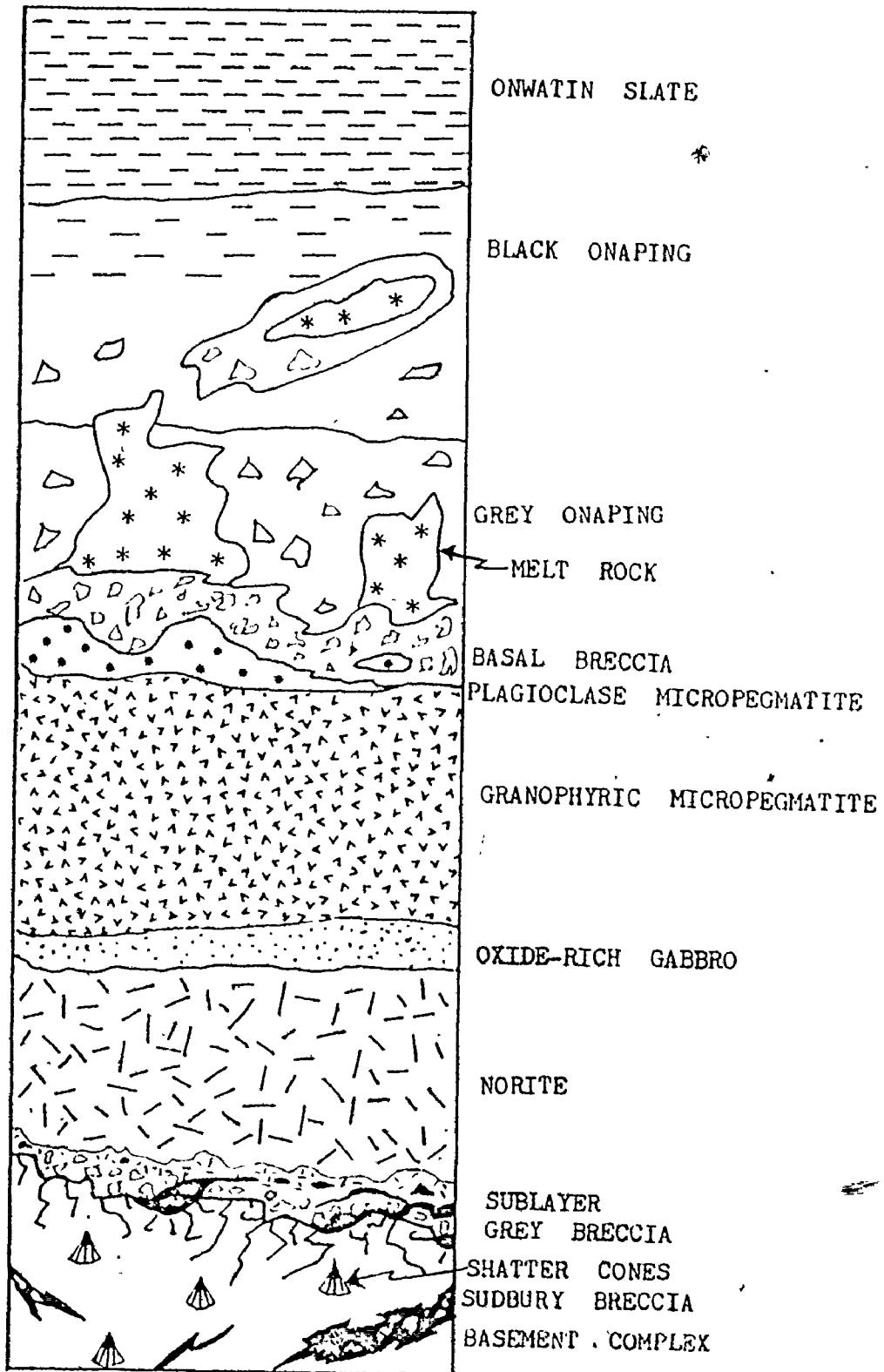


Figure 3-2. Diagrammatic representation of the contact relationships of the rock units of the Sudbury Basin (after Peredery, 1972b).



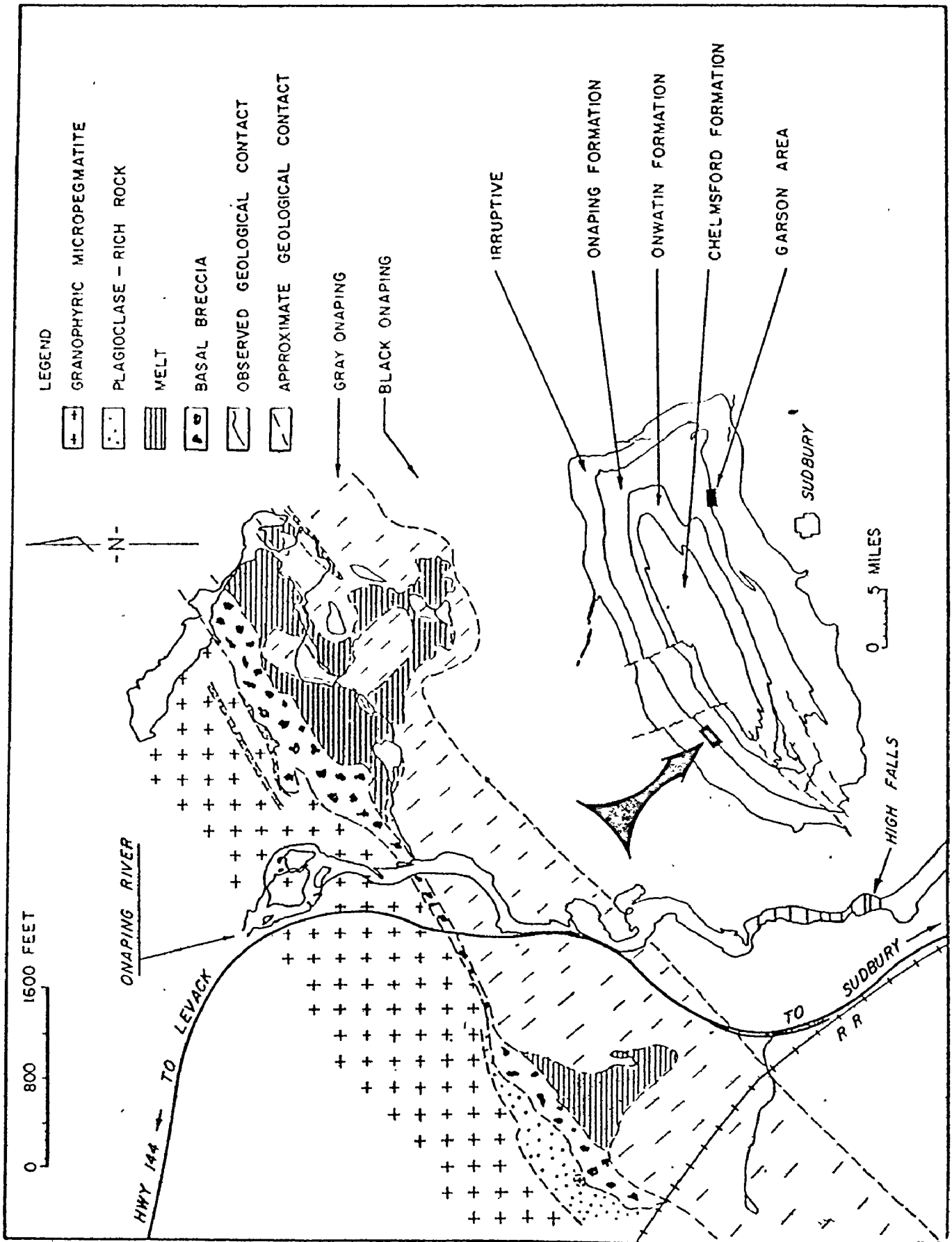


Figure 3-3. Geological Map of the upper Irruptive in the Dowling area (from Peredery & Naldrett, 1975).

into the basal breccia and there are a few inclusions of basal breccia within the plagioclase micropegmatite. The base of the unit is somewhat irregular with the thickness of the plagioclase micropegmatite varying from a few to one hundred feet (Peredery & Naldrett, 1975). It also occurs as discontinuous bands up to 100 feet thick and as blocks tens of feet in diameter, both enclosed within the granophyric micropegmatite. The contact between the two rocks is either sharp or gradational over a few feet. In places close to the basal breccia contact, the plagioclase micropegmatite is intruded by oval masses of granophyric micropegmatite approximately fifty feet in diameter. These relationships provide strong evidence for the later intrusive nature of granophyric micropegmatite into plagioclase micropegmatite (Peredery & Naldrett, 1975).

The plagioclase and granophyric varieties are distinguished on the basis of their weathering, modal mineralogy and textural features. From the detailed descriptions (Peredery & Naldrett, 1975 p.167), the main differences between these two rocks are in the variation in granophyre content (Grano. Micropeg.: 60-80%; Plag. Micropeg.: 20-40%) and the plagioclase content (Grano. Micropeg.: 5-15%; Plag. Micropeg.: 25-40%). However it is important to note that alteration has affected both rock types as illustrated by the albitization of the

plagioclase, the alteration of ilmenite to sphene and leucoxene, and the occurrence of epidote, chlorite and green amphibole (Peredery & Naldrett, 1975).

### 3.4 Chemistry of the Upper Irruptive

The relationships of the different rock units in the upper Irruptive have been examined using the trace elements Nb, Zr, Y, Sr, Rb, Th, Pb, Zn, Cu, Ni (Appendix F) with Correspondence Analysis, a type of factor analysis (David & Woussen, 1973; Appendix D), on a 72 sample data base consisting of samples of plagioclase micropegmatite, granophyric micropegmatite, fluidal glasses, melt, country rock inclusions from the Onaping Formation, basal breccia matrix and Sudbury breccia. Q-mode analysis was used to detect patterns and relationships between the samples of the different rock units.

The first four factors extracted account for 85.98% of the total variability of the samples (Table 3-1). These factors are linear combinations of variable proportions of the ten trace elements and they are used to provide a concise description of the data without significant loss of information. Binary factor diagrams can be used as a generalized petrographic variation diagram to present the interrelationships of the samples in a

single diagram for all the trace elements together. For the Sudbury rocks, a plot of factor 4 against factor 1 (Fig. 3-4; Table 3-1) provides a good separation of the different rock units where the relative relationships between the samples can be observed. The plagioclase micropegmatite can be observed to form a coherent group but with considerable scatter (Fig. 3-4). To compare the plagioclase micropegmatite to the other Irruptive units, the samples from Gibbins' (1973) traverse across the South range and those of the plagioclase micropegmatite were compared on the basis of horizontal distance from the lower contact of the Irruptive. The amount of factor 3 in each sample, as determined by correspondence analysis on the traverse samples, was used as an index of variation of all trace elements together while the concentration of Rb and Sr are also presented for comparative purposes (Fig. 3-5). These plots (Fig. 3-5) show the high degree of variability in the plagioclase micropegmatite samples as compared to the other Irruptive units and the lack of any trend from any of the other units. The Sr plot is particularly interesting. If the plagioclase micropegmatite is related to the upper gabbro (Peredery & Naldrett, 1975), the Sr, an element normally enriched in plagioclase, should be present in the plagioclase micropegmatite in a concentration similar to the upper gabbro and higher than the granophyric micropegmatite. Actually, its average composition is considerably lower than the upper gabbro and

TABLE 3-1 CORRESPONDENCE ANALYSIS RESULTS

| FACTOR   | 1     | 2     | 3     | 4     | Cumulative % |
|----------|-------|-------|-------|-------|--------------|
| Percent* | 38.17 | 20.68 | 13.87 | 13.26 | 85.98        |

\* Percent contribution of each factor to total variation among the samples.

| ELEMENT | FACTOR 1<br>#CA (%) | FACTOR 2<br>#CA (%) | FACTOR 3<br>#CA (%) | FACTOR 4<br>#CA (%) |
|---------|---------------------|---------------------|---------------------|---------------------|
| Nb      | 1.94                | .92                 | .05                 | .33                 |
| Zr      | 23.91               | 25.14               | 14.68               | 2.98                |
| Y       | .80                 | 2.54                | .16                 | .03                 |
| Sr      | 49.27               | .61                 | 8.77                | .86                 |
| Rb      | 16.11               | 61.17               | 1.28                | 6.13                |
| Th      | 1.03                | .18                 | .02                 | .00                 |
| Pb      | 1.04                | .44                 | 7.33                | 2.65                |
| Zn      | .76                 | .05                 | 48.18               | 21.08               |
| Cu      | 5.00                | .01                 | 6.55                | .01                 |
| Ni      | .15                 | 8.98                | 13.00               | 65.93               |

#CA - Absolute contribution of element to dispersion along each factor.

Figure 3-4. Correspondence analysis factor plot for the impact generated rocks from Sudbury. \* symbol indicates the zero point which is the center of the diagram. Irregular solid lines are the boundaries for the rock groups indicated by the large letter in the central portion of the enclosed area and the • symbol is a data point for that rock type.

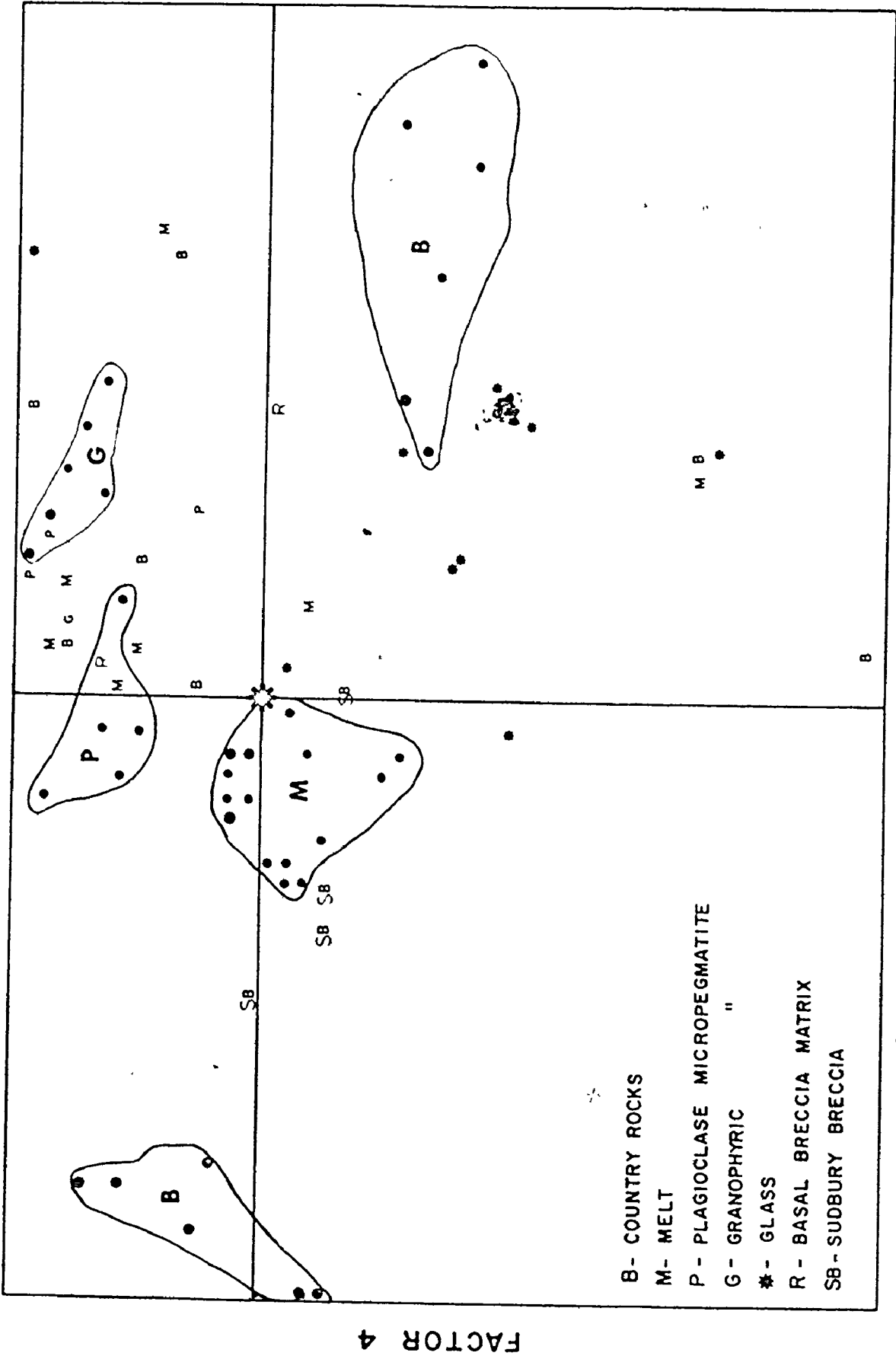
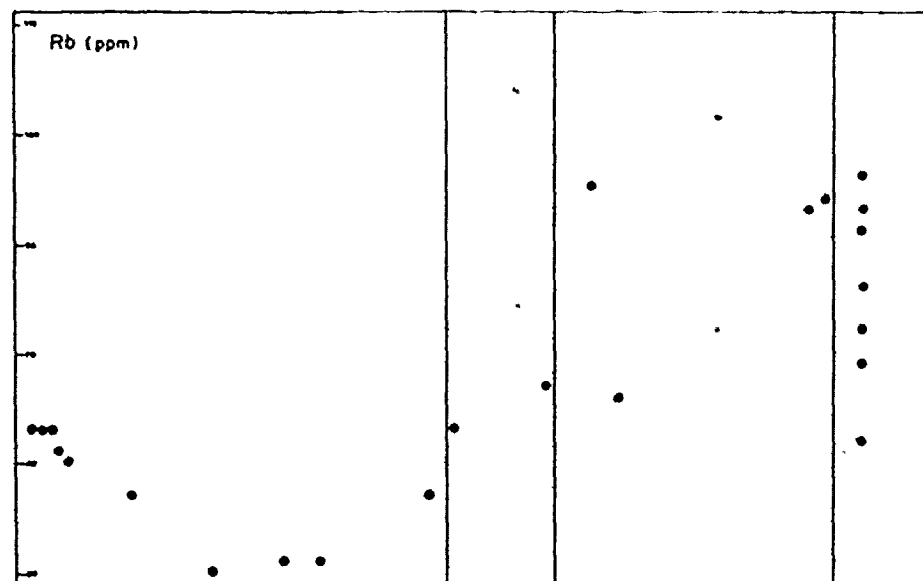
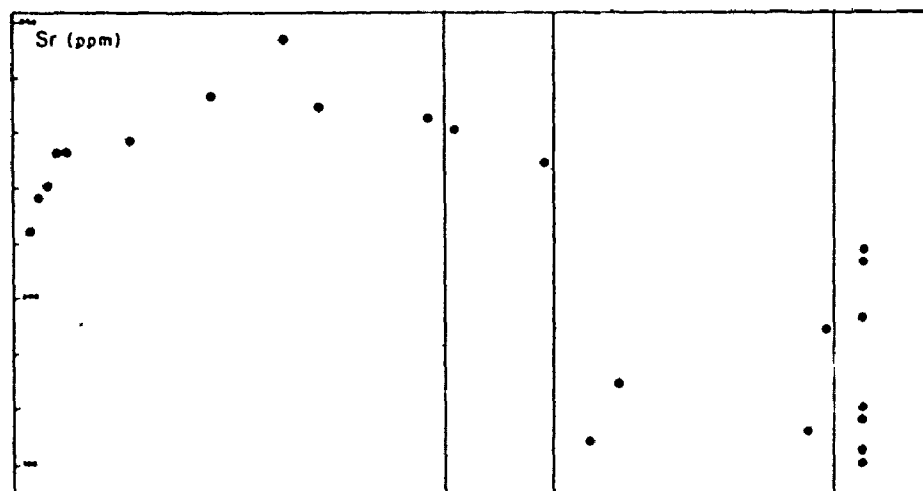
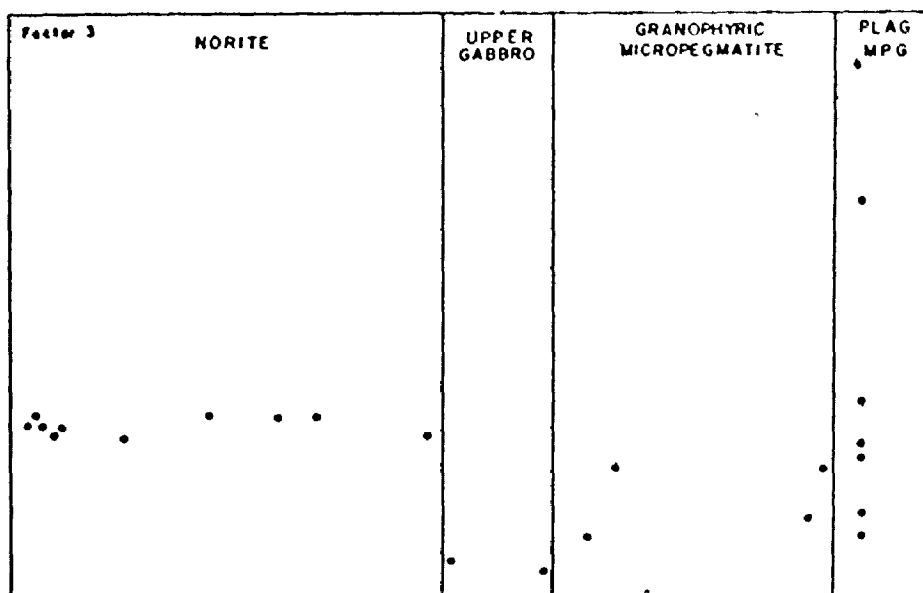


Figure 3-5. Variation in Factor 3 from correspondence analysis, Strontium, and Rubidium in the norite, upper gabbro, and granophyric micropegmatite across the South Range Blezard traverse [Fig. 3-4, Gibbins, 1973] and in the samples of plagioclase micropegmatite.





more comparable to the granophyric micropegmatite. Inspection of the modal data presented by Peredery & Naldrett (1975) shows little mineralogical similarity between the plagioclase micropegmatite and the upper gabbro and the four determinations of clinopyroxene compositions show the heterogeneity of this mineral in the unit, a factor which makes the comparison with clinopyroxene trends in the upper gabbro tenuous. The major elements also show heterogeneity in the plagioclase micropegmatite (Peredery & Naldrett, 1975, Fig. 9). It is therefore difficult to support Peredery and Naldrett's correlation of these two units since compositional heterogeneity is the outstanding characteristic of the plagioclase micropegmatite. A rock unit formed as a result of fractional crystallization would be more homogeneous than the plagioclase micropegmatite.

What then is the origin of the plagioclase micropegmatite if it is not a result of fractional crystallization from the magma that gave rise to the norite? Inspection of the factor plot (Fig. 3-4) reveals several rock groupings; especially important is the distribution of the country rock inclusions as the most extreme members of the sample population. The country rock groupings do not reflect a particular rock type since the granite, gneiss, quartzite and arkose

samples are distributed within both country rock groupings and throughout the dispersed samples. The melt rocks tend to lie grouped near the center of the diagram where the average sample of the population plots. It would therefore be reasonable to interpret them as some mixture of the country rocks. The plagioclase micropegmatite forms a scattered group near a more homogeneous granophyric micropegmatite grouping. It is difficult to establish a definitive interpretation of the plagioclase micropegmatite based on the trace element data but it should be noted that because the country rocks fall to the extreme of the diagram, all other groups could conceivably be formed from mixtures of the appropriate country rocks. This very likely is the origin of the plagioclase micropegmatite since its heterogeneity can be interpreted as arising from incomplete homogenization of a diverse source (eg. the country rocks). It also agrees with the hypothesis of Dence (1972) that the plagioclase micropegmatite is an impact melt.

### 3.5 Basal Breccia

The basal breccia (Peredery, 1972a) occurs as a discontinuous band up to 400 feet wide at the base of the Onaping Formation and is equivalent to the South range 'Quartzite Breccia' (Stevenson, 1961). The upper contact

of this unit is sharp but irregular and can be either with the Grey Onaping or with melt rock bodies. The matrix of the breccia is of quartzofeldspathic composition with minor chlorite, epidote, sphene and in rare spots, quartz pseudomorphs after tridymite. It is inhomogeneous in composition with an hypidiomorphic granular texture. The various country rocks including granites, gneisses, quartzites, arkoses, and cherts form the fragments which vary in size from a few inches to three feet, and in rare cases up to 100 feet in diameter. The fragments show abundant shock features including deformation lamellae and spherulitic devitrification textures, and rarely, quartz pseudomorphs after tridymite.

In the past the basal breccia has been identified as a quartzite conglomerate (Bell, 1891), as the Trout Lake conglomerate of Coleman (1905), a pyroclastic rock (Burrows & Rickaby, 1929), rhyolite (Williams, 1956), pelean domes (Thompson, 1956), and quartzite breccia (Stevenson, 1961). Peredery (1972b) interprets the basal breccia as a shock breccia that was subjected to hydrothermal alteration by emanations from the underlying micropegmatite. The disparate locations of the basal breccia matrix samples on the factor diagram (Fig. 3-4), one close to the plagioclase micropegmatite and the other isolated but tending towards one group of country rocks may support Peredery's (1972 a,b) observations of inhomogeneity and possible metasomatic

alteration, but it is difficult to be definitive on the basis of only two samples.

### 3.6 The Onaping Formation

The Onaping Formation is a 4500 foot thick sheet of fragmental and vitrophyric material that has been divided into the lower Grey Onaping and the upper Black Onaping (Peredery, 1972a). All the glass fragments in the Onaping have been devitrified or recrystallized. The Grey Onaping consists of abundant country rock fragments and large bombs and fragments of fluidal glass in a very fine-grained grey to grey-green matrix. The transition to Black Onaping is a gradual increase in the amount of carbonaceous material which imparts the black colour to the rock. There are a few country rock fragments in the lower part of the Black Onaping but these decrease progressively upwards in abundance and size. The Black Onaping has a crude bedding developed in the upper portion where it grades into the Onwatin Formation. The sedimentary character of the Onaping Formation suggests that it has accumulated very quickly (Peredery, 1972a,b; Beales & Lozej, 1975).

There are five major groups of country rock fragments in the Onaping, basal breccia and melt bodies (Peredery, 1972b). Metasediments, which comprise 60-80% of the fragments,

consist of quartzites, arkoses, cherts and argillites. Equal proportions of granites and gneisses form 10-30% of the fragments while the remaining two groups, which are uncommon, are basic rocks (diabases and amphibolites) and fragments of microbreccia. The country rock fragments have abundant shock metamorphic features (French, 1967, 1968, 1972), the most common of which include multiple planar elements of the decorated variety in quartz and feldspar, plastically deformed feldspar, devitrification textures in some feldspars indicating a previous glassy state and the development of granophyre along grain boundaries in highly shocked fragments (shock melting). In some of the fragments the habit of the quartz suggests pseudomorphism after tridymite, in other cases probably after glass (Peredery, 1972b). Peredery (1972b) suggests that the chert fragments may be completely recrystallized fragments of quartzite that have been shock melted.

There are three main types of (devitrified) glasses in the Onaping Formation; complex inhomogeneous glasses varying in composition, texture, and colour (shades of grey, green and blue); fluidal glasses showing colour banding of grey and green; black chloritized glasses consisting only of black chlorite. Some of the glasses are bomb-shaped and flow textures are common in all (Peredery, 1972b).

### 3.7 Chemistry of the Glasses and Country Rocks

Peredery (1972a) discusses the major element chemistry of the glasses from the Onaping Formation. Many glasses are alkaline in composition and some are nepheline and corundum normative while others are silica saturated. Soda is enriched in some (up to 10%) and others show potash enrichment (up to 13%). The glasses cover a very wide compositional field (Fig. 3-6) in an apparently random fashion. The scatter of the glasses on the factor diagram (Fig. 3-4) is an indication of their trace element inhomogeneity. The glasses seem to form no trend or association with any particular rock group and do not form their own grouping, though they can obviously be formed by melting of the appropriate country rocks or combinations thereof.

The country rocks, a combination of quartzites, granites and gneisses (Appendix F), form two main groups on the factor diagram (Fig. 3-4) with seven samples lying outside the main groupings. The different country rock types do not seem to partition to any specific group, so the diagram illustrates the high variability of these rocks for the ten trace elements. Since the samples are nearly all inclusions in the Onaping Formation it is very likely that they are representative of the rocks melted by the impact. However, they may also have been affected

by any post-impact events that occurred.

### 3.8 The Melt Rocks

The melt rocks (Peredery, 1972a,b) are irregular bodies of felsic composition occurring on top of the basal breccia and projecting into the Onaping Formation. The bodies have a massive and fine-grained character and contain abundant country rock inclusions that have planar features in their quartz and feldspar. Margins of the melt bodies are chilled or chill-brecciated and commonly show flow banding. Some bodies have dyke-like apophyses with flow lines, and extend up to 100 feet into the Onaping Formation. Melt bodies show diverse contact relationships with the basal breccia. Some are totally enclosed in basal breccia and others contain inclusions of basal breccia. Still other bodies are in sharp contact with plagioclase micropegmatite where it intrudes the basal breccia.

Peredery, (1972b) has distinguished two facies of melt bodies: a chilled marginal phase showing evidence of devitrification, such as spherulites of feldspar and acicular pyroxenes, and the main portion of a typical melt body, termed the crystalline melt, and interpreted as having crystallized from a liquid. The original mineralogy consisted of highly varying proportions of quartz, plagioclase, and clinopyroxene with minor opaques and



orthoclase. However, there is abundant evidence of alteration in that the plagioclase is now albite, the pyroxene converted to chlorite and/or green amphibole, and epidote and chlorite are dispersed throughout the rock. Peredery (1972b) pointed out that the plagioclase commonly occurs in sheaf-like and radial patterns and that the mafics exhibit radial patterns, always in acicular habit. Peredery (1972a,b) interprets these textures as being a result of a quench from a liquid but they are also typical of textures described by Lofgren (1971a,b) as being due to devitrification. The melt rocks are quite felsic in composition, having an average of 67%  $\text{SiO}_2$  (Peredery, 1972b). This indicates that they may have been too viscous to form quench crystals, and that in fact a glass was formed on cooling with subsequent devitrification to produce the textures now seen. This interpretation allows for the potential movement of elements during devitrification.

### 3.9 Geochemistry of the Melt Rocks

Based on the major element composition, the melt rocks show a wide range in composition (Fig. 3-6) with a marked tendency toward  $\text{Na}_2\text{O}$  enrichment. On variation diagrams, not only is their heterogeneity pronounced but no trends are evident (Peredery, 1972b). Peredery (1972a) points out that compared to the composition of a single

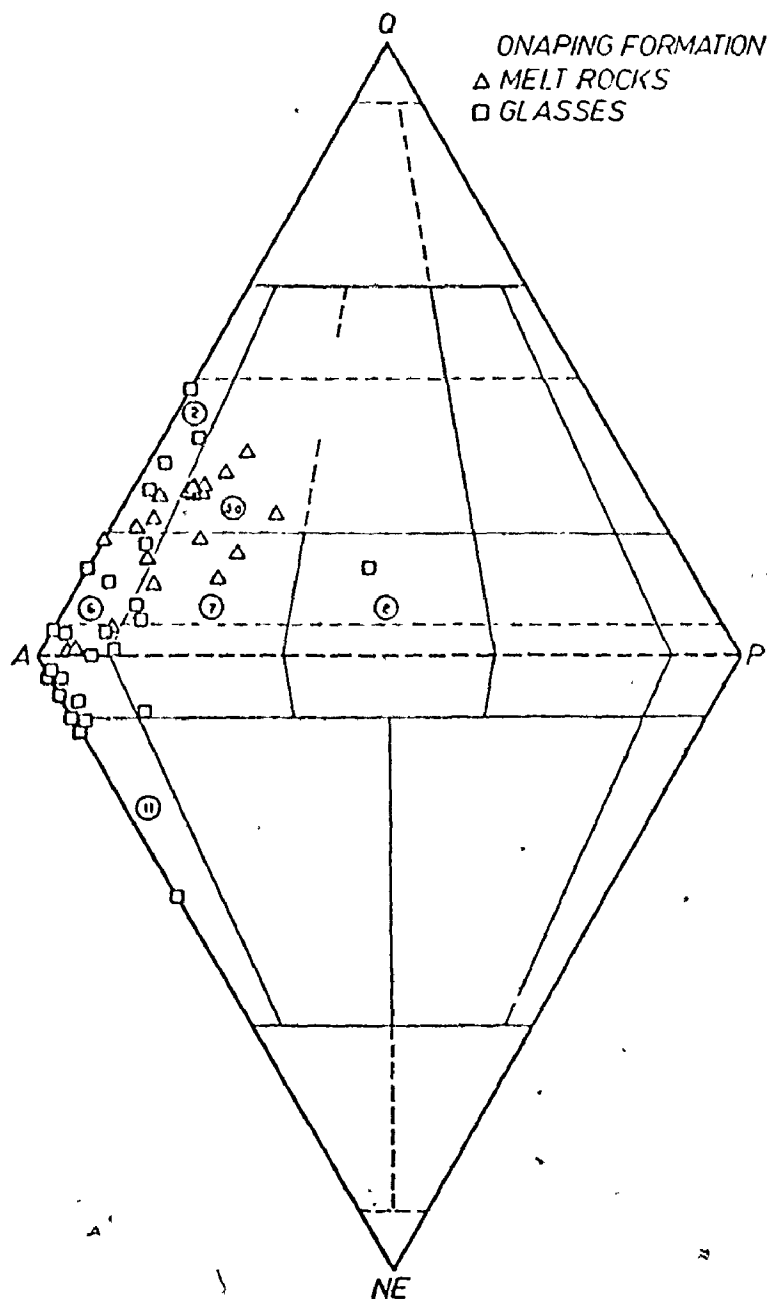


Figure 3-6. Streckeisen's (1965) double-triangle diagram on which the fluidal glasses and the melt rocks are plotted in terms of their normative mineralogy. In the diagram Q represents quartz, A represents alkali feldspar + sodic plagioclase up to  $An_5$ , P represents plagioclase with  $An > 5$ , and NE represents nepheline. According to this classification Area 2 is alkali-rhyolite, Area 3a is granite, Area 6 is alkali-trachyte, Area 7 is trachyte, Area 8 is latite, and Area 11 is phonolite [ from Peredery, 1972a, p.54 ].

volcanic pile, the melt rocks are much more heterogeneous. The factor diagram (Fig. 3-4) presents the melt rocks in terms of the trace elements and shows them forming a restricted grouping but with a significant number of exceptions. The melt shows no trend within its own group but if the mixing model demonstrated at Mistastin Lake is valid, the melt could have been formed from a mixture of the two groups of country rocks (as seen in Fig. 3-4), a conclusion also arrived at by Peredery (1972b) using the major element compositions.

### 3.10 Geochronology

For the most part only samples from the northern half of the Sudbury Basin have been used because of good geological and petrological control provided by Peredery (1972b) and because they are the farthest removed from the metamorphism and tectonism evident in the southern portion of the basin. Splits of Peredery's samples were used for geochronological analysis. While there are no effects of deformation in this area (Brocum & Dalziel, 1974) the whole rock data were found to be reset by the post-Irruptive events which have been previously identified and which extend out into the Archean basement (Hurst & Wetherill, 1974; Gibbins & McNutt, 1975b; Fairbairn et al., 1965). The ages found in this study fit the groupings of ages described

in Gibbins & McNutt (1975b) and demonstrate that these later events have completely wiped out geochronologic evidence for meteorite impact.

The new data obtained here are presented in Table (3-2) with the isochrons for the different rock units in Table (3-3). Standard techniques (Appendix A) were used in the analytical determinations and the isochron ages reported were obtained using the York (I) regression treatment (York, 1966) from the computer program of Brooks et al. (1972). The Mean Square of Weighted Deviates [MSWD] (McIntyre et al., 1966) is reported for the isochrons which are considered statistically perfect where the MSWD is less than the F-ratio (Brooks et al., 1972). All errors are reported at the one standard deviation (1s) level.

The country rock fragments from the Onaping Formation adjacent to the melt bodies were analysed to determine if they had remained undisturbed during and following the impact event because they should provide the most useful information on the nature of the rocks melted by impact. Some of the data is taken from Fullagar et al., (1971) and the larger error estimates from their work are used wherever one of their samples is included in an isochron calculation. The fragments analysed consisted of two main types, granites and quartzites. Visual inspection of the isochron plot of the granite samples indicated that

TABLE 3-2  
Rb-Sr Analytical Data

| Samples by group     | Rb <sup>87</sup> /Sr <sup>86</sup> | Sr <sup>87</sup> /Sr <sup>86</sup> <sub>n</sub> |
|----------------------|------------------------------------|---|
| <u>Granite No. 1</u> |                                    |   |
| DW-433               | .755                               | .7301   |
| C 670385*            | 1.29                               | .7450   |
| CSF-67-67B*          | 1.57                               | .7505   |
| CSF-66-501-1C*       | 2.22                               | .7655   |
| CSF-66-54-1*         | 2.66                               | .7705   |
| CSF-66-50-2*         | 2.68                               | .7735   |
| CSF-67-35*           | 2.79                               | .7735   |
| DW-418               | 3.52                               | .7902   |
| CSF-67-94*           | 5.02                               | .8239   |
| CSF-67-100*          | 7.67                               | .8802   |
| DW3759               | 14.73                              | 1.0150  |
| <u>Granite No. 2</u> |                                    |   |
| DW-414               | .490                               | .7203   |
| CSF-66-39*           | 1.03                               | .7323   |
| DW-180               | 1.490                              | .7419   |
| DW-167               | 6.461                              | .8388   |
| <u>Quartzites</u>    |                                    |   |
| DW-210               | .801                               | .7269   |
| DW-417               | 4.308                              | .7986   |
| DW-276               | 4.766                              | .8245   |
| CSF-67-66A*          | 7.19                               | .8625   |
| DW-206               | 17.979                             | 1.1233  |

\* samples from Fullagar et al. (1971)  
n = normalized to Sr<sup>86</sup>/Sr<sup>88</sup> = .1194

TABLE 3-2 cont'd

| Samples by group   | Rb <sup>87</sup> /Sr <sup>86</sup> | Sr <sup>87</sup> /Sr <sup>86</sup> <sub>n</sub> |
|--|------------------------------------|---|
| <u>Melt No. 1</u>  |                                    |   |
| DW297B   | .278                               | .7187   |
| DW1969   | .320                               | .7208   |
| DW235X   | .567                               | .7271; .7276                                    |
| DW221B   | .700                               | .7314   |
| DW-245   | .892                               | .7359   |
| DW-443   | 1.029                              | .7384   |
| DW343B   | 1.045                              | .7392   |
| <u>Melt No. 2</u>  |                                    |   |
| DW-431   | .593                               | .7223; .7225                                    |
| DW2489   | .863                               | .7294; .7297                                    |
| DW-552   | 1.082                              | .7340   |
| DW-550   | 1.188                              | .7386   |
| DW-551   | 1.200                              | .7356   |
| DW-109   | 1.213                              | .7389   |
| DW472X   | 1.392                              | .7424; .7420                                    |
| DW-388   | 1.458                              | .7453; .7457                                    |
| DW61A9   | 1.774                              | .7505   |
| <u>Plagioclase Micropegmatite</u>                            |                                    |   |
| DW3069   | .625                               | .7271   |
| G-205B   | .914                               | .7323   |
| DW3369   | 1.440                              | .7437   |
| DW42A9   | 1.699                              | .7478   |
| DW-382   | 1.946                              | .7514   |
| <u>Basal Breccia Matrix</u>                                  |                                    |   |
| G-205A   | .965                               | .7334   |
| DW-384   | 3.076                              | .7754   |
| n = normalized to Sr <sup>86</sup> /Sr <sup>88</sup> = .1194 |                                    |   |

TABLE 3-2 cont'd

| Samples by group       | Rb <sup>87</sup> /Sr <sup>86</sup> | Sr <sup>87</sup> /Sr <sup>86</sup> <sub>n</sub> |
|------------------------|------------------------------------|---|
| <u>Foy Offset</u>      |                                    |   |
| 1426-B                 | .398                               | .7147   |
| 1426-A                 | .542                               | .7195   |
| <u>Sub-layer</u>       |                                    |   |
| MS811V                 | .117                               | .7093   |
| WHL-A                  | .176                               | .7089   |
| WHL-AA                 | .187                               | .7102; .7109                                    |
| MS-777                 | .257                               | .7102   |
| <u>Grey Breccia</u>    |                                    |   |
| LF-1                   | .086                               | .7043   |
| 811FGR                 | .089                               | .7082   |
| 811FPI                 | .093                               | .7067; .7064                                    |
| MS811D                 | .123                               | .7060   |
| ST2900                 | .124                               | .7060   |
| MS811R                 | .128                               | .7042   |
| <u>Sudbury Breccia</u> |                                    |   |
| SBR-1                  | .680                               | .7229   |
| SBR-2                  | .552                               | .7208   |
| SBR-3                  | 2.038                              | .7559   |
| SBR-A                  | .313                               | .7130   |
| SBR-B                  | .146                               | .7075   |

n = normalized to Sr<sup>86</sup>/Sr<sup>88</sup> = .1194

TABLE 3-3 Geochronological Results

| NAME                          | AGE +/- | IR    | +/- | MSWD  | No. | F    | Ref. |
|-------------------------------|---------|-------|-----|-------|-----|------|------|
| Granite No. 1                 | 1495    | .7166 | 9   | 2.08  | 11  | 2.30 | 1    |
| Granite No. 2                 | 1429    | .7122 | 8   | 1.44  | 4   | 3.40 | 1    |
| Quartzites                    | 1601    | .7086 | 26  | 10.90 | 5   | 3.01 | 1    |
| Melt No. 1                    | 1891    | .7119 | 6   | 2.14  | 7   | 2.62 | 1    |
| Melt No. 2                    | 1782    | .7076 | 13  | 2.98  | 9   | 2.42 | 1    |
| Plagioclase<br>Micropegmatite | 1361    | .7151 | 8   | 1.52  | 5   | 3.01 | 1    |
| NASA Strong Shock             | 1431    | .7177 | 8   | .29   | 5   | --   | 2    |
| NASA Glasses                  | 1476    | .7142 | 11  | .50   | 5   | --   | 2    |
| Norite-Oxford                 | 1859    | .7067 | 1   | .90   | 6   | --   | 3    |
| Foy Offset                    | 1854    | .7053 | --  | --    | 2   | --   | 1    |
| Basal Breccia                 | 1417    | .7142 | --  | --    | 2   | --   | 1    |

+/- = one standard deviation (1s)

AGE in m.y.

MSWD - Mean square of weighted deviates, a measure of goodness of fit (Brooks et al., 1972)

F - F-ratio for 24 replicates (Brooks et al., 1972)

IR - Initial Ratio ( $Sr^{87}/Sr^{86}$ ).

No. - Number of samples regressed

Ref. - Reference: 1- This work; 2- Fullagar et al., 1971; 3- Gibbins & McNutt, 1975a

Errors used in the isochron calculations: Ref.  $Rb^{87}/Sr^{86}$   $Sr^{87}/Sr^{86}$

|   |      |       |
|---|------|-------|
| 1 | 2.0% | .046% |
| 2 | 1.5% | .2%   |
| 3 | 1.0% | .08%  |

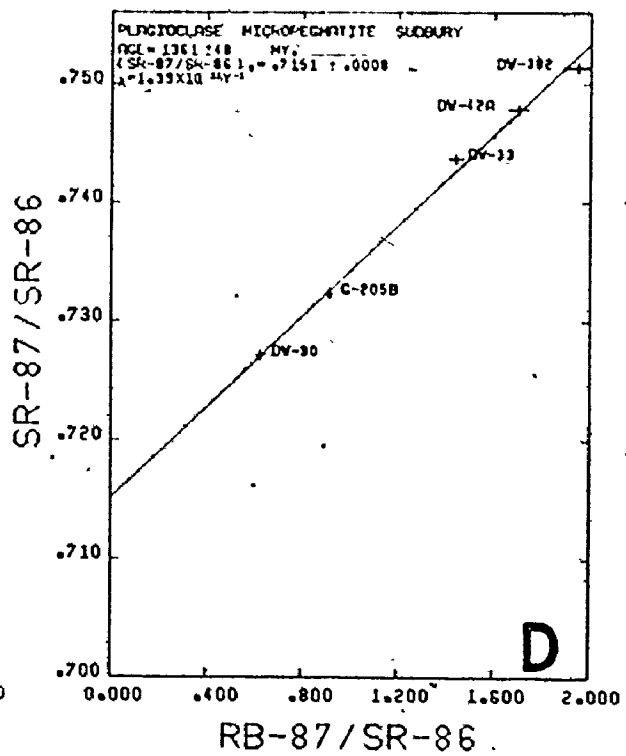
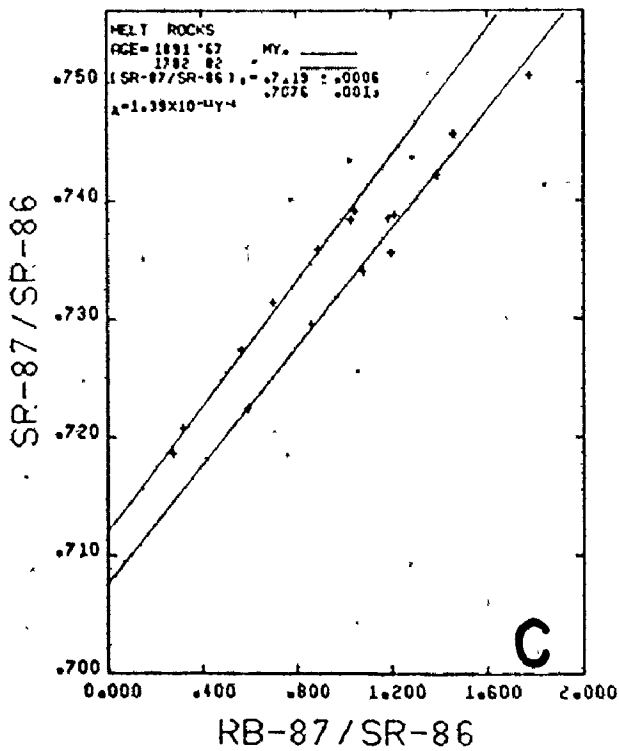
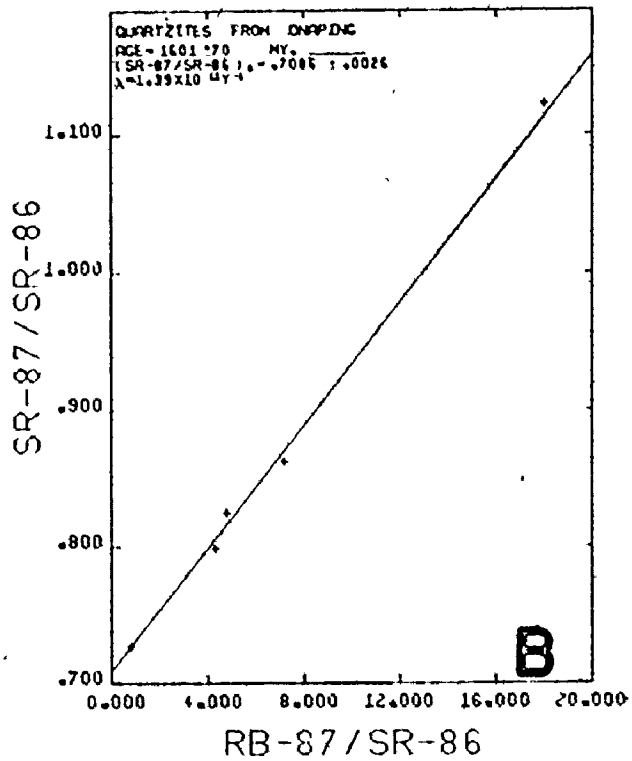
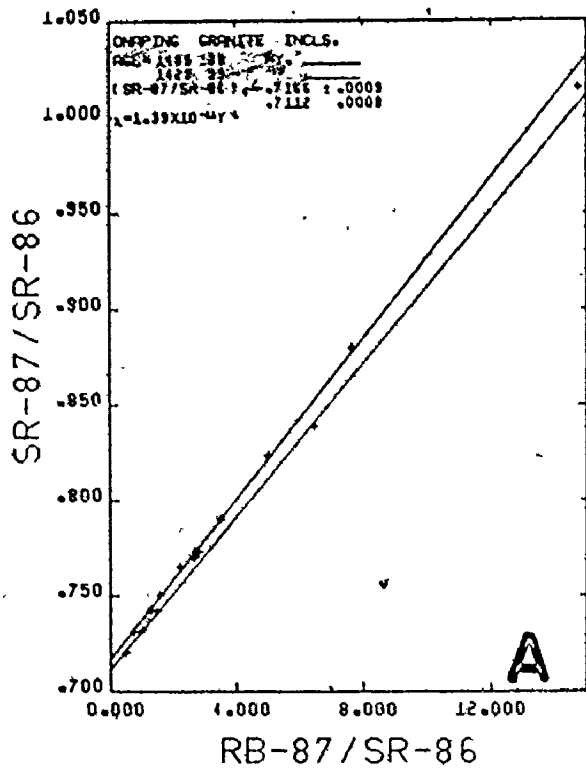


there might be two distinct groups. Consequently, the granites were divided on the basis of those groups that produced the best straight lines, that is the lowest MSWD. This produced two isochrons of  $1429 \pm 39$  m.y. and  $1495 \pm 28$  m.y. (Table 3-3; Fig. 3-7a), both essentially the same age but with different initial ratios (Table 3-3). As there are presently no other criteria available for dividing these granites, it may be premature to assign different sources to the groups as suggested by the different initial ratios (Table 3-3), but these could be the Birch Lake batholith and the Levack migmatite complex. The alternative of grouping all the granites together would produce an errorchron of  $1556 \pm 54$  m.y. The quartzites produce an errorchron of  $1601 \pm 70$  m.y. (Fig. 3-7b) and the errorchron ages are likely meaningless, possibly the result of open system behaviour caused by the same thermal episode that affected the granophyric micropegmatite ( $1680 \pm 31$  m.y.; Gibbins & McNutt, 1975a).

Sixteen samples of impact melt were analysed. The isochron diagram (Fig. 3-7c) shows that the samples may visually be assigned to two linear groups which were regressed separately. Melt No. 1 forms an isochron of  $1891 \pm 67$  m.y. while melt No. 2 produces an errorchron of  $1782 \pm 81$  m.y. The MSWD of melt No. 2 is 2.98, only slightly above the F-ratio of 2.42 and since there seems

Figure 3-7.

- A - The two isochrons for the granite inclusions from the Onaping Formation.
- B - The errorchron for the quartzite inclusions from the Onaping Formation.
- C - The two isochrons for the impact melt.
- D - The isochron for the plagioclase micropegmatite.

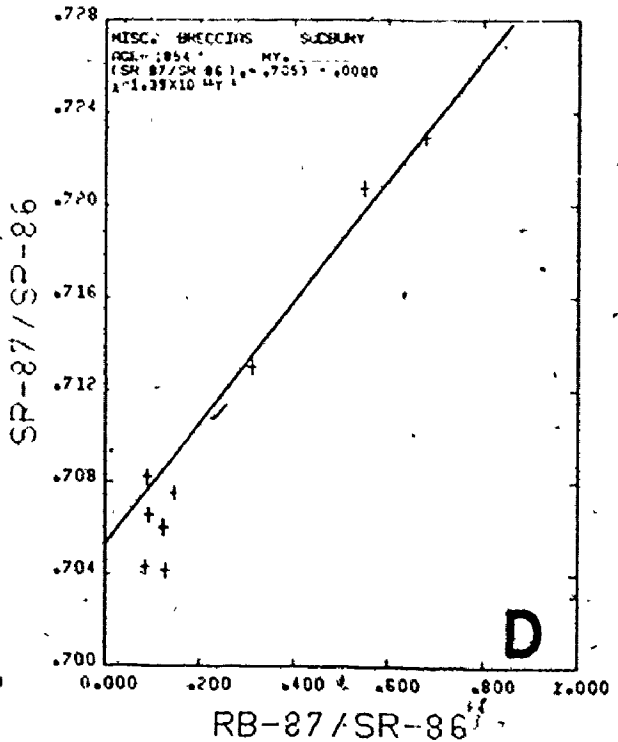
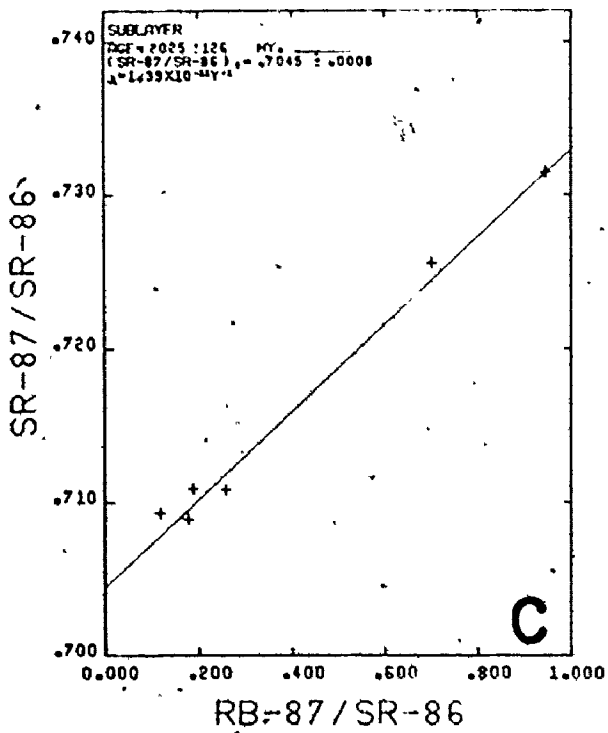
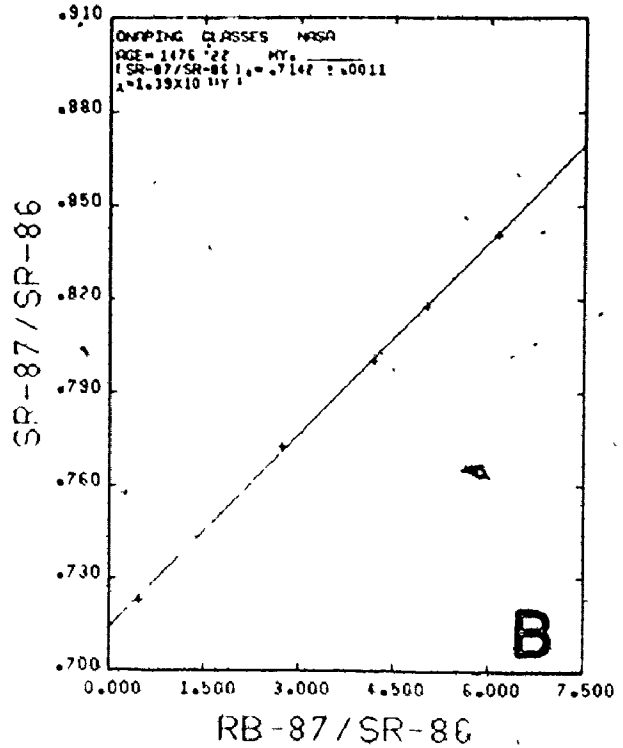
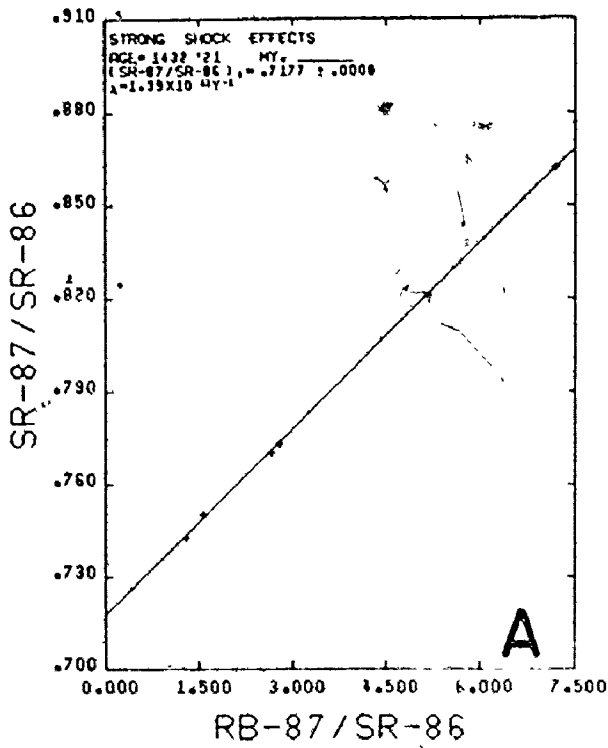


to be no geological evidence for a different history, this age is likely representative of system closure. The errors on the melt rocks are large so it seems reasonable to assume that both melt groups and the norite ( $1844 \pm 3$  m.y.; Krogh & Davis, 1974) were formed more or less contemporaneously. Since there are no samples of target rock that have retained their pre-impact Rb-Sr system, it is impossible to relate the melt rock to a closed system melting of target rock as was done at Mistastin Lake. The ages of the melt rocks likely represent response to the effects of the Sudbury event, particularly to hydrothermal fluids circulating during the cooling of the Irruptive.

The plagioclase micropegmatite forms an isochron of  $1316 \pm 48$  m.y. (Fig. 3-7d), the lowest whole rock isochron age in the Sudbury Basin area. The event that it records is possibly the cryptic thermal event (Gibbins & McNutt, 1975b) but it is difficult to explain why only this rock unit produced such a low age; perhaps it is an indication of its previous physical state. The data of Fullagar et al. (1971) for the strongly shocked inclusions (Fig. 3-8a) and the glasses in the Onaping Formation (Fig. 3-8b) show perfect linear relationships [MSWD < 1], possibly due to their physical state prior to homogenization and system closure.

Figure 3-8.

- A - The isochron for fragments in the Onaping Formation that show strong shock effects [from Fullagar et al., 1971].
- B - The isochron for fluidal glasses from the Onaping Formation [from Fullagar et al., 1971].
- C - Isochron diagram presenting the data on the sub-layer rocks from the Irruptive. The line plotted is the errorchron for the data presented.
- D - Isochron diagram presenting the various breccias with an 1854 m.y. reference line.



Some additional sub-layer samples were analysed but as illustrated (Fig. 3-8c) there is considerable scatter and very little variation in the  $\text{Rb}^{87}/\text{Sr}^{86}$  ratio. The two high points are the sub-layer samples from the Copper Cliff North mine (Gibbins & McNutt, 1975a)

Two samples from the far northern end of the Foy offset in S.W. Tyrone township, about seven miles north of the main Irruptive contact, were analysed. No other Irruptive samples yet analysed have come from such a large distance away from the post-Irruptive tectonic and thermal effects that increase southwards across the Irruptive. One sample is the normal fine-grained variety of sub-layer and the other is the quench variety as described by Hewins and Pattison (1972). An age of 1854 m.y. (Table 3-3) is obtained for a two sample isochron.

The age of the Sudbury Irruptive has been sought by numerous investigators over the past fifteen years but the recent result of 1844  $\pm$  3 m.y. obtained on zircons separated from the norite (Krogh & Davis, 1974) is perhaps the best age yet determined. This is primarily due to the freshness and concordant nature of the zircons and the high precision of the analytical technique, all of which produced an uncertainty of only  $\pm$  3 m.y. At the present time there has only been one set of high precision

Rb-Sr data published. This is the Oxford data from Gibbins and McNutt (1975a) which gives an age of  $1859 \pm 30$  m.y. for the norite. This agrees within error with the more extensive data from Gibbins and McNutt (1975a) that give the age of the Sudbury event as  $1900 \pm 100$  m.y. However, now that there is some high precision data available, it would seem preferable to use this data as the basis for the age of the Sudbury event at about 1850 m.y. The age of 1854 m.y. obtained for the Foy offset agrees well with this.

Samples of grey breccia (Greenman, 1970; Naldrett et al., 1972), Sudbury breccia, and basal breccia were analysed (Table 3-2) to ascertain if they could provide the age of the country rocks or the age of granulation and impact. The isochron plot (Fig. 3-8d) displays the data for the grey breccia and the Sudbury breccia. The data is inconclusive and can be interpreted as either an unequilibrated open system or a mixture of unrelated rocks. A two-sample isochron for the basal breccia matrix gives an age of 1417 m.y. (Table 3-3), very similar to that of the plagioclase micropegmatite and the strongly shocked inclusions.

### 3.11 $\text{Sr}^{87}/\text{Sr}^{86}$ Ratios

The Sr development diagram can be rigorously applied only if the average  $\text{Rb}^{87}/\text{Sr}^{86}$  ratio of the system has not been changed after the formation of the original



system. Starting with this assumption, which is not likely true for many of the Sudbury area rocks, a strontium development diagram was constructed (Fig. 3-9). Since the rocks are either older or contemporaneous with the Sudbury event, their  $\text{Sr}^{87}/\text{Sr}^{86}$  ratios at 1844 m.y. should be comparable (Table 3-4). At 1844 m.y. the ratios tend to cluster within the range of the norite initial ratio, between .7053 and .7067 and it is impossible to separate these diverse rock units at 1844 m.y. based on their  $\text{Sr}^{87}/\text{Sr}^{86}$  ratios. Some other interesting  $\text{Sr}^{87}/\text{Sr}^{86}$  relationships observed (Table 3-4) are: (1) melt No. 1 has a higher ratio than all other rocks including the the average Superior Province granite basement; this is not the expected relationship for a rock that was formed by melting of lower ratio rocks, (2) the quartzite, which is likely Huronian in age (~2.0 b.y.) has an unreasonably low ratio for a quartzite at 1844 m.y. These anomalous relationships and the suite of ages in the 1350-1600 m.y. range indicate that the development diagram can not be extrapolated back to 1844 m.y. because the average  $\text{Rb}^{87}/\text{Sr}^{86}$  of many of the systems was changed at a more recent time. This metasomatic event (or events) is indicated by the intersection of the development lines in the 1300-1600 m.y. region. It is suggested that the various rock units have responded differently and perhaps at somewhat different times to this event but the lack of additional geochronologic

TABLE 3-4  
 $Sr^{87}/Sr^{86}$  Ratios at 1844 m.y.

| Unit                          | $Rb^{87}/Sr^{86}$<br>average | $Sr^{87}/Sr^{86}$ | +/-       |
|-------------------------------|------------------------------|-------------------|-----------|
| Plagioclase<br>Micropegmatite | 1.3                          | .7064             | .0008     |
| Granophyric<br>Micropegmatite | 1.5                          | .7049             | .0014     |
| Norite/Oxford                 | .28                          | .7067             | .0001     |
| Norite/Foy Offset             | .47                          | .7053             | ----      |
| Norite/Sub-layer              | --                           | .7045             | estimated |
| Melt No. 1                    | .56                          | .7128             | .0006     |
| Melt No. 2                    | 1.2                          | .7066             | .0013     |
| Granite No. 1                 | 1.9                          | .7020             | .0009     |
| Granite No. 2                 | 1.0                          | .7055             | .0008     |
| Quartzite                     | 1.7                          | .7029             | .0026     |

$$Sr^{87}/Sr^{86} = (Sr^{87}/Sr^{86})_{\text{initial}} + [(Rb^{87}/Sr^{86})_{\text{average}} \lambda^t]$$

$$\lambda = 1.39 \times 10^{-11} \text{y}^{-1}$$

t = time

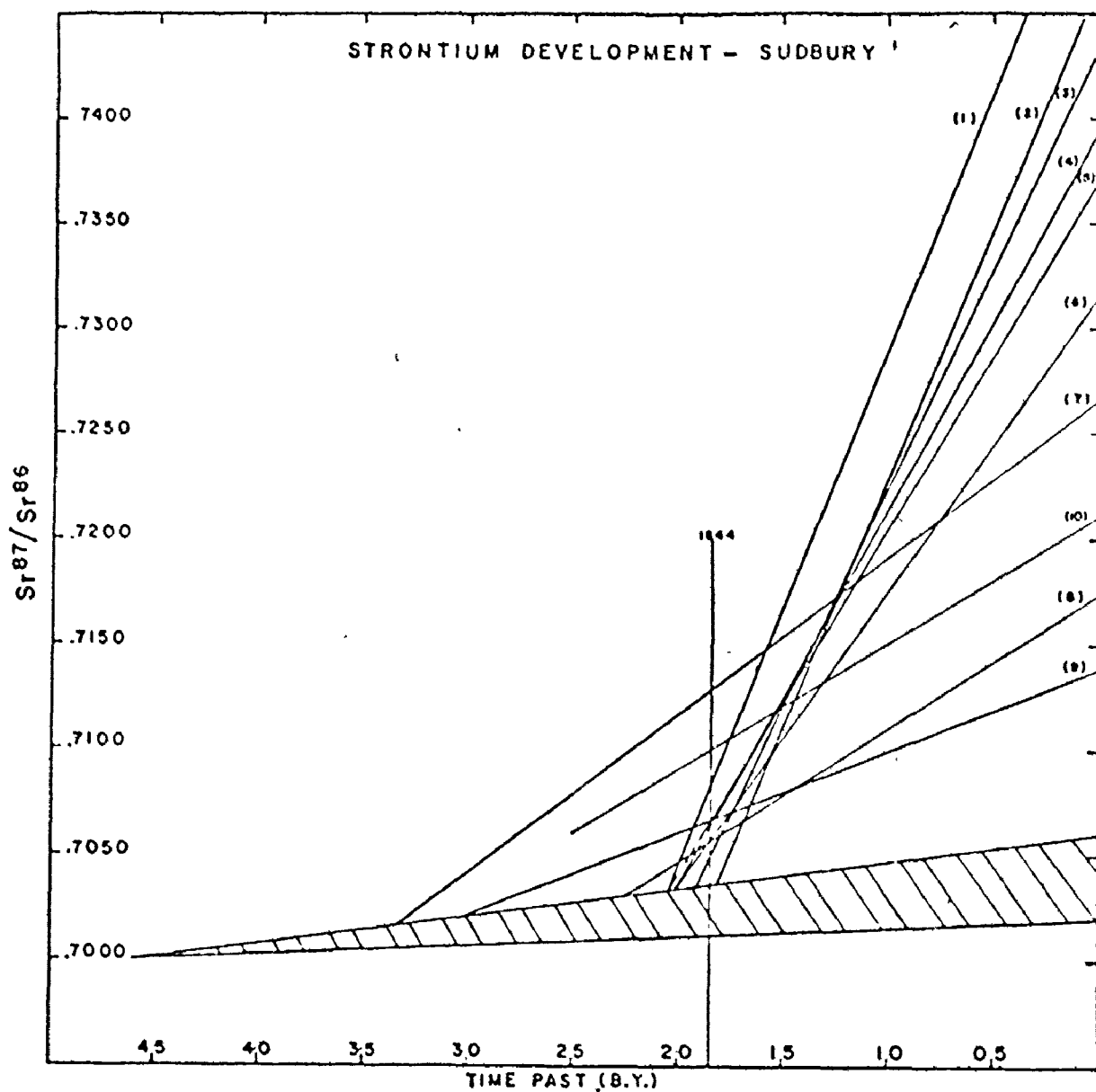


Figure 3-9. Strontium development diagram for the various rock types from the Sudbury Basin: (1) Granite No. 1, (2) Quartzite, (3) Granophyric Micropegmatite, (4) Plagioclase Micropegmatite, (5) Melt No. 2, (6) Granite No. 2, (7) Melt No. 1, (8) Foy Offset, (9) Norite-Oxford Data, (10) Average Superior Province Granite Basement (Fairbairn *et al.*, 1968). Shaded zone = source region for basalt.

evidence, such as U-Pb ages on whole rocks and zircons, does not allow any distinction between the ages. It may be concluded from the development diagram that there has been movement of Rb and/or Sr within the time period 1300-1600 m.y.

The initial ratios for the norite and sub-layer were probably not affected by these metasomatic events since they still have reasonably low initial ratios. Even the lowest estimated initial ratio for the sub-layer, .7054 (Fig. 3-9) is somewhat higher than expected for magma originating in the mantle. This implies that the norite producing magma was contaminated by crustal material prior to crystallization.

The two groups of melt rocks give quite different initial ratios, .7076 and .7119. Since they show no geochronologic evidence of being affected by later events, the differing initial ratios could be interpreted as due to different parental source rocks, a factor consistent with the inhomogeneous character of the melt.

### 3.12 Discussion

The isochron ages determined in this study have been assigned to the events summarized by Gibbins and McNutt (1975b) for which a correlation chart is presented in Table 3-5. The impact melts are correlated with the

TABLE 3-5

Ages from the Sudbury Region

| Sudbury Basin                                  | Southern Province<br>Grenville Province  | Event   |
|--|--|---|
| Melt Rocks<br>1891 ± 125 (1)<br>1782 162       |  | 1900 ± 100 (13)<br>Meteorite impact and<br>intrusion of Irruptive,<br>initiation of hydrothermal<br>convection system |
| Norite<br>1956 ± 98 (3)<br>*1844 ± 3 (2)       |  |   |
| Granophyric<br>Micropegmatite<br>1680 ± 62 (3) | Cutler granite 1750 ± 50 (4)<br>Mongowin pluton 1770 ± 140 (5)<br>Bell L. granite *1730 (6)<br>French River<br>paragneiss *1682 (2)<br>Basement north<br>of Irruptive 1701 ± 148 (7) | 1600-1800 (13)<br>Penocean-Hudsonian Orogeny.<br>metamorphism and<br>deformation                                      |

TABLE 3-5 cont'd

|                            |              |                        |                                 |                              |
|----------------------------|--------------|------------------------|---------------------------------|------------------------------|
| Granite No. 1              | 1495 ± 58(1) | Croker Is. intr.       | 1510 <sup>±</sup> 50(5)         | 1300-1450 (13)               |
| Granite No. 2              | 1429 ± 78(1) | Muskoka granite        | 1497 ± 32(9)                    | Cryptic Thermal Event        |
| Shocked Incls.             | 1431 ± 42(8) | Lamprophyre dykes      | 1414 ± 40(5)                    | Elsonian intrusive episode   |
| Onaping Glass              | 1476 ± 44(8) | Manitoulin Is. granite | 1454 ± 57(10)<br>*1500 ± 20(10) | a period of igneous activity |
| Basal Breccia matrix       | 1417 (1)     | Cosby batholith        | *1420 (11)                      |                              |
|                            |              | Olivine diabase dykes  | 1460 ± 130(12)                  |                              |
| Plagioclase Micropegmatite | 1361 ± 96(1) | North Bay granites     | 1330 <sup>±</sup> 70(9)         | ?? part of the Elsonian ??   |

\* indicates a zircon age, all others Rb-Sr isochron ages (in m.y.).

All errors are quoted at the 2 sigma level (2s).

Numbers in brackets (1) are the reference numbers as listed below:

- (1) This work
- (2) Krogh & Davis, 1974
- (3) Gibbins & McNutt, 1975a
- (4) Wetherill et al., 1960
- (5) Van Schmus, 1971
- (6) Krogh et al., 1971
- (7) Hurst & Wetherill, 1974
- (8) Fullagar et al., 1971
- (9) Krogh et al., 1968
- (10) Van Schmus, 1975a
- (11) Lumbers, 1975
- (12) Gates & Hurley, 1973
- (13) Gibbins & McNutt, 1975b

Sudbury event and since these rocks show no evidence of the closed system impact melting of the country rocks from which they were derived, they must have become an open system at the time of impact, probably due to circulating fluids. The next event that affected the area, the Penokean-Hudsonian Orogeny, produced an age of  $1680 \pm 30$  m.y. (Gibbins & McNutt, 1975a) for the granophyric micropegmatite and also an errorchron of  $1701 \pm 74$  m.y. for the Archean basement north of the Irruptive (Hurst & Wetherill, 1974). The ages of other impact produced units of the lower Onaping Formation, including granite inclusions, shocked fragments, glasses, and basal breccia matrix, have been assigned to the Cryptic Thermal Event (1300-1450 m.y.; Gibbins & McNutt, 1975b). The age of the plagioclase micropegmatite is somewhat lower than these other units (Table 3-5) but this age is also likely a manifestation of this event. In the vicinity of the Irruptive, the Cosby Monzonite batholith, just south of the Grenville Front (Lumbers, 1975) and the widespread olivine diabase dykes cutting the Irruptive are intrusives that are probably related to the Cryptic Thermal Event, which is correlative with the widespread Elsonian intrusive episode that affected the whole continent. The youngest event in the area is the Grenville Orogeny, 1100-1200 m.y. ago but it has left little effect on the Irruptive except for some discordant mineral

ages in the South range norite (Gibbins & McNutt, 1975b).

Though the various rock types analysed form valid isochrons and their ages can be assigned to the regional tectonic events, the rocks have had a very complex history. They come from a restricted geographic area and were formed either during or prior to the impact event. All these rocks have therefore had the same post-Irruptive history yet their ages differ significantly. This is an indication of post-Irruptive metasomatic and/or metamorphic events that affected the rocks in a very irregular and complex manner.

There are several lines of evidence for post-Irruptive episodes of chemical migration. Devitrification textures similar to those described by Lofgren (1971a,b) are abundant in the glasses in the Onaping Formation (Peredery, 1972a,b) and also the melt rocks and plagioclase micropegmatite show some coarse grained devitrification textures. Passage of groundwater through volcanic glasses produce similar textures and causes movement of alkalies and silica (Smith & Bailey, 1961; Noble, 1967; Scott, 1971). The alkaline nature of some of the Onaping glasses (Peredery, 1972a) is very likely due to such movement. Taylor and Forester (1971), studying the oxygen isotopic effects in shallow igneous intrusions, list the following as mineralogical criteria for meteoric [groundwater] activity within and adjacent to the intrusive: alteration of pyroxenes to chlorite,



green amphibole, epidote, magnetite, and biotite; alteration of plagioclase to epidote and albite; clouded and turbid feldspars with numerous fluid inclusions; feldspathic veinlets consisting of epidote and plagioclase [eg. found in the country rocks close to the Irruptive]; granophyric textures; and miarolitic cavities. They also state that this activity affects the trace element geochemistry of the rocks. Peredery (1972a,b) has described the ubiquitous presence of albite, epidote, chlorite, green amphibole, and sphene in the granophyric and plagioclase micropegmatite, the basal breccia, the melt rocks and throughout the Grey Onaping. Fluid inclusions are found oriented along modified shock lamellae in the fragments in the Onaping Formation indicating the action of fluids after the impact. The high  $Sr^{87}/Sr^{86}$  ratio of melt No. 1 at 1844 m.y. (Table 3-4), higher even than its probable source rock of Superior Province granite, could have occurred through the enrichment of Rb in the rock at that time by the action of hydrothermal fluids. Sodium metasomatism, particularly as albite and epidote replacing plagioclase, has affected the country rocks up to a distance of 50-100 feet from the norite contact near the Strathcona mine (Naldrett & Kullerud, 1967) and all along the Foy offset (Card & Meyn, 1969). Peredery (1972b) recognized a metasomatic effect in the basal breccia but noted that it was very erratic and probably due to the

variation in residual heat in the different clasts. This is similar to the metasomatic effects observed in the Brent crater (Dence & Guy-Bray, 1972) where potash metasomatism is found in an extremely erratic fashion in the breccias and has been interpreted as due to the effects of groundwater on shock heated fragments. Hydrothermal effects are in fact quite common at most craters.

Fullagar et al. (1971) suggested that the shocked inclusions and glasses preferentially lost their radiogenic strontium during an event at 1400-1500 m.y. ago because of the shock damage to the samples. This may be only partly correct since if the samples were affected by circulating groundwaters within the hot crater, they would have reacted geochemically at this time (1844 m.y.) and not at 1400-1500 m.y. However, the samples may have reacted proportionately to their degree of shock and temperature, acquiring a Rb-Sr system that was more susceptible to later events than the surrounding rocks. The small system size may actually be the most important reason why these rocks give younger ages. U-Pb data on zircons and whole rocks for these systems are needed before they can be completely explained.

### 3.13 Model of Crater and Irruptive Formation

The geochemical and isotopic data presented is consistent with the meteorite impact origin for the Sudbury

Basin as outlined by French (1970), Peredery (1972a,b) and Naldrett et al. (1972). The scenario envisaged begins with the impact occurring in a shallow marine continental shelf (Peredery, 1972a,b). The impact melt collects along the bottom of the crater in a pool or pools and is overlain by the graded sequence of the Grey Onaping, the fallback breccia. The basal breccia is the coarse grained lowermost unit of the fallback breccia. The Black Onaping and the sediments above it form in the manner described by Beales and Lozej (1975). The impact triggers the intrusion of the parental magma of the norite below the pool of molten melt. The noritic magma and melt will tend to mix only slowly, mainly due to viscosity differences, resulting in a case of kinetic immiscibility similar to that described in Yoder (1973). Since the initial ratio of the norite, even along the Foy offset, is higher than expected for a pristine mantle derived magma, there must have been some degree of instant contamination on intrusion between the noritic magma and the impact melt. The subaqueous crater is now filled with the shock-heated impact debris, the molten impact melt, and the noritic magma, all of which provide a large heat source. It is a comparable situation to that of shallow intrusions and caldera collapse structures where oxygen isotope studies (Taylor & Forester, 1971) have indicated the operation of hydrothermal convection systems during the cooling of the rocks. A hydrothermal convection

system was established sending sea water through the Irruptive complex and the fractured country rocks causing metasomatism to the shock heated fragments and continuously diffusing into the magma.

Irvine (1975), using as a base the model of Naldrett et al. (1973), developed his own model for the formation of the sulphide deposits. It relies on the contamination of the magma by melted roof rocks to cause precipitation of the sulphides. However, this can be accomplished easier by the molten impact melt, which would contaminate the magma faster since it would already be in the molten state. As crystallization of the magma proceeded with continuous diffusion of water into it, the magma became progressively more contaminated until the crystallization of the upper [oxide-rich] gabbro started. Irvine (1975) proposed that the sudden formation of continuous layers of magnetite in igneous intrusions is the result of almost instantaneous contamination of the magma. At Sudbury, the upper gabbro contains continuous layers of magnetite. What possibly happened was that during the time of crystallization of the upper gabbro the remaining magma blended together with the impact melt, resulting in a change of bulk composition of the system that caused precipitation of the oxide-rich layers. Concomitantly the influx of water

allowed the remaining magma, which now consisted mainly of impact melt, to crystallize as a granophyre, the granophyric micropegmatite. The plagioclase micropegmatite represents that portion of the impact melt which was not as seriously affected by the water. The melt rocks themselves, which occur as isolated bodies above the plagioclase micropegmatite, likely represent large blocks or bombs of impact melt that were separated from the main body during crater formation.

## APPENDIX A

## Geochronological Procedures

## A-1. Analytical Procedures in Sr Isotope Determinations

The basic analytical procedures and techniques have been in use for many years and are described in detail in Wanless and Loveridge (1972). Since only the  $\text{Sr}^{87}/\text{Sr}^{86}$  ratio was determined in this study, spikes were not used and Rb was not collected. The strontium was mounted as nitrate on a single tantalum filament in a Nier type 90 degree 10 inch radius mass spectrometer with a Faraday cup collector. The measurements were recorded on a digital voltmeter and printer. Peak switching was accomplished by switching the accelerating voltage of the source. Each peak was counted for ten seconds with an eight second delay for peak switching. The data was transferred to computer cards and the program of Stacey (1971) was used to reduce the data after the program was modified for compatibility with the spectrometer and the university computer. Normally each run consisted of 10-15 scans on each of the 86, 87, and 88 peaks after steady Sr emission was achieved. Details are on file in the Geochronology Laboratory of the Geology Department at McMaster University.

## A-2. Analytical Technique for Rb/Sr Determination

The Rb/Sr ratios were determined directly on rock powder pellets by X-ray fluorescence according to an improved version of Doering's (1968) technique. The method and computer programs for data reduction are described in detail in Marchand (1973), on file in the Geology Department of McMaster University.

## A-3. Precision and Accuracy in the Determination of $\text{Sr}^{87}/\text{Sr}^{86}$ and $\text{Rb}^{87}/\text{Sr}^{86}$

Precision in this study is based on replicate analyses of rock powders and on repeat determinations of the NBS standard strontium carbonate SRM-987. Precision is reported at the 1(s) level. The values obtained for SRM-987 (Table A-1) were measured throughout the course of this study. Accuracy is based on the value obtained for SRM-987 and is the basis for interlaboratory comparisons. The average value for 15 replicates is  $.70995 \pm .0003$  with a standard deviation (1s) of  $.046\%$ . This value is slightly lower than those reported from other laboratories (Table A-2). The difference from the accepted value of  $.71014$  is  $-.00019$ . This is identical to the difference of  $-.0002$  obtained by Gibbins (1973) in this laboratory for the E & A strontium carbonate from its accepted value. Thus the values of this study and

TABLE A-1

## Replicate Determinations of SRM-987

| $\text{Sr}^{87}/\text{Sr}^{86}_n$ |               |               |
|-----------------------------------|---------------|---------------|
| <u>.71016</u>                     | <u>.70951</u> | <u>.71026</u> |
| <u>.71013</u>                     | <u>.70933</u> | <u>.70970</u> |
| <u>.70984</u>                     | <u>.71024</u> | <u>.70950</u> |
| <u>.71030</u>                     | <u>.70995</u> | <u>.71034</u> |
| <u>.70986</u>                     | <u>.71021</u> | <u>.70994</u> |

AVERAGE .70995

Standard Deviation: .0003

Standard Deviation of the Mean: .0001

Percent Standard Deviation (%): .046



TABLE A-2

## Comparison of Analyses of SRM-987

| Reference   | Laboratory     | $\text{Sr}^{87}/\text{Sr}^{86}$<br>n | N  | 2 Sigma Mean |
|---|----------------|--------------------------------------|----|--------------|
| This work   | McMaster       | .70995                               | 15 | .0002        |
| Hart et al. (1973)                                      | D.T.M.         | .71018                               | 5  | .00002       |
| Evensen et al. (1973)                                   | U. of Minn.    | .71018                               | 8  | .00005       |
| Mark et al. (1973)                                      | U.C.L.A.       | .71039                               | -  | .00006       |
| Nyquist et al. (1973)                                   | NASA - Johnson | .71029                               | -  | .00008       |
| Pankhurst & O'Nions (1973)                              | Oxford         | .71039                               | -  | .00004       |
| National Bureau of Standards<br>Certificate of Analysis |                | .71014 ± .00020                      |    |              |

n = normalized to  $\text{Sr}^{86}/\text{Sr}^{88} = .1194$       N = No. of determinations

those of Gibbins (1973, 1975a, 1975b) are directly comparable. Any data used from the literature has been normalized to a value of .7078 for the E & A standard. The Sr blank for this laboratory was determined to be .0016  $\mu$  gms./100 gms. of sample (Gibbins, 1973) and is considered to be insignificant.

The reproducibility as determined by replicate analyses of rock samples, which should indicate the precision of the complete analytical process (Brooks et al., 1972) is presented in Table A-3. The percent error as determined on the replicate rock powders is slightly lower than that on the replicate SRM-987 determinations. In the regression treatments used in this study, the larger value of .046% error in the  $\text{Sr}^{87}/\text{Sr}^{86}$  values has been used since this is the maximum possible error. The error estimates for data taken from the literature are those listed by the authors and for mixed data the highest error estimates have been used in the regressions.

For the  $\text{Rb}^{87}/\text{Sr}^{86}$  value, the error is mostly due to X-ray fluorescence counting statistics. Since the same counting time was used for all samples, the precision based on replicate determinations varied from 0.1 to 3.0%, depending on the amount of Rb and Sr present. Most precision values were below 1.0% and nearly all below 2.0%. Therefore a 2.0% (1s) variation in the  $\text{Rb}^{87}/\text{Sr}^{86}$  value is a conservative estimate of the precision and has been used in the regression treatments.

TABLE A-3

| Sample  | Sr <sup>87</sup> /Sr <sup>86</sup> <sub>n</sub> | Mean   | S.D.   | % S.D. | D.F. |
|---------|---|--------|--------|--------|------|
| DW-248  | .72943<br>.72973                                | .72958 | .00021 | .02908 | 1    |
| DW-235  | .72524<br>.72579                                | .72552 | .00039 | .05360 | 1    |
| DW235X  | .72714<br>.72761                                | .72738 | .00033 | .04569 | 1    |
| DW-388  | .74532<br>.74574                                | .74553 | .00030 | .03384 | 1    |
| DW-431  | .72238<br>.72247                                | .72243 | .00006 | .00881 | 1    |
| DW472X  | .74241<br>.74202                                | .74222 | .00028 | .03716 | 1    |
| WHL-AA  | .71087<br>.71022                                | .71055 | .00046 | .06469 | 1    |
| 811FPI  | .70673<br>.70638                                | .70656 | .00025 | .03503 | 1    |
| LM-32   | .71333<br>.71410                                | .71372 | .00054 | .07629 | 1    |
| LM-33A  | .70369<br>.70381                                | .70375 | .00008 | .01206 | 1    |
| LM-41M  | .70483<br>.70550                                | .70517 | .00047 | .06718 | 1    |
| LM-51B  | .70468<br>.70477                                | .70473 | .00006 | .00903 | 1    |
| LM-56D  | .72828<br>.72819                                | .72824 | .00006 | .00874 | 1    |
| LM-57   | .70737<br>.70772                                | .70755 | .00025 | .03498 | 1    |
| TA-553  | .76069<br>.76038                                | .76054 | .00022 | .02882 | 1    |
| TA-601  | .83157<br>.83148                                | .83153 | .00006 | .00765 | 1    |
| TA-606  | .76650<br>.76655<br>.76627                      | .76644 | .00015 | .01948 | 2    |
| TA-609  | * .71363<br>.71275                              | .71319 | .00062 | .08725 | 1    |
| TA-612  | .72522<br>.72514                                | .72518 | .00006 | .00780 | 1    |
| TA-633  | .72006<br>.72007                                | .72007 | .00001 | .00098 | 1    |
| TA-678  | .80116<br>.80047<br>.80127                      | .80097 | .00043 | .05414 | 2    |
| BT-143  | .74466<br>.74535                                | .74501 | .00049 | .06549 | 1    |
| AVERAGE |   |        |        | .03943 | 24   |

S.D. = Standard Deviation

D.F. = Degrees of Freedom

## APPENDIX B

## Trace Element Analysis

The trace elements were determined by X-ray fluorescence on 3 grams of finely (200 mesh) ground rock powders pressed into pellets. The fluorescent peak intensities were corrected for background, background curvature, dead time, and peak overlap for each element. The mass absorption correction was applied by use of the Mo-Compton scattered radiation peak (Reynolds, 1963,1967). Detection limits were calculated on the calibration standards using the formula of Jenkins and DeVries (1970, p.52) and all raw data was reduced by computer programs developed by the author. Similar programs and detailed technical procedures are listed in Tech. Memo 73-2 of the Department of Geology, McMaster University (Marchand, 1973). Table B-1 below lists the analytical conditions used, the calibration standards for each element and the calibration value for the standards in ppm. The precision for each element is estimated to vary from 50% at 2 ppm, 10% at 10 ppm to 5% at 100 ppm.

TABLE B-1

| Element           | Nb    | Zr    | Y    | Sr    | U     | Rb   | Th    | Pb   | Zn    | Cu    | Ni    |
|-------------------|-------|-------|------|-------|-------|------|-------|------|-------|-------|-------|
| Standard          | BCR   | BCR   | BCR  | BCR   | NIM-G | BCR  | GSP   | GSP  | BCR   | W-1   | BR    |
| Calibration Value | 11.3  | 192.0 | 33.4 | 332.0 | 14.0  | 48.0 | 106.0 | 58.7 | 120.0 | 110.0 | 270.0 |
| Detection Limit   | 2.0   | 1.7   | 1.2  | 1.2   | 4.1   | 1.5  | 3.6   | 4.6  | 2.6   | 3.2   | 5.4   |
| Radiation         | W     | W     | Mo   | Mo    | Mo    | Mo   | Mo    | Mo   | Mo    | Mo    | Mo    |
| KV                | 90    | 90    | 60   | 60    | 60    | 60   | 60    | 60   | 60    | 60    | 60    |
| Ma                | 25    | 25    | 30   | 30    | 30    | 30   | 30    | 30   | 30    | 30    | 30    |
| Precision (ppm)   | 2.4   | 4.8   | 1.1  | 20.3  | 1.2   | 1.7  | 1.7   | 3.0  | 2.3   | 2.5   | 1.7   |
| Replicate Value   | 125.9 | 257.8 | 18.2 | 652.0 | 6.0   | 68.2 | 9.3   | 39.8 | 81.2  | 58.0  | 17.1  |
| No. of Replicates | 3     | 3     | 19   | 19    | 19    | 19   | 19    | 19   | 19    | 19    | 19    |

Standard: the rock standard used for the element listed

Calibration Value: The value in ppm assigned to the standard

Precision: The value in ppm determined by replicate analyses of the rock standard AGV, except for the elements Nb & Zr which were determined on the rock standard BR. Reported at the one sigma (1s) level.

Replicate Value: The amount of the element in ppm found in the rock standard used in the determination of precision. This is the value to which the precision must be compared (eg. Nb  $125.9 \pm 2.4$  ppm).

Analysing Crystal: LiF (100); Fine Collimator; Scintillation Counter;  
Counting Time: 40 sec.

## APPENDIX C

## Major Element Analysis

The major elements were determined on a Philips PW-1450 automatic X-ray fluorescence spectrometer. The technique and computer program used was obtained from Brown et al. (1973), but it is essentially the same procedure as that of Holland and Brindle (1966). The same rock powder pellets used for trace element analysis were utilized. A suite of twenty-eight rock standards, covering the range basalt to granite were used for calibration curves. These consisted of the international rock standards and some rocks analysed wet chemically at McMaster. However it was discovered that this technique (Brown et al., 1973) has a serious flaw in that only a mass absorption correction is applied and enhancement effects are ignored. There is a serious enhancement of Mg by Al which in turn falsifies the mass absorption correction and invalidates the analysis, particularly with respect to the light elements. This effect did not seem important at low concentrations of Mg. All MgO values below 1.0% are considered reliable, those between 1.0% and 2.0% fair but usable, but higher MgO values are subject to error. The error seems to be in the order of + 0.4% MgO for rocks containing up to 4.0% MgO. Table C-1 shows the variation of MgO values obtained by

this technique as compared to the fusion technique. Table C-1 also presents some replicate analyses to illustrate the level of precision obtained. Table C-2 presents a comparison of chemical and XRF analyses for 'Benchmark Sample B-3'.

In retrospect, the use of pure rock powder pellets for major element analysis suffers from uncertainties and its use is not recommended, even for granites, since the use of the fusion technique is more reliable.

TABLE C-1  
Replicate Analyses

|                                | LM-10B |      | LM-29A |      | LM-38A |      |
|--------------------------------|--------|------|--------|------|--------|------|
|                                | Mean   | S.D. | Mean   | S.D. | Mean   | S.D. |
| SiO <sub>2</sub>               | 62.71  | .17  | 57.77  | .24  | 58.96  | .29  |
| Al <sub>2</sub> O <sub>3</sub> | 13.87  | .07  | 23.05  | .14  | 18.90  | .13  |
| TiO <sub>2</sub>               | 1.02   | .01  | .21    | .01  | .86    | .03  |
| MgO                            | 1.24   | .17  | 1.07   | .01  | 1.90   | .16  |
| Fe <sub>2</sub> O <sub>3</sub> | 9.29   | .16  | 1.48   | .01  | 6.22   | .14  |
| MnO                            | .10    | .04  | .07    | .01  | .16    | .06  |
| CaO                            | 4.47   | .03  | 9.39   | .11  | 7.07   | .08  |
| Na <sub>2</sub> O              | 2.98   | .23  | 5.30   | .05  | 3.68   | .02  |
| K <sub>2</sub> O               | 3.52   | .07  | 2.08   | .01  | 2.24   | .01  |
| P <sub>2</sub> O <sub>5</sub>  | .68    | .01  | .05    | .02  | .31    | .05  |
| No. of Analyses                | 3      |      | 4      |      | 3      |      |

Comparison of MgO Analyses

|        | U of Oregon | U of Toronto | McMaster |
|--------|-------------|--------------|----------|
| DW-28  | --          | .84          | .98      |
| DW-29  | --          | .95          | 1.00     |
| DW-42A | --          | 1.36         | 1.30     |
| DH-8R  | 1.44        | --           | 1.35     |
| DH-8PB | 1.53        | --           | 1.54     |

analyses at Oregon and Toronto by fusion technique



TABLE C-2

Benchmark Sample B-3

|                                | Suggested<br>Values* | McMaster<br>X.R.F. | McMaster<br>Chemical |
|--------------------------------|----------------------|--------------------|----------------------|
| SiO <sub>2</sub>               | 80.06                | 81.19              | 80.12                |
| Al <sub>2</sub> O <sub>3</sub> | 10.31                | 9.90               | 10.21                |
| TiO <sub>2</sub>               | .08                  | .08                | .07                  |
| Fe <sub>2</sub> O <sub>3</sub> | 1.44                 | 1.40               | 1.44                 |
| MnO                            | .02                  | .02                | .01                  |
| MgO                            | .01                  | .04                | .01                  |
| CaO                            | .09                  | .10                | .09                  |
| Na <sub>2</sub> O              | 2.26                 | 2.24               | 2.33                 |
| K <sub>2</sub> O               | 5.64                 | 5.42               | 5.69                 |
| P <sub>2</sub> O <sub>5</sub>  | .01                  | .01                | .00                  |

\* Abbey, S., 1974 personal communication

McMaster Chemical: analyst - J. Muysson [Lab No. 74003]

## APPENDIX D

## Correspondence Analysis

Correspondence factor analysis is a type of factor analysis developed by the French School under Prof. Benzercı (1970) at the Mathematical Statistics Laboratory, Faculty of Science, Paris. The general aim of the technique, as in other multivariate methods, is to find associations and oppositions between samples and variables. However, it differs from regular factor analysis in that its weighting scheme and data transformation allows it to operate in Q-mode and R-mode simultaneously. This facility has considerable advantage in conserving computer time and money. There have been numerous recent papers on the method and its applications; David & Woussen, 1973; David et al., 1974; David & Beauchemin, 1974; Dagbert & David, 1974; Teil, 1975; Teil & Cheminee, 1975. Only its uses and interpretational aspects are described here.

Correspondence analysis has been used in this study mainly for two reasons; (1) to consolidate and summarize the trace element data, (2) to demonstrate the behaviour of different rock groups using the ten trace elements simultaneously. Only the Q-mode portion of correspondence

analysis, that is the relationships between the samples, has been used. The results of correspondence analysis are factors which are combinations of the trace elements. They allow the variability of the data to be expressed in fewer components than originally present; usually 3 or 4 factors can account for 90% of the variation of the samples. Each sample is then expressed in terms of these factors and factor plots of two factors are constructed. For example, a factor plot of factor 1 vs. factor 2 will express in a two dimensional plot perhaps 80% of the sample variability. The factor plot can be considered a generalized petrographic diagram and the problem is then simply a visual one where it is necessary to interpret the sample patterns in terms of geologic processes. Similar samples plot close together.

## APPENDIX E

Analytical data and sample locations for Mistastin Lake.  
 Sample locations are given in terms of the Universal  
 Transverse Mercator Grid. Grid Zone: 20U

| SAMPLE                  | LOCATION  | SAMPLE | LOCATION  |
|-------------------------|-----------|--------|-----------|
| M A N G E R I T E S     |           |        |           |
| LM-2                    | MS 736897 | LM44-7 | MS 791870 |
| LM-5                    | MS 735899 | LM-46A | MS 795870 |
| LM-10B                  | MS 732336 | LM-560 | MS 741913 |
| LM-14                   | MS 782322 | LM-64A | MS 929992 |
| LM-22                   | MS 782333 | TA-609 | MT 763054 |
| LM-25                   | MS 783930 | TA-627 | MT 522005 |
| LM-32                   | MS 799948 | TA-634 | MS 909738 |
| LM-39                   | MS 702068 | TA-680 | MS 725530 |
| LM-40                   | MS 702901 | TA-T35 | MS 800940 |
| LM-43B                  | MS 779871 |        |           |
| A D A M E L L I T E S   |           |        |           |
| LM-8                    | MS 721888 | TA-706 | MS 690481 |
| LM-9A                   | MS 718885 | TA-728 | MS 322205 |
| LM-37C                  | MS 820003 | TA-729 | MS 386214 |
| LM-41C                  | MS 755967 | BT-24  | MS 574920 |
| LM-53                   | MS 750964 | BT-100 | MS 792535 |
| LM-54N                  | MS 747964 | BT-121 | MS 632329 |
| TA-518                  | MS 335795 | BT-143 | MS 528117 |
| TA-519                  | MS 400800 | BT-196 | MS 788663 |
| TA-555                  | MS 512032 | 12759  | MS 557842 |
| TA-601                  | MS 416073 | 12762  | MS 951765 |
| TA-606                  | MS 432143 | 12763  | MS 994861 |
| TA-633                  | MS 841778 | 12781  | MS 537977 |
| TA-654                  | MS 588277 | 12785  | MS 420847 |
| TA-678                  | MS 374408 |        |           |
| A N O R T H O S I T E S |           |        |           |
| LM-29A                  | MS 790940 | LM-51B | MS 753973 |
| LM-29G                  | MS 790940 | TA-707 | MS 612457 |
| LM-30A                  | MS 788945 | 11318  | MS 812932 |
| LM-33A                  | MS 806937 |        |           |
| M E L T                 |           |        |           |
| LM-F-1                  | MS 730913 | LM446A | MS 788872 |
| LM-4A                   | MS 725900 | LM446B | MS 788872 |
| LM-4B                   | MS 725900 | LM-45A | MS 791872 |
| LM-C                    | MS 726900 | LM-48A | MS 757882 |
| LM-7A                   | MS 727889 | LM-48B | MS 757882 |
| LM-7B                   | MS 727889 | LM-48D | MS 757882 |
| LM-34C                  | MS 802933 | LM-48F | MS 757882 |
| LM-38A                  | MS 798008 | LM-51Z | MS 751971 |
| LM-38B                  | MS 798008 | LM51BA | MS 751971 |
| LM-38C                  | MS 798008 | LM51EE | MS 751971 |
| LM-41A                  | MS 754966 | S1TTCE | MS 751971 |
| LM-41M                  | MS 754966 | S1TTTP | MS 751971 |
| LM-43A                  | MS 778872 | LM-52A | MS 752970 |
| LM-43D                  | MS 778872 | LM-52B | MS 752970 |
| LM-44A                  | MS 788872 | LM-52X | MS 752970 |
| LM442C                  | MS 788872 | LM-55A | MS 745942 |
| LM444B                  | MS 788872 | LM-55I | MS 745942 |
| LM444C                  | MS 788872 | LM-57  | MS 738909 |
| LM445A                  | MS 788872 | LM-58  | MS 731907 |
| LM445B                  | MS 788872 | TA-T30 | MS 727900 |

## M A N G E R I T E S

|         | NB   | ZR     | Y    | SR    | U   | RB    | TH   | PB   | ZN    | CU   | NI   |
|---------|------|--------|------|-------|-----|-------|------|------|-------|------|------|
| LM-2    | 21.9 | 644.5  | 50.3 | 294.3 | 0.0 | 57.8  | 9.9  | 20.5 | 105.1 | 19.7 | 8.5  |
| LM-5    | 25.4 | 613.9  | 44.4 | 303.9 | 0.0 | 83.1  | 10.8 | 29.9 | 107.5 | 0.0  | 22.8 |
| LM-1UB  | 20.6 | 692.7  | 43.9 | 252.1 | 1.0 | 67.7  | 9.1  | 23.2 | 132.3 | 8.8  | 8.4  |
| LM-14   | 29.5 | 854.9  | 73.5 | 269.0 | 0.0 | 46.0  | 5.3  | 21.4 | 193.3 | 0.0  | 29.2 |
| LM-22   | 18.0 | 656.6  | 50.0 | 321.9 | 0.0 | 56.8  | 6.5  | 21.3 | 131.2 | 0.0  | 18.4 |
| LM-25   | 32.9 | 1024.0 | 79.2 | 289.7 | .1  | 40.4  | 4.6  | 19.2 | 206.8 | 0.0  | 20.3 |
| LM-32   | 18.0 | 706.0  | 44.8 | 333.2 | .5  | 38.1  | 5.0  | 19.2 | 131.1 | 0.0  | 16.2 |
| LM-39   | 10.4 | 543.9  | 30.1 | 501.4 | 0.0 | 44.6  | 2.6  | 18.2 | 115.1 | 0.0  | 10.3 |
| LM-40   | 42.1 | 821.8  | 69.1 | 302.7 | 0.0 | 72.6  | 9.8  | 26.0 | 166.6 | 0.0  | 28.6 |
| LM44-3B | 25.0 | 793.7  | 53.5 | 286.3 | 0.0 | 68.3  | 9.3  | 23.6 | 158.3 | 0.0  | 23.0 |
| LM44-7  | 23.9 | 774.7  | 50.0 | 298.0 | 0.0 | 83.2  | 9.0  | 27.2 | 105.3 | 0.0  | 24.5 |
| LM-46A  | 20.9 | 636.2  | 47.0 | 304.2 | 0.0 | 62.8  | 6.5  | 24.5 | 108.2 | 0.0  | 22.6 |
| LM-50D  | 34.2 | 910.3  | 57.9 | 256.7 | 0.0 | 95.7  | 11.1 | 30.0 | 172.4 | 0.6  | 23.7 |
| LM-64A  | 36.8 | 745.1  | 68.4 | 292.5 | 0.0 | 97.8  | 15.9 | 28.3 | 130.1 | 0.0  | 31.4 |
| TA-609  | 18.7 | 574.2  | 41.7 | 445.5 | 1.3 | 47.4  | 4.3  | 20.1 | 129.5 | 0.0  | 17.8 |
| TA-627  | 18.5 | 745.7  | 35.8 | 324.7 | .2  | 73.6  | 8.3  | 24.5 | 104.5 | 0.0  | 11.8 |
| TA-634  | 37.4 | 572.4  | 30.3 | 348.3 | 0.0 | 90.9  | 3.7  | 25.0 | 56.8  | 0.0  | 12.4 |
| TA-68U  | 35.1 | 780.0  | 58.0 | 254.0 | 0.0 | 126.7 | 13.1 | 32.3 | 137.7 | 0.0  | 27.7 |
| TA-T35  | 28.3 | 904.3  | 67.6 | 319.8 | 1.3 | 43.5  | 5.9  | 21.7 | 189.1 | 0.0  | 26.1 |

## A D A M E L L I T E S

|        |      |        |       |       |     |       |       |      |       |     |      |
|--------|------|--------|-------|-------|-----|-------|-------|------|-------|-----|------|
| LM-8   | 2.3  | 221.4  | 16.1  | 387.4 | 0.0 | 256.9 | 6.7   | 52.1 | 9.5   | 0.0 | 25.4 |
| LM-9A  | 15.1 | 322.5  | 28.4  | 274.4 | 0.0 | 130.4 | 8.7   | 34.3 | 58.8  | 0.0 | 23.7 |
| LM-37C | 4.4  | 275.5  | 19.5  | 247.6 | 0.0 | 138.2 | 6.6   | 29.6 | 29.2  | 0.0 | 15.2 |
| LM-41C | 18.8 | 725.0  | 25.7  | 328.2 | 0.0 | 111.0 | 13.0  | 24.7 | 46.8  | 0.0 | 13.0 |
| LM-53  | 20.0 | 509.0  | 43.8  | 317.2 | 0.0 | 89.3  | 9.9   | 25.9 | 101.9 | .4  | 22.0 |
| LM-54H | 19.9 | 548.7  | 50.4  | 289.3 | .9  | 65.5  | 10.1  | 25.7 | 87.2  | 0.0 | 20.1 |
| TA-518 | 19.9 | 479.0  | 42.6  | 226.5 | 0.0 | 129.4 | 9.2   | 34.8 | 66.9  | 0.0 | 23.1 |
| TA-519 | 24.4 | 668.3  | 40.8  | 255.2 | 0.0 | 104.6 | 20.3  | 32.3 | 99.2  | 0.0 | 20.5 |
| TA-555 | 12.4 | 353.3  | 27.3  | 163.3 | 0.0 | 116.8 | 5.6   | 27.0 | 42.6  | 0.0 | 16.4 |
| TA-601 | 49.9 | 487.6  | 71.3  | 120.4 | 0.0 | 273.4 | 20.1  | 56.0 | 98.8  | 0.0 | 43.1 |
| TA-606 | 61.7 | 936.2  | 76.5  | 205.5 | 0.0 | 226.7 | 26.0  | 57.3 | 149.3 | 0.0 | 36.7 |
| TA-633 | 1.9  | 209.2  | 7.2   | 518.7 | .3  | 104.1 | 3.7   | 30.7 | 6.8   | 2.6 | 10.9 |
| TA-654 | 39.6 | 504.0  | 48.9  | 179.0 | 0.0 | 206.2 | 15.4  | 44.4 | 87.8  | 0.0 | 31.4 |
| TA-678 | 35.0 | 576.0  | 63.1  | 121.7 | 0.0 | 210.0 | 17.9  | 43.8 | 67.7  | 0.0 | 37.6 |
| TA-706 | 0.0  | 290.0  | 15.2  | 358.0 | 0.0 | 170.0 | 5.1   | 39.7 | 26.5  | 0.0 | 17.1 |
| TA-728 | 53.4 | 557.4  | 75.2  | 101.1 | 0.0 | 246.4 | 36.9  | 42.8 | 96.5  | 0.0 | 46.1 |
| TA-729 | 60.0 | 527.5  | 133.3 | 123.5 | 0.0 | 253.1 | 227.8 | 67.4 | 118.7 | 0.0 | 73.4 |
| BT-24  | 14.4 | 382.6  | 20.0  | 224.7 | 0.0 | 161.2 | 15.0  | 38.8 | 47.9  | 0.0 | 17.1 |
| BT-100 | 22.5 | 199.7  | 49.9  | 87.6  | 0.0 | 175.9 | 17.9  | 32.8 | 38.6  | 0.0 | 38.2 |
| BT-121 | 14.7 | 126.4  | 18.8  | 190.8 | 0.0 | 174.4 | 34.8  | 43.5 | 56.2  | 0.0 | 20.3 |
| BT-143 | 13.2 | 459.4  | 29.4  | 279.1 | 0.0 | 195.3 | 13.2  | 46.7 | 63.9  | 0.0 | 24.3 |
| BT-196 | 25.4 | 601.2  | 52.3  | 272.0 | 0.0 | 123.7 | 10.8  | 33.9 | 91.1  | 0.0 | 22.2 |
| 12759  | 21.4 | 491.2  | 32.0  | 225.2 | 0.0 | 137.3 | 13.2  | 34.9 | 66.6  | 0.0 | 25.3 |
| 12762  | 15.9 | 371.9  | 35.2  | 275.0 | 0.0 | 108.3 | 15.5  | 31.1 | 75.2  | 0.0 | 22.4 |
| 12763  | 9.4  | 253.5  | 32.1  | 307.9 | 0.0 | 95.5  | 16.6  | 27.7 | 63.5  | 0.0 | 23.8 |
| 12781  | 18.3 | 427.8  | 20.6  | 311.0 | 0.0 | 284.4 | 9.3   | 45.2 | 29.2  | 0.0 | 27.0 |
| 12785  | 0.0  | 1299.3 | 8.2   | 268.4 | 0.0 | 142.2 | 6.5   | 32.9 | 13.4  | .9  | 13.3 |

M A N G E R I T E S

|        | SI02  | AL 203 | TI02 | FE203 | MNO | MGO  | CAO  | NA2O | K2O  | P2O5 |
|--------|-------|--------|------|-------|-----|------|------|------|------|------|
| LM-2   | 62.96 | 14.51  | 1.10 | 8.76  | .08 | .95  | 4.85 | 3.09 | 3.28 | .50  |
| LM-5   | 63.32 | 14.64  | 1.04 | 8.30  | .07 | .78  | 4.28 | 3.10 | 3.96 | .57  |
| LM-10B | 62.71 | 13.87  | 1.02 | 9.29  | .10 | 1.24 | 4.47 | 2.98 | 3.52 | .68  |
| LM-14  | 55.81 | 13.18  | 1.42 | 14.33 | .28 | 2.06 | 6.16 | 2.56 | 2.55 | 1.17 |
| LM-22  | 61.66 | 14.43  | 1.07 | 9.64  | .07 | .99  | 4.87 | 3.14 | 3.54 | .76  |
| LM-25  | 57.47 | 13.01  | 1.63 | 13.61 | .19 | 1.54 | 5.48 | 2.82 | 2.50 | 1.34 |
| LM-32  | 62.29 | 14.71  | 1.04 | 8.79  | .08 | .89  | 5.16 | 3.37 | 3.04 | .75  |
| LM-39  | 63.62 | 16.58  | .85  | 5.63  | .07 | .65  | 5.80 | 3.38 | 4.17 | .53  |
| LM-40  | 60.51 | 14.78  | 1.35 | 10.66 | .07 | .89  | 4.52 | 3.46 | 3.39 | .74  |
| LM-43B | 63.42 | 13.94  | 1.28 | 8.37  | .07 | .86  | 4.53 | 3.13 | 3.67 | .75  |
| LM44-7 | 61.94 | 14.03  | 1.31 | 9.96  | .08 | .73  | 4.35 | 3.02 | 3.97 | .81  |
| LM-46A | 64.16 | 14.87  | .90  | 7.47  | .10 | .63  | 4.01 | 3.27 | 4.14 | .56  |
| LM-560 | 61.80 | 13.42  | 1.31 | 10.22 | .08 | .93  | 4.23 | 2.75 | 4.47 | .93  |
| LM-64A | 64.09 | 13.86  | 1.09 | 8.56  | .07 | .84  | 4.18 | 3.18 | 3.70 | .45  |
| TA-609 | 60.66 | 16.50  | 1.17 | 8.70  | .07 | .75  | 4.97 | 3.70 | 3.36 | .48  |
| TA-627 | 64.83 | 15.15  | .91  | 6.78  | .07 | .65  | 4.04 | 3.39 | 3.94 | .27  |
| TA-634 | 67.46 | 14.64  | 1.37 | 4.11  | .06 | .80  | 4.56 | 3.70 | 5.60 | .37  |
| TA-680 | 66.04 | 12.97  | 1.01 | 8.22  | .07 | .71  | 2.59 | 2.69 | 5.32 | .32  |
| TA-T35 | 57.53 | 13.80  | 1.47 | 12.25 | .18 | 1.44 | 5.57 | 2.78 | 3.29 | 1.28 |

A D A M E L L I T E S

|        |       |       |     |      |     |     |      |      |      |     |
|--------|-------|-------|-----|------|-----|-----|------|------|------|-----|
| LM-8   | 66.40 | 18.32 | .15 | 1.88 | .06 | .17 | .93  | 3.07 | 9.48 | .06 |
| LM-9A  | 68.11 | 15.04 | .53 | 4.20 | .06 | .46 | 2.41 | 3.20 | 5.75 | .20 |
| LM-37C | 76.75 | 11.19 | .32 | 2.20 | .06 | .23 | 2.98 | 2.53 | 5.61 | .07 |
| LM-41C | 70.53 | 13.69 | .72 | 3.54 | .06 | .29 | 2.28 | 2.34 | 5.44 | .15 |
| LM-53  | 64.78 | 15.03 | .88 | 6.80 | .06 | .54 | 3.85 | 3.26 | 4.43 | .37 |
| LM-54N | 65.59 | 16.15 | .73 | 5.16 | .06 | .55 | 4.00 | 3.71 | 3.94 | .25 |
| TA-518 | 68.24 | 14.25 | .53 | 4.73 | .18 | .58 | 2.39 | 3.11 | 5.58 | .15 |
| TA-519 | 64.36 | 15.80 | .86 | 6.64 | .07 | .57 | 3.52 | 3.90 | 4.75 | .24 |
| TA-555 | 77.42 | 10.63 | .33 | 2.50 | .06 | .25 | 1.20 | 2.46 | 4.18 | .04 |
| TA-EU1 | 70.01 | 15.11 | .28 | 2.82 | .06 | .12 | 1.16 | 3.38 | 7.01 | .07 |
| TA-60E | 63.55 | 17.63 | .50 | 4.97 | .07 | .27 | 2.63 | 4.26 | 6.34 | .14 |
| TA-653 | 71.51 | 16.07 | .12 | 3.93 | .06 | .16 | 2.63 | 4.14 | 7.70 | .05 |
| TA-654 | 67.61 | 16.12 | .35 | 3.80 | .06 | .19 | 1.68 | 3.64 | 6.58 | .09 |
| TA-678 | 72.17 | 13.21 | .36 | 3.29 | .06 | .17 | 1.18 | 2.94 | 6.55 | .08 |
| TA-706 | 66.02 | 18.51 | .20 | 1.81 | .06 | .23 | 1.22 | 3.28 | 9.17 | .07 |
| TA-728 | 72.37 | 12.39 | .45 | 3.77 | .06 | .23 | 1.12 | 2.73 | 6.27 | .09 |
| TA-729 | 69.38 | 15.01 | .35 | 3.51 | .06 | .12 | 1.72 | 3.56 | 6.44 | .07 |
| BT-24  | 70.53 | 14.55 | .47 | 5.09 | .06 | .21 | 1.81 | 3.44 | 5.70 | .12 |
| BT-180 | 76.94 | 10.71 | .30 | 2.96 | .06 | .31 | .78  | 2.50 | 5.02 | .06 |
| BT-121 | 73.61 | 13.40 | .17 | 2.18 | .06 | .19 | .51  | 2.81 | 6.90 | .05 |
| BT-143 | 67.41 | 15.42 | .53 | 3.99 | .06 | .34 | 1.46 | 2.79 | 7.82 | .14 |
| BT-196 | 65.93 | 14.80 | .78 | 6.08 | .07 | .62 | 2.96 | 3.35 | 5.11 | .26 |
| 12759  | 74.23 | 14.03 | .22 | 2.99 | .06 | .31 | 2.92 | 4.05 | 1.16 | .05 |
| 12762  | 66.27 | 15.77 | .61 | 5.01 | .06 | .42 | 3.19 | 3.77 | 4.81 | .19 |
| 12763  | 66.47 | 16.12 | .57 | 4.60 | .06 | .44 | 3.54 | 3.95 | 4.72 | .18 |
| 12781  | 66.34 | 17.99 | .27 | 2.25 | .06 | .19 | 1.83 | 3.76 | 7.72 | .10 |
| 12785  | 74.97 | 13.10 | .11 | 1.44 | .06 | .22 | .74  | 2.56 | 6.73 | .05 |

M E L T

|         | NB   | ZR    | Y    | SR    | U   | RB   | TH  | PB   | ZN    | CU   | NI   |
|---------|------|-------|------|-------|-----|------|-----|------|-------|------|------|
| LM-F-1  | 33.3 | 727.6 | 46.0 | 364.7 | 0.0 | 63.4 | 6.5 | 21.1 | 133.0 | 0.0  | 21.5 |
| LM-4A   | 16.0 | 438.1 | 32.1 | 476.1 | 7.5 | 51.1 | 7.3 | 14.7 | 99.0  | 0.0  | 15.0 |
| LM-4B   | 16.8 | 457.0 | 35.1 | 488.8 | 7.5 | 44.0 | 7.6 | 17.3 | 97.0  | 1.0  | 16.3 |
| LM-6    | 9.2  | 392.7 | 30.5 | 519.6 | 3.1 | 49.3 | 8.1 | 15.8 | 66.0  | 4.5  | 24.7 |
| LM-7A   | 9.4  | 370.0 | 25.5 | 543.2 | 3.1 | 43.8 | 8.0 | 15.1 | 66.6  | 9.9  | 20.9 |
| LM-7B   | 10.1 | 383.0 | 29.1 | 574.9 | 0.0 | 46.1 | 7.7 | 15.4 | 67.4  | 6.4  | 21.5 |
| LM-34C  | 0.0  | 209.5 | 14.9 | 974.9 | 5.7 | 17.2 | 1.1 | 1.9  | 28.4  | 1.1  | 15.8 |
| LM-38A  | 5.3  | 327.1 | 25.5 | 553.6 | 2.1 | 32.6 | 4.3 | 12.0 | 64.0  | 4.5  | 30.6 |
| LM-38B  | 3.4  | 378.8 | 26.8 | 507.4 | 3.4 | 39.7 | 4.3 | 14.7 | 79.7  | 1.1  | 31.2 |
| LM-38C  | 1.3  | 510.8 | 32.2 | 630.5 | 4.8 | 41.1 | 5.3 | 15.5 | 83.4  | 8.8  | 27.2 |
| LM-41A  | 3.0  | 165.5 | 13.3 | 810.5 | 4.3 | 22.2 | 3.3 | 7.7  | 54.9  | 8.7  | 17.8 |
| LM-41M  | 4.6  | 171.5 | 12.1 | 631.0 | 3.5 | 22.9 | 2.7 | 7.7  | 54.0  | 8.6  | 17.8 |
| LM-43A  | 5.9  | 205.9 | 23.4 | 528.6 | 3.6 | 22.8 | 5.7 | 10.4 | 73.7  | 11.3 | 20.2 |
| LM-43D  | 5.5  | 218.8 | 21.7 | 556.3 | 3.4 | 22.4 | 5.1 | 9.6  | 70.5  | 11.1 | 17.7 |
| LM-44A  | 7.1  | 197.8 | 22.6 | 585.4 | 2.2 | 30.5 | 5.5 | 11.1 | 70.5  | 11.1 | 17.7 |
| LM442C  | 0.0  | 15.0  | 3.3  | 598.8 | 8.4 | 2.7  | 1.1 | 5.5  | 0.9   | 14.3 | 6.7  |
| LM444B  | 2.9  | 160.3 | 15.8 | 655.5 | 4.3 | 23.8 | 2.2 | 7.7  | 6.4   | 14.4 | 25.6 |
| LM444C  | 4.4  | 153.3 | 14.7 | 622.4 | 6.1 | 21.9 | 6.4 | 8.8  | 5.3   | 10.7 | 19.0 |
| LM445A  | 5.0  | 203.8 | 17.6 | 512.6 | 5.5 | 13.3 | 3.3 | 7.7  | 5.8   | 10.9 | 16.5 |
| LM445B  | 8.6  | 232.3 | 22.7 | 552.4 | 7.5 | 11.1 | 3.6 | 9.9  | 5.4   | 9.9  | 15.0 |
| LM446A  | 3.8  | 177.8 | 16.1 | 584.9 | 2.2 | 22.8 | 6.4 | 6.6  | 11.9  | 9.9  | 19.2 |
| LM446B  | 6.4  | 181.0 | 14.5 | 588.5 | 2.2 | 20.3 | 5.5 | 9.9  | 11.1  | 10.4 | 20.5 |
| LM-45A  | 4.4  | 144.4 | 12.8 | 603.5 | 2.2 | 19.0 | 6.6 | 9.9  | 4.3   | 12.4 | 22.5 |
| LM-48A  | 8.7  | 251.0 | 22.6 | 537.3 | 7.9 | 4.0  | 1.1 | 13.3 | 6.8   | 13.4 | 23.4 |
| LM-48B  | 8.8  | 299.9 | 25.2 | 499.6 | 1.6 | 4.5  | 9.9 | 14.4 | 6.2   | 3.0  | 21.9 |
| LM-48D  | 6.9  | 231.7 | 18.8 | 565.0 | 1.1 | 3.4  | 9.9 | 9.9  | 7.7   | 1.0  | 18.5 |
| LM-48F  | 2.0  | 62.8  | 4.3  | 346.2 | 2.2 | 8.0  | 1.1 | 2.2  | 2.2   | 1.0  | 22.6 |
| LM-51Z  | 4.4  | 161.5 | 24.5 | 570.6 | 6.6 | 15.3 | 3.3 | 8.8  | 7.4   | 1.1  | 33.6 |
| LM51BA  | 8.3  | 277.4 | 24.0 | 522.2 | 5.0 | 31.7 | 3.3 | 12.2 | 6.0   | 1.1  | 33.3 |
| LM51EE  | 1.0  | 452.3 | 29.8 | 467.8 | 2.6 | 43.9 | 4.4 | 16.9 | 6.0   | 5.0  | 26.5 |
| LM51TT  | 2.4  | 158.9 | 12.8 | 648.8 | 7.9 | 10.0 | 8.8 | 6.6  | 7.7   | 10.0 | 22.2 |
| LM51TP  | 5.5  | 180.3 | 14.4 | 633.9 | 3.7 | 14.7 | 2.2 | 3.3  | 6.6   | 9.9  | 21.9 |
| LM-52A  | 8.2  | 289.3 | 22.9 | 579.9 | 3.3 | 32.9 | 2.2 | 10.0 | 5.5   | 1.1  | 33.3 |
| LM-52B  | 4.4  | 296.6 | 18.9 | 574.4 | 2.2 | 29.7 | 4.4 | 10.2 | 6.6   | 1.1  | 25.8 |
| LM-52XA | 7.4  | 290.3 | 19.2 | 555.0 | 2.0 | 25.1 | 3.3 | 10.8 | 5.5   | 1.1  | 17.9 |
| LM-55A  | 9.5  | 358.8 | 24.3 | 522.2 | 6.8 | 35.0 | 5.5 | 12.9 | 6.4   | 14.5 | 19.2 |
| LM-55I  | 1.0  | 363.6 | 26.7 | 527.8 | 6.8 | 31.0 | 5.5 | 12.2 | 6.6   | 13.5 | 19.0 |
| LM-57   | 9.4  | 360.4 | 29.0 | 586.5 | 7.9 | 30.3 | 3.3 | 13.3 | 8.8   | 20.6 | 29.3 |
| LM-58   | 14.7 | 366.1 | 31.1 | 468.3 | 6.6 | 49.6 | 9.9 | 17.3 | 9.3   | 11.3 | 17.5 |
| TA-T30  | 16.7 | 408.1 | 30.6 | 486.4 | 0.0 | 50.7 | 7.4 | 14.9 | 6.8   | 2.3  | 26.2 |

A N O R T H O S I T E S

|        |     |      |     |       |     |      |    |     |      |      |      |
|--------|-----|------|-----|-------|-----|------|----|-----|------|------|------|
| LM-29A | 0.0 | 6.2  | 1.1 | 742.3 | 4.7 | 31.2 | .1 | 2.1 | 8.1  | 17.6 | 12.8 |
| LM-29G | 0.0 | 10.2 | 2.0 | 735.1 | 4.7 | 9.1  | .9 | 2.7 | 0.6  | 15.3 | 29.9 |
| LM-30A | 0.0 | 21.1 | 5.2 | 752.6 | 7.4 | 4.5  | .8 | 5.2 | 11.9 | 11.7 | 12.1 |
| LM-33A | 0.0 | 23.7 | 5.5 | 724.4 | 7.0 | 4.9  | .7 | 5.8 | 20.3 | 10.2 | 9.6  |
| LM-51B | 1.1 | 22.7 | 3.0 | 773.7 | 6.7 | 10.4 | .0 | 7.7 | 19.6 | 14.2 | 16.3 |
| TA-707 | .8  | 51.0 | 9.9 | 732.3 | 7.2 | 7.1  | .4 | 6.5 | 4.5  | 54.9 | 57.3 |
| 11318  | 0.0 | 17.6 | 3.3 | 691.6 | 4.8 | 4.0  | .1 | 2.3 | 3.4  | 11.2 | 27.1 |

M E L T

|        | SI02   | AL203 | TIO2 | FE203 | MNO | MGO  | CAU  | NA2O | K2O  | P2O5 |
|--------|--------|-------|------|-------|-----|------|------|------|------|------|
| LM-F-1 | 561.85 | 14.96 | 1.25 | 9.63  | .07 | .80  | 4.35 | 3.31 | 3.76 | .28  |
| LM-4A  | 58.15  | 18.17 | 1.15 | 7.75  | .11 | 1.42 | 6.78 | 3.45 | 2.73 | .34  |
| LM-4B  | 58.18  | 17.92 | 1.19 | 8.26  | .13 | 1.22 | 6.86 | 3.65 | 2.27 | .35  |
| LM-6   | 59.40  | 19.16 | .96  | 6.24  | .08 | 1.00 | 6.87 | 3.79 | 2.54 | .37  |
| LM-7A  | 58.88  | 19.20 | .93  | 6.13  | .11 | 1.02 | 7.31 | 3.89 | 3.55 | .42  |
| LM-7B  | 59.16  | 18.96 | .96  | 6.19  | .10 | .88  | 7.13 | 3.93 | 2.52 | .40  |
| LM-34C | 57.13  | 22.00 | .78  | 4.49  | .09 | .80  | 9.93 | 3.44 | 1.47 | .19  |
| LM-38A | 58.96  | 18.90 | .86  | 6.22  | .16 | 1.90 | 7.07 | 3.68 | 2.24 | .31  |
| LM-38B | 60.29  | 18.28 | .87  | 6.10  | .11 | 1.52 | 6.53 | 3.45 | 2.71 | .25  |
| LM-38C | 60.41  | 17.38 | 1.01 | 7.03  | .10 | 1.38 | 6.17 | 3.36 | 2.79 | .33  |
| LM-41A | 57.23  | 21.59 | 1.01 | 4.68  | .08 | .74  | 8.80 | 4.29 | 1.55 | .37  |
| LM-41M | 57.58  | 22.12 | .98  | 4.52  | .07 | .67  | 8.52 | 4.16 | 1.57 | .40  |
| LM-43A | 53.89  | 18.31 | 1.26 | 9.47  | .23 | 2.31 | 9.61 | 3.26 | 1.46 | .30  |
| LM-43D | 55.47  | 18.94 | 1.25 | 9.72  | .15 | 2.35 | 8.08 | 3.52 | 1.43 | .29  |
| LM-44A | 57.11  | 20.38 | .85  | 5.47  | .09 | 2.16 | 8.51 | 3.89 | 1.72 | .28  |
| LM442C | 53.81  | 21.49 | .44  | 6.63  | .11 | 3.90 | 9.34 | 3.80 | 1.45 | .09  |
| LM444B | 56.01  | 21.22 | .78  | 5.13  | .08 | 2.03 | 8.81 | 4.17 | 1.54 | .25  |
| LM444C | 57.34  | 21.50 | .75  | 4.32  | .08 | 1.70 | 8.99 | 4.27 | 1.48 | .25  |
| LM445A | 56.61  | 20.98 | .88  | 4.07  | .09 | 1.07 | 8.94 | 4.10 | 1.50 | .33  |
| LM445B | 57.45  | 20.33 | .87  | 5.96  | .10 | 1.30 | 8.19 | 4.13 | 1.79 | .32  |
| LM446A | 57.21  | 20.75 | .83  | 5.24  | .09 | 1.94 | 8.55 | 3.97 | 1.69 | .26  |
| LM446B | 56.74  | 21.53 | .80  | 5.95  | .10 | 1.54 | 8.96 | 4.54 | 1.28 | .25  |
| LM-48A | 58.75  | 19.55 | .95  | 5.99  | .13 | 1.30 | 7.67 | 3.89 | 2.07 | .31  |
| LM-48B | 59.13  | 18.73 | .95  | 6.07  | .11 | 1.48 | 7.35 | 3.54 | 2.48 | .31  |
| LM-48D | 57.73  | 20.00 | .91  | 5.75  | .10 | 1.67 | 8.05 | 3.94 | 1.89 | .33  |
| LM-48F | 62.77  | 16.00 | 1.06 | 5.45  | .08 | .76  | 4.68 | 3.41 | 3.62 | .35  |
| LM-51Z | 55.45  | 21.41 | .93  | 5.63  | .11 | 1.99 | 9.13 | 4.39 | 1.21 | .40  |
| LM51BA | 58.28  | 19.66 | .94  | 5.86  | .09 | 1.51 | 7.67 | 4.03 | 2.02 | .25  |
| LM51EE | 59.05  | 16.86 | 1.25 | 8.47  | .14 | 1.48 | 6.26 | 3.26 | 2.70 | .41  |
| LM51TT | 55.55  | 21.46 | .92  | 5.62  | .10 | 2.04 | 9.19 | 4.44 | 1.08 | .25  |
| LM51TP | 56.01  | 21.27 | .93  | 5.56  | .09 | 1.83 | 8.91 | 4.47 | 1.25 | .27  |
| LM-52A | 58.18  | 19.86 | .96  | 5.84  | .09 | 1.36 | 7.71 | 4.09 | 2.00 | .27  |
| LM-52B | 57.53  | 20.36 | .98  | 5.65  | .10 | 1.60 | 8.00 | 4.13 | 1.81 | .28  |
| LM-52X | 57.78  | 20.31 | 1.00 | 6.09  | .10 | 1.36 | 7.67 | 3.99 | 1.67 | .27  |
| LM-55A | 58.03  | 18.90 | 1.10 | 7.04  | .12 | 1.22 | 7.29 | 3.97 | 2.16 | .37  |
| LM-55I | 57.75  | 18.45 | 1.17 | 7.74  | .12 | 1.37 | 7.14 | 3.70 | 2.21 | .46  |
| LM-57  | 54.62  | 19.37 | 1.35 | 8.62  | .12 | 1.93 | 8.42 | 3.81 | 1.68 | .32  |
| LM-58  | 58.24  | 17.83 | 1.12 | 7.85  | .10 | 1.96 | 6.70 | 3.41 | 2.50 | .30  |
| TA-T30 | 59.17  | 19.79 | .99  | 6.47  | .07 | .94  | 6.53 | 3.87 | 2.57 | .33  |

A N O R T H O S I T E S

|        |       |       |     |      |     |      |       |      |      |     |
|--------|-------|-------|-----|------|-----|------|-------|------|------|-----|
| LM-29A | 57.77 | 23.05 | .21 | 1.48 | .07 | 1.07 | 9.39  | 5.30 | 2.08 | .05 |
| LM-29G | 53.96 | 22.62 | .29 | 4.83 | .09 | 4.75 | 8.44  | 4.26 | .71  | .07 |
| LM-30A | 56.53 | 23.49 | .45 | 1.80 | .07 | .71  | 11.26 | 5.20 | .65  | .19 |
| LM-33A | 57.08 | 22.46 | .31 | 3.26 | .10 | .95  | 10.53 | 4.58 | .86  | .18 |
| LM-31B | 59.37 | 23.05 | .45 | 1.73 | .08 | .57  | 10.32 | 4.81 | .92  | .14 |
| TA-707 | 55.73 | 22.72 | .65 | 3.78 | .08 | .85  | 10.51 | 4.58 | 1.18 | .25 |
| 11318  | 55.93 | 22.08 | .41 | 4.93 | .09 | 2.61 | 10.16 | 3.59 | .72  | .14 |



## APPENDIX F

Sudbury samples: trace element data, descriptions and locations.

## Abbreviations

|        |                    |       |                   |
|--------|--------------------|-------|-------------------|
| BR.    | Breccia            | MG.   | Medium-grained    |
| COMP.  | Composition        | MPG.  | Micropegmatite    |
| D.D.H. | Diamond Drill Hole | N.    | North             |
| DEVIT. | Devitrified        | PL.   | Plagioclase       |
| DIFF.  | Different          | POP.  | Population        |
| DK.    | Dark               | PYRR  | Pyrrhotite        |
| FELD.  | Feldspathic        | QD    | Quartz Diorite    |
| FG.    | Fine-grained       | S.    | South             |
| FM.    | Formation          | SPHER | Spherulitic       |
| FRACT. | Fraction           | SUBL  | Sub-layer         |
| FRAG.  | Fragment           | TEXT  | Texture           |
| INCL.  | Inclusion          | VFG.  | Very Fine-grained |
| LT.    | Less Than          | XLINE | Crystalline       |

## SAMPLE LOCATIONS

Locations are easily placed by referring to the Ontario Department of Mines MAP 2170, 'The Sudbury Mining Area' (1968).

The samples of melt, country rock inclusions from the Onaping Formation, the basal breccia matrix, and the plagioclase micropegmatite are from Dowling Township near High Falls on the Onaping River; between the CPR railway tracks and Highway 144 (Fig. 3-3), unless otherwise indicated in the sample descriptions.

Norite samples: W- samples from Gibbins (1973); from Longvac Mine area near Levack; from the Whistle property in Norman Township.

Grey Breccia: From Longvac Mine and Strathcona Mine area near Levack; from Sultana property at western edge of the Irruptive in Drury Township.

Sub-layer: From Longvac Mine; from Sultana property; from Whistle property; from the Copper Cliff offset near the Copper Cliff North Mine; from the Foy offset at the northern end in southwest Tyrone Township.

M E L T R O C K

|        | NB   | ZR    | Y    | SR    | U   | RB    | TH   | PB   | ZN    | CU   | NI   |
|--------|------|-------|------|-------|-----|-------|------|------|-------|------|------|
| DW-19  | 7.4  | 169.9 | 22.1 | 269.1 | 4.9 | 31.4  | 12.7 | 5.8  | 67.5  | 51.7 | 79.2 |
| DW-61A | 8.5  | 120.1 | 12.6 | 180.6 | 0.0 | 108.0 | 10.2 | 70.8 | 79.3  | 64.0 | 32.4 |
| DW-102 | 7.4  | 145.1 | 16.2 | 240.2 | 6.8 | 89.0  | 13.8 | 18.6 | 65.1  | 71.5 | 42.1 |
| DW-108 | 5.2  | 159.4 | 16.2 | 292.6 | 6.8 | 89.8  | 15.8 | 9.5  | 65.7  | 10.8 | 48.6 |
| DW-109 | 7.9  | 137.0 | 25.1 | 253.6 | 3.1 | 103.3 | 11.3 | 7.1  | 63.2  | 17.9 | 48.3 |
| DW116B | 38.2 | 674.8 | 12.8 | 111.3 | 3.0 | 142.3 | 12.9 | 27.7 | 66.3  | 60.3 | 44.1 |
| DW-184 | 7.0  | 164.1 | 20.2 | 389.3 | 5.4 | 76.4  | 11.5 | 10.2 | 59.3  | 33.8 | 44.1 |
| DW-200 | 6.3  | 166.7 | 18.6 | 365.3 | 6.6 | 66.9  | 13.1 | 10.9 | 73.3  | 33.5 | 68.8 |
| DW221B | 7.6  | 150.6 | 15.1 | 308.4 | 5.8 | 74.8  | 13.0 | 12.9 | 60.7  | 43.0 | 42.8 |
| DW-235 | 2.4  | 121.7 | 13.3 | 342.0 | 5.1 | 65.4  | 8.4  | 8.8  | 66.6  | 3.3  | 64.5 |
| DW235X | 3.3  | 123.3 | 13.1 | 342.6 | 5.8 | 67.8  | 6.8  | 7.7  | 64.0  | 4.9  | 68.0 |
| DW-245 | 6.0  | 155.0 | 15.6 | 278.9 | 6.0 | 86.7  | 11.8 | 16.3 | 61.8  | 54.9 | 43.7 |
| DK245X | 6.1  | 154.4 | 15.9 | 282.3 | 1.7 | 86.5  | 10.5 | 12.9 | 57.6  | 57.9 | 43.5 |
| DW245A | 8.2  | 154.3 | 16.1 | 273.5 | 7.4 | 84.9  | 13.3 | 13.7 | 61.1  | 54.8 | 41.4 |
| DW-248 | 9.8  | 159.9 | 18.1 | 374.9 | 5.4 | 111.7 | 12.7 | 14.3 | 65.2  | 10.6 | 45.8 |
| DW297B | 11.0 | 135.5 | 15.8 | 52.2  | 3.9 | 51.1  | 10.2 | 13.6 | 21.3  | 2.5  | 91.5 |
| DW343B | 10.3 | 164.7 | 15.7 | 261.5 | 3.0 | 92.7  | 13.4 | 7.1  | 170.3 | 32.5 | 41.6 |
| DW-388 | 7.7  | 193.4 | 24.1 | 507.4 | 6.8 | 247.4 | 12.1 | 4.6  | 40.7  | 33.3 | 78.9 |
| DW-431 | 9.3  | 134.0 | 15.1 | 184.8 | 3.5 | 93.8  | 9.3  | 5.5  | 38.7  | 29.9 | 66.4 |
| DW-443 | 7.7  | 163.3 | 14.5 | 262.4 | 3.3 | 32.5  | 12.8 | 5.0  | 38.8  | 32.9 | 66.9 |
| DW-472 | 7.1  | 163.4 | 18.2 | 132.8 | 4.8 | 66.1  | 10.7 | 4.2  | 30.8  | 8.5  | 69.2 |
| DW472X | 8.4  | 160.1 | 18.5 | 137.8 | 4.3 | 64.6  | 12.6 | 6.9  | 32.9  | 4.7  | 68.2 |
| DW-550 | 7.9  | 165.1 | 14.2 | 285.6 | 3.2 | 115.8 | 13.6 | 4.1  | 58.9  | 53.8 | 54.1 |
| DW-551 | 9.0  | 160.4 | 16.1 | 163.6 | 4.0 | 66.4  | 10.6 | 5.0  | 44.4  | 4.8  | 47.2 |
| DW-552 | 12.5 | 159.4 | 12.9 | 118.1 | 4.4 | 44.1  | 12.9 | 7.7  | 179.6 | 45.7 | 50.7 |

DW-19 CHILLED MELT, OK. VFG., AT CONTACT OF BASAL BRECCIA  
 DW-61A CHILLED PHASE OF MELT ROCK AT CONTACT WITH BASAL BRECCIA  
 DW-102 MG. SPHEROIDAL MELT, LT. 1% INCL  
 DW-108 MELT WITH FRESH PYROXENES  
 DW-109 MG. MELT, LT. 1% INCL  
 DW116B MELT, LOWER MELTING FRACT., SPHER. TEXT.,  
 DW-184 MG. MELT  
 DW-200 FG. MELT  
 DW221B MG. FELDSPATHIC MELT, LT. 1% INCLUSIONS  
 DW-235 CHILLED MELT  
 DW235X CHILLED MELT, NO INCLUSIONS  
 DW-245 VFG. CHILLED MELT, CONTACT PHASE NEAR BASAL BRECCIA BODY  
 DW245X VFG. CHILLED MELT, CONTACT PHASE NEAR BASAL BRECCIA BODY, NO INCL  
 DW245A MELT ROCK WITH QUARTZITE INCLUSIONS  
 DW-248 CHILLED PHASE OF MELT ROCK  
 DW297B LT. GREY MELT WITH MAFIC BLOTCHES, NO INCLUSIONS  
 DW343B FG. CHILLED MELT, SPHERULITES, LT. 1% INCL.  
 DW-388 MELT DYKE, DEVIT., GLOBULES AND MATRIX DIFF. COMP., NOW CHLORITE  
 DW-431 VESICULAR MELT ROCK, CARBON + PYRR. IN VESICULES  
 DW-443 FG. MELT, LT 1% INCL.  
 DW-472 DK. GREY GLASS, CHILLED FLOW PHASE OF MELT  
 DW472X DK. GREY GLASS, CHILLED FLOW PHASE OF MELT, NO INCL.  
 DW-550 FG. FELTY MELT, LT 1% INCL.  
 DW-551 MG. FELTY MELT, LT. 1% INCL.  
 DW-552 FG. MELT, FELDSPATHIC, 1% INCL. AS SINGLE SILICA GRAINS

|        | G L A S S I N C L U S I O N S |       |      |       |     |       |      |      |       |      |       |
|--------|-------------------------------|-------|------|-------|-----|-------|------|------|-------|------|-------|
|        | NB                            | ZR    | Y    | SR    | U   | RB    | TH   | PB   | ZN    | CU   | NI    |
| DW-138 | 10.1                          | 168.0 | 18.1 | 186.8 | 3.5 | 52.4  | 11.7 | 7.6  | 74.1  | 21.4 | 63.0  |
| DW-391 | 7.5                           | 167.1 | 18.1 | 152.2 | 4.8 | 8.5   | 10.2 | 5.6  | 27.0  | 41.5 | 90.8  |
| DW-434 | 12.2                          | 178.8 | 29.9 | 52.8  | 4.4 | 12.8  | 10.8 | 21.6 | 32.8  | 3.6  | 82.5  |
| DW434X | 10.7                          | 179.7 | 30.8 | 64.8  | 4.5 | 11.1  | 11.4 | 8.9  | 33.2  | 5.6  | 86.2  |
| GG-2   | 7.7                           | 145.0 | 21.4 | 35.5  | 2.3 | 263.9 | 14.3 | 34.0 | 299.2 | 17.9 | 34.4  |
| GG-3   | 11.6                          | 113.1 | 13.4 | 121.8 | 3.2 | 197.7 | 12.5 | 7.0  | 22.8  | 11.6 | 103.7 |
| P-110  | 8.6                           | 158.8 | 22.6 | 98.4  | 1.9 | 157.8 | 12.3 | 13.9 | 75.7  | 41.3 | 70.4  |

DW-138 BLACK OR GREEN GLASS  
 DW-391 LT. GREY-GREEN GLASS WITH DK. GREY STREAKS, 1-3% INCL.  
 DW-434 MED. GREY GLASS, 1-5% FELD INCLUSIONS,  
 DW434X MED. GREY GLASS, CLEAN OF INCL.  
 GG-2 GREEN GLASS INCLUSION, ONAPING FM.  
 GG-3 GREEN GLASS INCLUSION, ONAPING FM.  
 P-110 FELDSPATHIC COMPLEX GLASS, ONAPING FORMATION, BLUE COLOUR

|        | B A S A L B R E C C I A M A T R I X |       |      |       |     |       |      |      |      |     |      |
|--------|-------------------------------------|-------|------|-------|-----|-------|------|------|------|-----|------|
|        | NB                                  | ZR    | Y    | SR    | U   | RB    | TH   | PB   | ZN   | CU  | NI   |
| DW-384 | 10.6                                | 171.5 | 13.6 | 131.5 | 3.0 | 139.6 | 11.1 | 9.8  | 30.2 | 6.1 | 19.5 |
| G-205A | 19.4                                | 122.1 | 12.6 | 207.6 | 3.7 | 67.3  | 12.7 | 10.7 | 73.7 | 4.8 | 13.3 |

DW-384 BASAL BRECCIA MATRIX, NO INCL.  
 G-205A CONTACT OF PL. MPG. AND LOW FRAG. POP. MATRIX OF QTZITE BR. (A)

|        | P L A G I O C L A S E M I C R O P E G M A T I T E |       |      |       |     |       |      |       |       |      |      |
|--------|---|-------|------|-------|-----|-------|------|-------|-------|------|------|
|        | NB  | ZR    | Y    | SR    | U   | RB    | TH   | PB    | ZN    | CU   | NI   |
| DW-30  | 4.6   | 182.3 | 19.1 | 344.2 | 4.2 | 73.9  | 13.8 | 100.4 | 375.7 | 23.5 | 7.8  |
| DW-32  | 12.1  | 223.0 | 25.7 | 328.6 | 5.7 | 84.0  | 13.6 | 11.6  | 59.9  | 32.6 | 7.3  |
| DW-33  | 9.0   | 209.0 | 25.3 | 200.7 | 2.8 | 96.9  | 12.2 | 15.4  | 108.4 | 32.7 | 6.7  |
| DW-36  | 5.3   | 146.8 | 13.4 | 276.1 | 5.9 | 66.4  | 11.7 | 7.8   | 607.3 | 27.6 | 15.6 |
| DW-37  | 2.2   | 147.6 | 12.0 | 259.3 | 5.5 | 46.1  | 11.9 | 3.8   | 103.3 | 19.2 | 17.3 |
| DW-39A | 6.0   | 147.8 | 14.7 | 302.6 | 5.4 | 101.2 | 11.5 | 13.1  | 82.1  | 26.5 | 14.3 |
| DW-42A | 10.7  | 205.3 | 19.3 | 189.3 | 4.0 | 110.1 | 14.5 | 18.2  | 114.2 | 24.6 | 8.4  |
| DW-65  | 4.7   | 144.1 | 16.2 | 255.5 | 5.5 | 110.6 | 10.8 | 19.0  | 77.6  | 51.9 | 19.2 |
| DW-382 | 7.2   | 151.2 | 17.4 | 151.6 | 3.3 | 101.9 | 12.1 | 10.3  | 36.9  | 5.8  | 12.3 |
| G-205B | 17.9  | 134.7 | 12.7 | 157.3 | 5.1 | 50.0  | 7.3  | 12.6  | 42.2  | 8.0  | 11.8 |

DW-30 MICROPEGMATITE, PLAGIOCLASE  
 DW-32 MICROPEGMATITE, PLAGIOCLASE, FOLIATED  
 DW-33 MICROPEGMATITE, PLAGIOCLASE  
 DW-36 SILICEOUS PLAG. MICROPEG. LENS IN BASAL BRECCIA  
 DW-37 SILICEOUS PLAG. MICROPEG. LENS IN BASAL BRECCIA  
 DW-39A SILICEOUS PLAG. MICROPEG. LENS IN BASAL BRECCIA  
 DW-42A MICROPEGMATITE, PLAGIOCLASE  
 DW-65 MICROPEGMATITE, PLAGIOCLASE, SILICEOUS, LENS IN BASAL BRECCIA  
 DW-382 MICROPEGMATITE, PLAGIOCLASE, TOP, IN A LENS IN BASAL BRECCIA  
 G-205B CONTACT OF PL. MPG. (B) AND LOW FRAG. POP. MATRIX OF QTZITE BR.

## U P P E R G A B B R O

|       | NB   | ZR    | Y    | SR    | U   | RB   | TH   | PB  | ZN   | CU   | NI   |
|-------|------|-------|------|-------|-----|------|------|-----|------|------|------|
| W-159 | 10.3 | 114.6 | 29.6 | 445.6 | 6.0 | 53.3 | 9.4  | 7.9 | 83.3 | 56.9 | 21.4 |
| W-153 | 11.6 | 180.8 | 29.0 | 416.6 | 4.0 | 63.4 | 13.3 | 9.9 | 71.0 | 10.3 | 15.9 |

W-159 UPPER GABBRO, SOUTH RANGE  
W-153 UPPER GABBRO, SOUTH RANGE

## M I C R O P E G M A T I T E

|        | NB   | ZR    | Y    | SR    | U   | RB    | TH   | PB   | ZN    | CU   | NI  |
|--------|------|-------|------|-------|-----|-------|------|------|-------|------|-----|
| DW-28  | 12.6 | 226.3 | 25.2 | 174.6 | 4.7 | 101.0 | 17.5 | 15.8 | 56.4  | 20.2 | 6.1 |
| DW-29  | 8.4  | 227.3 | 24.4 | 206.8 | 6.2 | 95.8  | 15.9 | 26.7 | 94.7  | 35.4 | 5.3 |
| DW-42B | 10.5 | 203.1 | 21.1 | 188.9 | 3.4 | 117.9 | 16.1 | 23.6 | 102.6 | 22.8 | 5.7 |
| W-150  | 18.4 | 299.0 | 31.2 | 168.3 | 2.8 | 106.4 | 20.4 | 7.1  | 60.1  | 5.5  | 5.3 |
| W-154  | 17.5 | 338.2 | 42.9 | 216.2 | 7.0 | 59.9  | 19.9 | 7.9  | 49.7  | 3.0  | 4.3 |
| W-156  | 16.1 | 300.8 | 33.6 | 184.3 | 5.8 | 101.7 | 19.9 | 9.1  | 73.3  | 2.1  | 5.8 |
| W-155  | 10.5 | 217.7 | 28.3 | 266.1 | 5.4 | 104.6 | 15.1 | 18.7 | 95.9  | 20.9 | 6.8 |

DW-28 MICROPEGMATITE, GRANOPHYRIC  
DW-29 MICROPEGMATITE, GRANOPHYRIC  
DW-42B MICROPEGMATITE, GRANOPHYRIC, BLOTCHY  
W-150 MICROPEGMATITE, SOUTH RANGE  
W-154 MICROPEGMATITE, SOUTH RANGE  
W-156 MICROPEGMATITE, SOUTH RANGE  
W-155 MICROPEGMATITE, SOUTH RANGE

## O N A P I N G M A T R I X

|      | NB   | ZR    | Y   | SR   | U   | RB    | TH   | PB  | ZN   | CU   | NI   |
|------|------|-------|-----|------|-----|-------|------|-----|------|------|------|
| DW-6 | 18.2 | 118.7 | 8.6 | 64.5 | 2.4 | 205.2 | 14.9 | 9.0 | 10.4 | 28.1 | 17.3 |

DW-6 FINE GRAINED DARK GREY SILTY MUD FROM ONAPING FM.

S U B U R Y B R E C C I A

|       | NB   | ZR    | Y    | SR    | U   | RB    | TH   | PB   | ZN    | CU    | NI    |
|-------|------|-------|------|-------|-----|-------|------|------|-------|-------|-------|
| SBR-1 | 7.6  | 163.0 | 22.2 | 382.9 | 3.5 | 90.2  | 18.2 | 13.1 | 96.4  | 100.5 | 95.0  |
| SBR-2 | 6.3  | 148.5 | 21.5 | 381.2 | 2.8 | 72.3  | 11.3 | 11.3 | 86.3  | 108.7 | 90.4  |
| SBR-3 | 7.2  | 195.9 | 18.3 | 454.4 | 0.0 | 316.3 | 22.6 | 9.2  | 127.7 | 55.6  | 95.6  |
| SBR-A | 19.4 | 150.3 | 14.9 | 144.6 | 3.0 | 15.2  | 10.3 | 12.7 | 137.9 | 18.9  | 376.1 |
| SBR-B | 7.9  | 167.9 | 21.7 | 464.7 | 5.8 | 23.2  | 11.1 | 11.3 | 91.9  | 84.4  | 84.6  |

SBR-1 SUDBURY BRECCIA, NORTH OF LEVACK ON HWY. 144, VFG. MATRIX  
 SBR-2 SUDBURY BRECCIA, VFG. BLACK MATRIX WITH UP TO 10% INCL  
 SBR-3 SUDBURY BRECCIA, 3 IN. VEIN, FAR N. FOY OFFSET NEAR SHAFT 2  
 SBR-A SUDBURY BRECCIA, WINDY LAKE RD., XLINE MATRIX  
 SBR-B SUDBURY BRECCIA, WINDY LAKE RD., XLINE MATRIX

C O U N T R Y R O C K S

|        | NB   | ZR    | Y    | SR    | U   | RB    | TH  | PB   | ZN    | CU    | NI    |
|--------|------|-------|------|-------|-----|-------|-----|------|-------|-------|-------|
| UW469A | 5.0  | 2.1   | .6   | 1.0   | 0.0 | 2.3   | .5  | 3.7  | 0.0   | 4.3   | 4.6   |
| DW-417 | 1.6  | 48.4  | 1.0  | 48.3  | 1.1 | 72.2  | 6.6 | 19.1 | 61.4  | 5.9   | 5.4   |
| DW-210 | 2.3  | 55.2  | 3.5  | 70.3  | .8  | 19.3  | 4.4 | 4.2  | 19.1  | 6.8   | 11.5  |
| DW-276 | 2.3  | 55.0  | 5.9  | 80.9  | 0.0 | 126.5 | 4.6 | 2.7  | 6.4   | 7.9   | 7.7   |
| DW-206 | 3.3  | 53.7  | 6.2  | 20.3  | 0.0 | 114.1 | 5.1 | 2.1  | 9.7   | 2.3   | 7.4   |
| DW-8   | 3.4  | 64.3  | 5.9  | 10.5  | 0.0 | 126.6 | 5.5 | 2.1  | 9.7   | 2.3   | 7.4   |
| DW-27  | 0.7  | 3.1   | 2.5  | 453.3 | 4.7 | 39.4  | 0.8 | 6.7  | 4.5   | 2.5   | 5.0   |
| DW-167 | 0.7  | 3.2   | 1.3  | 91.7  | 0.0 | 199.5 | 4.3 | 10.2 | 10.7  | 13.5  | 5.0   |
| DW-180 | 5.6  | 96.8  | 4.2  | 185.9 | .8  | 98.5  | 3.7 | 2.2  | 10.7  | 6.0   | 3.6   |
| DW-375 | 4.0  | 45.3  | .7   | 224.8 | 0.0 | 126.5 | 3.1 | 5.5  | 6.6   | 3.7   | 3.6   |
| DW-414 | 0.0  | 41.8  | 4.2  | 660.2 | 4.1 | 109.3 | 3.7 | 1.4  | 20.0  | 15.6  | 15.0  |
| DW-418 | 0.0  | 522.3 | 7.9  | 167.7 | 0.0 | 193.9 | 2.0 | 3.4  | 10.4  | 7.0   | 13.8  |
| DW-433 | 0.0  | 222.8 | 2.2  | 148.0 | 1.8 | 37.0  | 2.4 | 10.6 | 21.0  | 10.4  | 18.2  |
| DW-474 | 3.3  | 104.0 | 5.7  | 620.8 | 4.3 | 117.3 | 2.8 | 8.6  | 10.7  | 15.8  | 14.1  |
| XL-1   | 12.3 | 55.6  | 4.3  | 98.7  | 2.3 | 90.9  | 5.0 | 7.7  | 21.1  | 21.6  | 105.5 |
| PX-HFS | 0.0  | 67.3  | 18.6 | 556.2 | 5.0 | 14.8  | 9.7 | 13.1 | 128.0 | 126.9 | 34.8  |
| B-29   | 0.0  | 108.4 | 1.3  | 509.2 | 5.3 | 27.0  | 1.5 | 6.8  | 16.8  | 5.8   | 8.1   |

DW-469 PINKISH WHITE CHERTY QUARTZITE  
 DW-417 PINK ARKOSIC QUARTZITE  
 DW-210 MG. ARKOSE WITH BLACK QUARTZITE BANDS  
 DW-276 ARKOSIC QUARTZITE  
 DW-206 SERICITIC QUARTZITE  
 DW-8 SPOTTED QUARTZITE  
 DW-27 FELDSPATHIC INCLUSION IN BASAL BRECCIA, ANEAELED, STAGE 5  
 DW-167 MG. SALMON PINK GRANITE  
 DW-180 MG. GRANITE  
 DW-375 MED. GR. PINK GREY GRANITE  
 DW-414 CG. PINK GREY GRANITE  
 DW-418 CG. GRANITE  
 DW-433 PEGMATITIC GRANITE  
 DW-474 DK. GREY GRANODIORITIC GNEISS  
 XL-1 GRANITE INCLUSION IN THE BLACK ONAPING, STAGE 3 SHOCK  
 PX-HFS STRATHCONA MINE, PYROXENE HORNFELS  
 B-29 LEVACK COMPLEX, 0.5 MI. NORTH OF IRRUPTIVE, ALTERED AND SHATTERED

## GREY BRECCIA

|        | NB   | ZR    | Y    | SR    | U   | RB   | TH   | PB   | ZN    | CU     | NI     |
|--------|------|-------|------|-------|-----|------|------|------|-------|--------|--------|
| MS776C | 6.8  | 74.0  | 21.7 | 420.1 | 5.7 | 15.8 | 6.6  | 16.4 | 93.5  | 48.0   | 121.1  |
| MS811D | 1.3  | 152.1 | 8.3  | 533.8 | 4.4 | 23.6 | 5.7  | 60.5 | 90.3  | 884.9  | 523.7  |
| 811FPI | .8   | 106.1 | 5.9  | 566.2 | 5.0 | 18.8 | 3.2  | 24.4 | 54.9  | 789.5  | 467.1  |
| 811FGR | 11.2 | 130.7 | 4.9  | 375.5 | 4.0 | 11.9 | 4.2  | 19.7 | 55.0  | 1178.0 | 593.1  |
| MS811R | 9.0  | 105.2 | 4.6  | 753.3 | 5.6 | 34.3 | 2.1  | 12.5 | 44.6  | 159.7  | 98.8   |
| ST2900 | .1   | 143.4 | 6.3  | 565.4 | 5.1 | 25.0 | 4.0  | 14.6 | 45.7  | 535.6  | 975.7  |
| LF-1   | 0.0  | 56.9  | 12.9 | 523.9 | 4.3 | 14.9 | 10.8 | 59.7 | 43.27 | 314.27 | 7747.6 |

MS776C SULTANA, GREY BRECCIA  
MS811D LONGVAC, AGMATITE-GREY BRECCIA  
811FPI LONGVAC, AGMATITE-GREY BRECCIA, PINK MATRIX  
811FGR LONGVAC, AGMATITE-GREY BRECCIA, GREY MATRIX  
MS811R LONGVAC, D.D.H. CORE 1325 FT., SUDBURY BRECCIA  
ST2900 STRATHCONA MINE 2900 LEVEL, S. OF 2901 BYPASS, GREY BRECCIA  
LF-1 LONGVAC, GREY BRECCIA RICH IN SULPHIDES

## SUBLAYER

|        | NB   | ZR    | Y    | SR    | U   | RB   | TH   | PB   | ZN    | CU     | NI     |
|--------|------|-------|------|-------|-----|------|------|------|-------|--------|--------|
| MS776A | 1.8  | 53.6  | 10.3 | 44.1  | 2.3 | 17.9 | 8.0  | 9.9  | 113.2 | 118.72 | 424.3  |
| MS776E | 17.1 | 79.6  | 18.4 | 446.3 | 4.6 | 13.9 | 6.9  | 12.1 | 100.2 | 184.8  | 104.7  |
| MS-777 | 4.4  | 85.2  | 22.9 | 396.1 | 4.7 | 34.8 | 7.3  | 11.7 | 106.4 | 271.1  | 653.1  |
| MS805A | 18.5 | 134.1 | 29.8 | 244.1 | 1.0 | 75.8 | 12.8 | 30.6 | 99.7  | 152.8  | 189.4  |
| MS811P | 0.0  | 9.2   | 9.6  | 137.0 | 1.2 | 9.9  | 7.4  | 10.5 | 62.1  | 195.6  | 192.7  |
| MS811V | 0.0  | 37.6  | 7.7  | 255.5 | 4.0 | 10.5 | 5.3  | 11.4 | 110.7 | 342.7  | 316.4  |
| WHL-AA | 3.8  | 78.4  | 9.1  | 516.0 | 2.1 | 34.0 | 8.3  | 66.9 | 59.0  | 1320.8 | 2362.1 |
| WHL-A  | 0.0  | 37.7  | 19.5 | 291.9 | 5.3 | 18.4 | 6.2  | 12.7 | 130.8 | 73.2   | 470.4  |
| WHL-B  | 0.0  | 30.3  | 16.8 | 238.4 | 4.4 | 13.8 | 7.6  | 15.1 | 122.0 | 675.8  | 303.4  |
| WHL-C  | 0.0  | 30.6  | 19.5 | 289.2 | 2.9 | 20.2 | 7.4  | 11.7 | 119.7 | 26.6   | 217.3  |
| 1426-A | 24.6 | 208.2 | 19.9 | 401.7 | 4.1 | 74.5 | 15.0 | 22.6 | 81.5  | 46.6   | 41.4   |
| 1426-B | 12.3 | 185.6 | 16.9 | 479.3 | 0.0 | 64.3 | 11.3 | 16.9 | 85.5  | 124.2  | 155.0  |
| E-2-70 | 6.7  | 173.6 | 19.2 | 406.1 | 4.0 | 64.2 | 11.7 | 27.7 | 80.6  | 63.7   | 48.2   |

MS776A SULTANA AREA, SUBLAYER WITH LITTLE SULPHIDE  
MS776E SULTANA, OK, VFG. SUBLAYER WITH SULPHIDES AND QTZ INCL.  
MS-777 SULTANA, MG. SUBLAYER WITH SULPHIDE SEGREGATIONS  
MS805A COPPER CLIFF OFFSET, QD  
MS811P LONGVAC, SUBLAYER  
MS811V LONGVAC, SUBLAYER  
WHL-AA WHISTLE, SUBLAYER, CG. PHASE WITH SULPHIDES  
WHL-A WHISTLE, SUBLAYER, CG. PHASE WITH SULPHIDES  
WHL-B WHISTLE, SUBLAYER, MG. EQUIGRANULAR, WITH BIOTITE AND SULPHIDES  
WHL-C WHISTLE, SUBLAYER, MG. EQUIGRANULAR, WITH BIOTITE  
1426-A FOY OFFSET, CONTACT BETWEEN QD + SUBLAYER, NICKEL LAKE, A=QD  
1426-B FOY OFFSET, CONTACT BETWEEN QD + SUBLAYER, NICKEL LAKE, B=SUBL  
E-2-70 FOY OFFSET, QD. NEAR NICKEL LAKE

N O R I T E

|        | NB  | ZR    | Y    | SR    | U   | RB   | TH   | PB   | ZN    | CU    | NI    |
|--------|-----|-------|------|-------|-----|------|------|------|-------|-------|-------|
| 811 NF | 5.2 | 166.1 | 27.4 | 523.9 | 4.8 | 39.8 | 7.4  | 13.2 | 83.2  | 107.5 | 122.8 |
| MS809M | 0.0 | 59.5  | 25.3 | 269.1 | 3.8 | 27.0 | 7.7  | 4.2  | 19.8  | 115.5 | 131.2 |
| WHL-FN | 4.4 | 98.5  | 10.1 | 311.1 | 3.0 | 61.0 | 6.8  | 4.9  | 69.4  | 127.1 | 128.3 |
| W-101  | 3.2 | 117.4 | 16.6 | 427.1 | 4.3 | 47.6 | 7.0  | 1.1  | 84.8  | 39.6  | 53.9  |
| W-102  | 6.4 | 112.0 | 16.5 | 401.6 | 3.6 | 22.3 | 8.1  | 1.1  | 33.3  | 33.5  | 47.1  |
| W-103  | 6.2 | 118.4 | 16.4 | 389.7 | 3.3 | 11.6 | 8.8  | 1.1  | 33.3  | 33.3  | 47.1  |
| W-104  | 7.7 | 114.0 | 16.1 | 365.0 | 3.3 | 11.6 | 8.8  | 1.1  | 33.3  | 33.3  | 47.1  |
| W-110  | 4.3 | 108.4 | 15.4 | 434.1 | 7.7 | 46.2 | 10.2 | 1.1  | 89.8  | 60.9  | 50.0  |
| W-113  | 3.4 | 88.1  | 12.8 | 435.9 | 4.4 | 33.6 | 4.4  | 1.1  | 70.6  | 48.2  | 61.7  |
| W-116  | 1.8 | 55.0  | 7.8  | 473.6 | 6.6 | 20.3 | 4.4  | 1.1  | 67.5  | 22.4  | 44.9  |
| W-118  | 0.0 | 55.4  | 7.7  | 471.9 | 3.3 | 11.6 | 2.2  | 1.1  | 64.9  | 22.4  | 33.6  |
| W-120  | 2.5 | 58.1  | 7.6  | 464.0 | 3.3 | 7.7  | 2.2  | 1.1  | 55.4  | 22.4  | 33.6  |
| W-124  | 0.0 | 73.7  | 11.9 | 464.0 | 3.3 | 7.7  | 2.2  | 1.1  | 79.4  | 43.2  | 64.7  |
| W-126  | .5  | 95.6  | 15.9 | 352.6 | 5.8 | 22.4 | 1.1  | 1.1  | 55.4  | 22.4  | 33.6  |
| W-127  | .5  | 102.4 | 13.5 | 457.3 | 6.8 | 31.4 | 6.6  | 1.1  | 66.8  | 21.3  | 16.5  |
| W-129  | 0.0 | 116.3 | 14.1 | 472.0 | 2.2 | 11.6 | 9.9  | 1.1  | 87.5  | 14.3  | 24.8  |
| W-134  | 1.6 | 100.3 | 13.8 | 440.9 | 6.3 | 27.7 | 9.5  | 3.0  | 95.0  | 27.9  | 30.6  |
| W-132  | .6  | 96.8  | 13.8 | 440.9 | 5.3 | 27.7 | 8.2  | 1.1  | 87.5  | 27.9  | 30.6  |
| W-136  | 0.0 | 113.4 | 15.4 | 454.4 | 3.5 | 48.4 | 7.7  | 1.1  | 101.4 | 33.1  | 46.4  |

811 NF LONGVAC, NORITE FRAGMENT IN THE SUBLAYER  
 MS609M WHISTLE, NORITE  
 WHL-FN WHISTLE, FELSIC NORITE FROM D.O.H. CORE, MG. EQUIGRANULAR  
 W-101 NORITE, SOUTH RANGE  
 W-102 NORITE, SOUTH RANGE  
 W-103 NORITE, SOUTH RANGE  
 W-104 NORITE, SOUTH RANGE  
 W-110 NORITE, SOUTH RANGE  
 W-113 NORITE, SOUTH RANGE  
 W-116 NORITE, SOUTH RANGE  
 W-118 NORITE, SOUTH RANGE  
 W-120 NORITE, SOUTH RANGE  
 W-124 NORITE, SOUTH RANGE  
 W-126 NORITE, SOUTH RANGE  
 W-127 NORITE, NORTH RANGE  
 W-129 NORITE, NORTH RANGE  
 W-134 NORITE, NORTH RANGE  
 W-132 NORITE, NORTH RANGE  
 W-136 NORITE, NORTH RANGE



REFERENCES CITED

- Ahrens, T.J., and Rosenberg, J.T., 1968, Shock metamorphism: experiments on quartz and plagioclase, in Shock Metamorphism of Natural Materials, eds. B.M. French and N.M. Short, Mono Book Corp., Baltimore, p. 59-82.
- Beales, F.W. and Lozej, G.P., 1975, Sudbury Basin sediments and the meteorite impact theory of origin for the Sudbury structure; *Can. Jour. Earth Sci.*, 12, p. 629-635.
- Bell, R., 1891, On the Sudbury mining district; *Rept. Geol. Surv. Can.*, v. 5, pt. F, 95 pp.
- Benzercı, J.P., 1970, La pratique de l'analyse des correspondences: Cahier N°2 du Laboratoire des Statistiques Mathematiques, Faculte des Sciences, Paris, 35 pp.
- Brocum, S.J. and Dalziel, I.W.D., 1974, The Sudbury Basin, the Southern Province, the Grenville Front, and the Penokean Orogeny; *Bull. Geol. Soc. Amer.*, 85, p. 1571-1580.
- Brooks, C., Hart, S.R., and Wendt, I., 1972, Realistic use of two-error regression treatments as applied to Rubidium-Strontium data; *Rev. Geophy. and Space Phy.*, 10, p. 551-577.
- Brown, G.C., Hughes, D.J., and Esson, J., 1973, New X.R.F. data retrieval techniques and their application to U.S.G.S. standard rocks; *Chem. Geol.*, 11, p.223-229.
- Bryan, W.B., Finger, L.W., and Chayes, F., 1969, Estimating proportions in petrographic mixing equations by least-squares approximation; *Science*, 163, p.926-927.

- Bunch, T.E., and Cassidy, W.A., 1972, Petrographic and electron microprobe study of the Monturaqui impactite; *Contr. Mineral. Petrol.*, 36, p.95-112.
- Burrows, A.G., and Rickaby, H.C., 1929, Sudbury Basin area; *Ont. Dept. Mines Rpt.* 38, pt.3.
- Cantin, R. and Walker, R.G., 1972, Was the Sudbury Basin circular during deposition of the Chelmsford Formation ? ; *Geol. Assoc. Can. Spec. Paper* 10, p. 93-101.
- Card, K.D., and Meyn, H.D., 1969, Geology of the Leinster-Bowell area; *Ont. Dept. Mines Geol. Rpt.* 65.
- \_\_\_\_\_, Church, W.R., Franklin, J.M., Frarey, J.A., Robertson, J.A., West, G.F., and Young, G.M., 1972, The Southern Province; *Geol. Assoc. Can. Spec. Paper* 11, p. 335-380.
- Carter, N.L., 1965, Basal quartz deformation lamellae - a criterion for recognition of impactites; *Amer. Jour. Sci.*, 263, p.786-806.
- \_\_\_\_\_, 1968, Dynamic deformation of quartz; *in Shock Metamorphism of Natural Materials*, eds. B.M. French and N.M. Short, Mono Book Corp., Baltimore, p.453-474.
- Chao, E.C.T., 1974, Impact cratering models and their application to lunar studies - a geologist's view; *Proc. Fifth Lunar Sci. Conf.*, 1, p.35-52.
- Coleman, A.P., 1905, The Sudbury nickel field; *Ont. Bur. Mines, Ann. Rpt.*, 14, pt.3, p.1-188.
- Compston, W., and Taylor, S.R., 1969, Rb-Sr study of impact glass and country rocks from the Henbury meteorite crater field; *Geochim. Cosmoch. Acta*, 33, p.1037-1043.

Currie, K.L., 1971a, Origin of igneous rocks associated with shock metamorphism as suggested by geochemical investigations of Canadian craters; Jour. Geophys. Res., 76, p. 5575-5585.

\_\_\_\_\_, 1971b, Geology of the resurgent cryptoexplosion crater at Mistastin Lake, Labrador; Geol. Surv. Can. Bull. 207, 62 pp.

Dagbert, M., and David, M., 1974, Pattern recognition and geochemical data: an application to Montereian Hills; Can. Jour. Earth Sci., 11, p.1577-1585.

David, M., and Woussen, G., 1973, Correspondence analysis, a new tool for geologists; Proc. Mining Pribram, 1, p.41-65.

\_\_\_\_\_, Campiglio, C., and Darling, R., 1974, Progress in R- and Q-mode analysis and its application to the study of geological processes, Can. Jour. Earth Sci., 11, p.131-146.

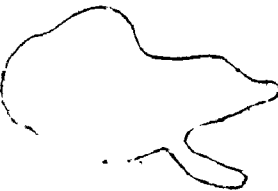
\_\_\_\_\_, and Beauchemin, Y, 1974, The correspondence analysis method and a FORTRAN IV program; Geocom Programs 10.

Dence, M.R., 1971, Impact Melts; Jour. Geophys. Res. 76, p.5552-5565.

\_\_\_\_\_, 1972, Meteorite impact craters and the structure of the Sudbury Basin; Geol. Assoc. Can. Spec. Paper 10, p.7-18.

\_\_\_\_\_ and Guy-Bray, J.V., 1972, Some astroblemes, craters and cryptovolcanic structures in Ontario and Quebec; Excursion Guidebook A65, XXIV Int. Geol. Cong., Montreal, 61 pp.

Dietz, R.S., 1963, Astroblemes: ancient meteorite impact structures on the earth; in The Moon, Meteorites and Comets, eds. Middlehurst and Kuiper, Univ. Chicago Press, Chicago, p.285-300.



Dietz, R.S., 1964, Sudbury structure as an astrobleme; *J. Geol.* 72, p.412-434.

\_\_\_\_\_, 1968, Shatter cones in cryptoexplosion structures; in *Shock Metamorphism of Natural Materials*, eds. B.M. French and N.M. Short, Mono Book Corp., Baltimore, p.267-285.

\_\_\_\_\_, and Butler, L., 1964, Shatter cone orientation at Sudbury, Canada; *Nature*, 204, p.4955.

Doering, W.P., 1968, A rapid method for measuring the Rb/Sr ratio in silicate rocks; U.S.G.S. Prof. Paper 600C, p. 164-168.

Emslie, R.F., 1975, Nature and origin of anorthositic suites; *Geoscience Canada*, 2, p.99-104.

\_\_\_\_\_, Morse, S.A., and Wheeler, E.P. II, 1972, Igneous rocks of central Labrador, with emphasis on anorthositic and related intrusions; *Excursion Guidebook A54, XXIV Int. Geol. Cong., Montreal*, 72 pp.

Engelhart, W. von, 1967, Chemical composition of Ries glass bombs; *Geochim. Cosmochim. Acta*, 31, p.1677-1688.

Evensen, N.M., Murthy, V.R., and Coscio Jr., M.R., 1973, Rb-Sr ages of some mare basalts and the isotopic and trace element systematics in lunar fines; in *Proc. Fourth Lunar Sci. Conf.*, 2, p.1707-1724.

Fairbairn, H.W., and Robson, G.M., 1944, Breccia at Sudbury; *Rept. Ont. Dept. Mines*, 50, pt.6, p.18-33.

\_\_\_\_\_, Hurley, P.M., and Pinson, W.H., 1965, Re-examination of Rb-Sr whole-rock ages at Sudbury, Ontario; *Proc. Geol. Assoc. Can.*, 16, p.95-101.

- Fairbairn, H.W., Faure, G., Pinson, W.H., and Hurley, P.M., 1968, Rb-Sr whole-rock age of the Sudbury lopolith and basin sediments; *Can. Jour. Earth Sci.*, 5, p.707-714.
- French, B.M., 1967, Sudbury structure, Ontario: some petrographic evidence for origin by meteorite impact; *Science*, 156, p.1094-1098.
- \_\_\_\_\_, 1968, Shock metamorphism as a geological process; in *Shock Metamorphism of Natural Materials*, eds. B.M. French and N.M. Short, Mono Book Corp., Baltimore, p.1-18.
- \_\_\_\_\_, 1970, Possible relations between meteorite impact and igneous petrogenesis, as indicated by the Sudbury structure, Ontario, Canada, *Bull. Volcanologique*, 34, p.446-517.
- \_\_\_\_\_, and Short, N.M., 1968, *Shock Metamorphism of Natural Materials*, Mono Book Corp., Baltimore, 644 pp.
- \_\_\_\_\_, Hartung, J.B., Short, N.M., and Dietz, R.S., 1970, Tenoumer crater, Mauritania: age and petrologic evidence for origin by meteorite impact; *Jour. Geophys. Res.*, 75, p.4396-4406.
- Fullagar, P.D., Bottino, M.L., and French, B.M., 1971, Rb-Sr study of shock-metamorphosed inclusions from the Onaping Formation, Sudbury, Ontario; *Can. Jour. Earth Sci.*, 8, p.435-443.
- Gates, T.M., and Hurley, P.M., 1973, Evaluation of Rb-Sr dating methods applied to the Matachewan, Abitibi, Mackenzie, and Sudbury dike swarms in Canada; *Can. Jour. Earth Sci.*, 10, p.900-919.

- Gault, D.E., Quaide, W.L., and Oberbeck, V.R., 1968, Impact cratering mechanics and structures; in Shock Metamorphism of Natural Materials, eds. B.M. French and N.M. Short, Mono Book Corp., Baltimore, p.87-99.
- Gibbins, W.A., 1973, Rubidium-Strontium mineral and rock ages at Sudbury, Ontario; Ph.D. Thesis, McMaster University, Hamilton, Ont., 230 pp.
- \_\_\_\_\_, and McNutt, R.H., 1975a, The age of the Sudbury Nickel Irruptive and the Murray Granite; Can. Jour. Earth Sci., 12, p.1970-1989.
- \_\_\_\_\_, 1975b, Rubidium-Strontium mineral ages and polymetamorphism at Sudbury, Ontario; Can. Jour. Earth Sci., 12, p.1990-2003.
- Greenman, L., 1970, The petrology of the footwall breccias in the vicinity of the Strathcona Mine, Levack, Ontario; Ph.D. thesis, Univ. of Toronto, Toronto, Ont.
- Grieve, R.A.F., 1975, Petrology and chemistry of the impact melt at Mistastin Lake crater, Labrador; Bull. Geol. Soc. Amer., 86, p.1617-1629.
- Guy-Bray, J.V.; et al., 1966, Shatter cones at Sudbury; J. Geol., 74, p.243-245.
- Hart, S.R., Schilling, J.G., and Powell, J.L., 1973, Basalts from iceland and along the Reykjanes ridge: Sr isotope geochemistry; Nature Phys. Sci., 246, p.104-107.
- Hawley, J.E., 1962, The Sudbury ores; their mineralogy and origin; Can. Mineral., 7, p.1-207.
- Hewins, R.H., and Pattison, E.F., 1972, Bronzite-ferrohypersthene, pigeonite and augite in quenched Foy offset, Sudbury nickel irruptive, Ontario; Geol. Soc. Amer. Abstracts with programs, 4, p.366-367.

- Holland, J.G. and Brindle, D.W., 1966, A self-consistent mass absorption correction for silicate analysis by X-ray fluorescence; *Spectrochimica Acta*, 22, p.2083-2093.
- Hörz, F., ed., 1971, Meteorite impact and volcanism; *Jour. Geophys. Res.*, 76, p.5381-5798.
- Hurley, P.M., 1969, Rb-Sr isotopic investigation of crater rocks of possible impact origin; MIT 17th Ann. Prog. Rpt., p.27-28.
- Hurst, R.W. and Wetherill, G.W., 1974, Rb-Sr study of the Sudbury Nickel Irruptive; *Trans. Amer. Geophys. Union*, 55, p.488.
- Irvine, T.N., 1975, Crystallization sequences in the Muskox intrusion and other layered intrusions - II. Origin of chromite layers and similar deposits of other magmatic ores; *Geochim. Cosmochim. Acta*, 39, p.991-1020.
- Jenkins, R.H. and De Vries, B., 1970, Worked examples in X-ray spectrometry; Springer Verlag Inc., N.Y., 129 pp.
- Kolbe, P., Pinson, W.H., Saul, J.M., and Miller, E.W., 1967, Rb-Sr study on country rocks of the Bosumtwi crater, Ghana; *Geochim. Cosmochim. Acta*, 31, p869-875.
- Kraut, F., and French, B.M., 1971, The Rochechouart meteorite impact structure, France: preliminary geological results; *Jour. Geophys. Res.*, 76, p. 5407-5413.
- Krogh, T.E., Davis, G.L., Aldrich, L.T., Hart, S.R. and Steuber, A., 1968, Geological history of the Grenville province; *Carnegie Inst. Washington Yearbook* 66, p.528-536.

Krogh, T.E., Davis, G.L., and Frarey, M.J., 1971, Isotopic ages along the Grenville front in the Bell Lake area, southwest of Sudbury, Ontario; Carnegie Inst. Washington Yearbook 69, p.337-339.

---

\_\_\_\_\_, 1973, The significance of inherited zircons on the age and origin of igneous rocks - an investigation of the ages of the Labrador adamellites; Carnegie Inst. Washington Yearbook 72, p.610-613.

---

\_\_\_\_\_, 1974, The age of the Sudbury Nickel Irruptive; Carnegie Inst. Washington yearbook 73, p.567-569.

Lofgren, G., 1971a, Experimentally produced devitrification textures in natural rhyolitic glass; Bull. Geol. Soc. Amer., 82, p.111-124.

---

\_\_\_\_\_, 1971b, Spherulitic textures in glassy and crystalline rocks; Jour. Geophys. Res., 76, p.5635-5648.

Lumbers, S.B., 1975, Geology of the Burwash area, districts of Nipissing, Parry Sound, and Sudbury; Ont. Div. Mines Geol. Rpt. 116, p.160.

Mak, E.K.C., 1973, Ar<sup>40</sup>/Ar<sup>39</sup> dating of shock-metamorphosed rocks from Mistastin Lake meteorite impact crater, Unpub. M.Sc. Thesis, Univ. of Toronto, 74 pp.

Marchand, M., 1973, Determination of Rb, Sr, and Rb/Sr by XRF; Tech. Memo 73-2, Dept. of Geology, McMaster University, Hamilton, Ont.

Mark, R.K., Cliff, R.A., Lee-Hu, C., and Wetherill, G.W., 1973, Rb-Sr studies of lunar breccias and soils; Proc. 4th Lunar Sci. Conf., 2, p.1785-1795.

McIntyre, G.A., Brooks, C., Compston, W., and Turek, A., 1966, The statistical assessment of Rb-Sr isochrons; Jour. Geophys. Res., 71, p.5459-5468.



Naldrett, A.J. and Kullerud, G., 1967, A study of the Strathcona Mine and its bearing on the origin of the nickel-copper ores of the Sudbury district, Ontario; *J. Petrol.*, 8, p.453-531.

\_\_\_\_\_, Guy-Bray, J.V., Gasparri, E.L., Podolsky, T., and Rucklidge, J.C., 1970, Cryptic variation and the petrology of the Sudbury Nickel Irruptive; *Econ. Geol.*, 65, p.122-155.

\_\_\_\_\_, Greenman, L., and Hewins, R.H., 1972, The main irruptive and the sub-layer at Sudbury, Ontario; *Proc. XXIV Int. Geol. Cong., Sect 4*, p.206-214.

Noble, D.C., 1967, Sodium, potassium and ferrous iron contents of some secondarily hydrated natural silicic glasses; *Amer. Mineral.*, 52, p.280-286.

Nyquist, L.E., Hubbard, N.J., Gast, P.W., Bansal, B.M., and Weismann, H., 1973, Rb-Sr systematics for chemically defined Apollo 15 and 16 materials; *Proc. 4th Lunar Sci. Conf.*, 2, p.1823-1846.

Pankhurst, R.J., and O'Nions, R.K., 1973, Determination of Rb/Sr and  $^{87}\text{Sr}/^{86}\text{Sr}$  ratios of some standard rocks and evaluation of X-ray fluorescence spectrometry in Rb-Sr geochemistry; *Chem. Geol.*, 12, p.127-136.

Peredery, W.V., 1972a, Chemistry of fluidal glasses and melt bodies in the Onaping Formation; *Geol. Assoc. Can. Spec. Paper 10*, p.49-59.

\_\_\_\_\_, 1972b, The origin of rocks at the base of the Onaping Formation, Sudbury, Ontario; Ph.D. Thesis, Univ. of Toronto, 366 pp.

\_\_\_\_\_, and Naldrett, A.J., 1975, Petrology of the upper irruptive rocks, Sudbury, Ontario; *Econ. Geol.* 70, p.164-175.

Reynolds, R.C., 1963, Matrix corrections in trace element analysis by X-ray fluorescence: estimation of the mass absorption coefficient by Compton scattering; Amer. Mineral., 48, p.1133-1143.

\_\_\_\_\_, 1967, Estimation of mass absorption coefficients by Compton scattering: improvements and extensions of the method; Amer. Mineral. 52, p.1493-1502.

Robertson, P.B., Dence, M.R., and Vos, M.A., 1968, Deformation in rock-forming minerals from Canadian craters; in Shock Metamorphism of Natural Materials, eds. B.M. French and N.M. Short, Mono Book Corp., Baltimore, p.433-452.

Rousell, D.H., 1972, The Chelmsford Formation of the Sudbury Basin - a Precambrian turbidite; Geol. Assoc. Can. Spec. Paper 10, p.79-91.

Schnetzler, C.C., Philpotts, J.A., and Thomas, H.H., 1967, Rare-earth and Barium abundances in Ivory Coast tektites and rocks from the Bosumtwi crater area, Ghana; Geochim. Cosmochim. Acta, 31, p.1987-1993.

\_\_\_\_\_, and Pinson Jr., W.H., 1969, Rubidium-strontium correlation study of moldavites and Ries crater material; Geochim. Cosmochim. Acta, 33, p.1015-1021.

Schonfeld, E. and Meyer, C., 1972, The abundances of components in the lunar soils by a least-squares mixing model and the formation age of KREEP; Proc. 3rd. Lunar Sci. Conf., 2, p.1397-1420.

Scott, R.B., 1971, Alkali exchange during devitrification and hydration of glasses in ignimbrite cooling units; J. Geol., 179, p.100-110.

- Smith, R.L., and Bailey, R.A., 1966, The Bandelier tuff: a study of ash-flow eruption cycles from zoned magma chambers; Bull. Volcanologique, 29, p.83-104.
- Souch, B.E., Podolsky, T., and geological staff, 1969, The sulfide ores at Sudbury: their particular relationship to a distinctive inclusion-bearing facies of the Nickel Irruptive; Econ. Geol., Mon. 4, p.252-261.
- Speers, E.C., 1957, The age relation and origin of common Sudbury breccia; J. Geol., 65, p.497-514.
- Stacey, J.S., Wilson, E.E., Peterman, Z.E., and Terrazas, R., 1971, Digital recording of mass spectra in geologic studies I; Can. Jour. Earth Sci., 8, p.371-377.
- Stevenson, J.S., 1961, Recognition of the quartzite breccia in the Whitewater Series, Sudbury basin, Ontario; Roy. Soc. Can. Trans., 55, p.57-66.
- Stoffler, D., 1971, Progressive metamorphism and classification of shocked and brecciated crystalline rocks at impact craters; Jour. Geophys. Res., 76, p.5541-5551.
- Streckeisen, A., 1965, Die Klassifikation der Eruptivgesteine; Geol. Rundschau; 55, p.478-491.
- Taylor, F.C., 1969, Reconnaissance geology of a part of the Precambrian shield, northeastern Quebec and northern Labrador, 14L(N1/2), 14M, 23P(W1/2), 24B,G,J,P, 25A; Geol. Surv. Can., Paper 68-43, 13 pp.
- \_\_\_\_\_, 1970, Reconnaissance geology of a part of the Precambrian shield northeastern Quebec and Northern Labrador; Part II; Geol. Surv. Can., Paper 70-24, 10pp.
- \_\_\_\_\_, 1972, Reconnaissance geology of a part of the Precambrian shield northeastern Quebec and northern Labrador; Part III; Geol. Surv. Can. Paper 71-48, 14 pp.

- Taylor, F.C. and Dence, M.R., 1969, A probable meteorite origin for Mistastin Lake; Can. Jour. Earth Sci., 6, p. 39-45.
- Taylor, H.P., and Forester, R.W., 1971, Low  $O^{18}$  igneous rocks from the intrusive complexes of Skye, Mull, and Arnamurchan, Western Scotland; J. Petrol., 12, p. 465-497.
- Taylor, S.R., 1967, Compositions of meteorite impact glass across the Henbury strewnfield; Geochim. Cosmochim. Acta, 31, p.961-968.
- Teil, H., 1975, Correspondence factor analysis: an outline of its method; Math. Geol., 7, p.3-12.
- \_\_\_\_\_ and Cheminee, J.L., 1975, Application of correspondence analysis to the study of major and trace elements in the Erta Ale chain (Afar, Ethiopia); Math. Geol., 7, p.13-30.
- Thompson, J.E., 1956, Geology of the Sudbury Basin; Ont. Dept. Mines Ann. Rpt., 65, pt.3, p.1-56.
- Van Schmus, R., 1971, Ages of lamprophyre dykes and of the Mongowin pluton, North shore of Lake Huron, Ontario, Canada; Can. Jour. Earth Sci., 8, p.1203-1209.
- \_\_\_\_\_, Card, W.D., and Harrower, K.L., 1975, Geology and ages of buried Precambrian basement rocks, Manitoulin Island, Ontario; Can. Jour. Earth Sci., 12, p.1175-1189.
- Wanless, R.K., and Loveridge, W.D., 1972, Rubidium-Strontium isochron age studies, Report 1; Geol. Surv. Can. Paper 72-23, 77 pp.

- Wetherill, G.W., Davis, G.L., and Tilton, G.R., 1960, Age measurements on minerals from the Cutler batholith, Cutler, Ontario; Jour. Geophys. Res., 65, p.2461-2466.
- Wheeler, E.P. II, 1942, Anorthosite and associated rocks about Nain, Labrador; J. Geol., 50, p.611-642.
- \_\_\_\_\_, 1955, Adamellite intrusive north of Davis Inlet, Labrador; Bull. Geol. Soc. Amer., 66, p.1031-1059.
- \_\_\_\_\_, 1960, Anorthosite-adamellite complex of Nain, Labrador; Bull. Geol. Soc. Amer., 71, p. 1755-1762.
- \_\_\_\_\_, 1968, Minor intrusives associated with the Nain anorthosite; in Origin of Anorthosite and Related Rocks, N.Y. Museum and Sci. Service Memoir 18, p.189-206.
- Williams, H., 1957, Glowing avalanche deposits of the Sudbury basin; Ont. Dept. Mines Ann. Rpt., 65, pt.3, p.57-89.
- Wright, T.L., and Doherty, P.C., 1970, A linear-programming and least-squares computer method for solving petrologic mixing problems; Bull. Geol. Soc. Amer., 81, p.1995-2007.
- Yoder, H.S., 1973, Contemporaneous basaltic and rhyolitic magmas; Amer. Mineral., 58, p.153-171.
- York, D., 1966, Least-squares fitting of a straight line; Can. Jour. Physics, 44, p.1079-1086.